THE RELATIONSHIP BETWEEN ENSO, SEASONAL RAINFALL, AND CIRCULATION PATTERNS IN SOUTH AFRICA

A. C. KRUGER

A dissertation submitted in partial fulfilment of the requirements for the degree

MASTER OF SCIENCE (ATMOSPHERIC SCIENCES)

in the

FACULTY OF SCIENCE

UNIVERSITY OF CAPE TOWN

1999

DISSERTATION SUMMARY

THE RELATIONSHIP BETWEEN ENSO, SEASONAL RAINFALL AND CIRCULATION PATTERNS IN SOUTH AFRICA

Supervisor:	Dr. B. Hewitson
Co-supervisor:	Mr. W. A. Landman
Department:	Environmental and Geographical Science
Faculty:	Science
University:	Cape Town
Degree:	Master of Science (Atmospheric Sciences)

Key Words: El Niño, La Niña, Sea-surface temperature, Seasonal rainfall, South Africa, Circulation patterns, Canonical correlation analysis, Southern Oscillation, El Niño-Southern Oscillation, General circulation model

Abstract

Relationships between the El Niño-Southern Oscillation phenomenon (ENSO), seasonal rainfall, and atmospheric circulation patterns at the 1000 hPa and 500 hPa levels are investigated. Firstly, correlations between early-summer (October to December), late-summer (January to March) rainfall over South Africa, and sea-surface temperatures in the NINO3 region in the equatorial Pacific Ocean were investigated, where the correlations in the case for late-summer showed much better spatial coherence than in the case for early-summer. Consequently, the study further concentrated only on late summer. The influence of the quasi 18-20 year oscillation of summer rainfall on the effect of El Niño and La Niña events was also investigated, and it was found that during an epoch of above-normal/below-normal rainfall a moderating effect is evident on the severity of El Niño/La Niña events so that on average even above-normal/below-normal rainfall is experienced during such events. Canonical correlation analysis (CCA) was applied to different combinations of years, to find associations between equatorial Pacific sea-surface temperatures and deviations in circulation patterns during certain years. Some of the above results were then verified by model runs, to further prove the relationships not to be coincidental, and to add more degrees of freedom. The results of CCA were then separately interpreted for each combination of seasons (e. g. El

Niño during the above-normal phase at the 500 hPa level) with the aid of average circulation maps for different combinations of years. Above- or below-normal rainfall during such years could then be explained in terms of deviations of general synoptic features at the surface and 500 hPa levels.

ACKNOWLEDGEMENTS

- Rainfall data was obtained from the South African Weather Bureau. Data of equatorial Pacific sea-surface temperatures was obtained from the Climate Prediction Center (CPC) at the National Oceanic and Atmospheric Administration (NOAA).

- Supervisor Dr. Bruce Hewitson, especially for obtaining and explaining the GCM model data.

- Co-supervisor Willem Landman, for the CCA analyses and weekly discussions.

- The South African Weather Bureau for computer facilities.

CONTENTS

LIST OF FIGURES

LIST OF TABLES

CHAPTER 1

INTRODUCTION

1.1. The South African rainfall climate

Unlike most countries the size of South Africa (1 219 090 km^2), which usually have only one or two rainfall regimes, the rainfall climate of the country can be divided into four regimes according to the annual march in precipitation (Schulze, 1965). Reasons for this are mainly the influences of the extent of the coastal border of the country, the orography, and the latitudinal position; the latter having the effect that the country is influenced by tropical weather from the north during summer, as well as frontal weather in the south, mainly during the winter months. The four types are:

a) The "Mediterranean" type, with the main rainy season extending from about the middle of April to September.

b) "All seasons type", with a double maximum, namely in February to March and again in September to November.

c) The "monsoonal" type with maximum in midsummer.

d) The "monsoonal" type with maximum in late summer or autumn.

The spatial extent of these types is shown in Figure 1.1. The regions covered by types c and d, spanning the eastern and central parts of the subcontinent, are collectively known as the summer rainfall region of South Africa. This area is the most important with regards to the production of food for the area, whether in the form of crops or livestock. This is also the area, because of its significance, this study will mainly concentrate upon. Although South Africa and the subcontinent can be subdivided into more rainfall regions e. g. regions of higher and lower annual or monthly rainfall, rainfall differences due to orographic influences etc., this brief description of the rainfall can be considered sufficient as an introduction, keeping in mind the aims of the study, which is to find general associations between ENSO, rainfall and circulation patterns over southern Africa.

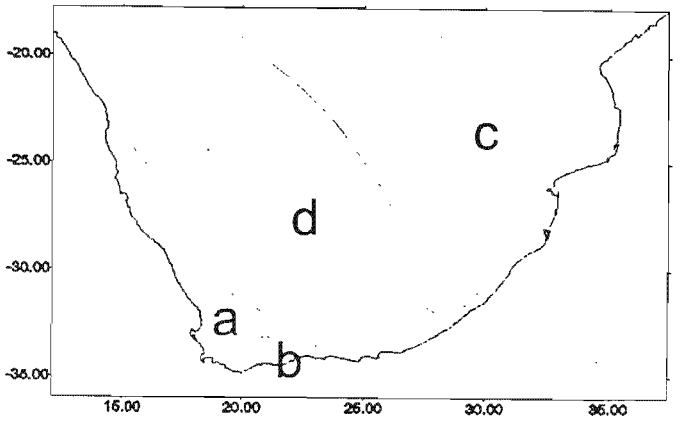

Figure 1.1. Outline of southern Africa, showing rainfall regimes a to d over South Africa, with a, indicating the region of maximum rainfall in winter, b indicating all year rainfall, c. monsoonal type, with maximum rainfall in midsummer, and d, monsoonal type rainfall with maximum rainfall during late summer or autumn (after Schulze, 1965).

1.2. Mean circulation patterns over South Africa and its relation to rainfall distribution during austral summer

"It is necessary to identify the circulation patterns over South Africa to be able to proceed with the establishment of the characteristic weather associated with each pattern"- (Taljaard, 1995). In this study only typical summer circulation patterns and its associated weather are considered. In summer, rainfall is concentrated mainly in the northern and eastern regions, i.e. type c and d regions indicated in Figure 1.1. Figure 1.2 shows the mean 850 hPa geopotential height pattern for January for the period 1981 to 1990, as shown in Taljaard (1995).

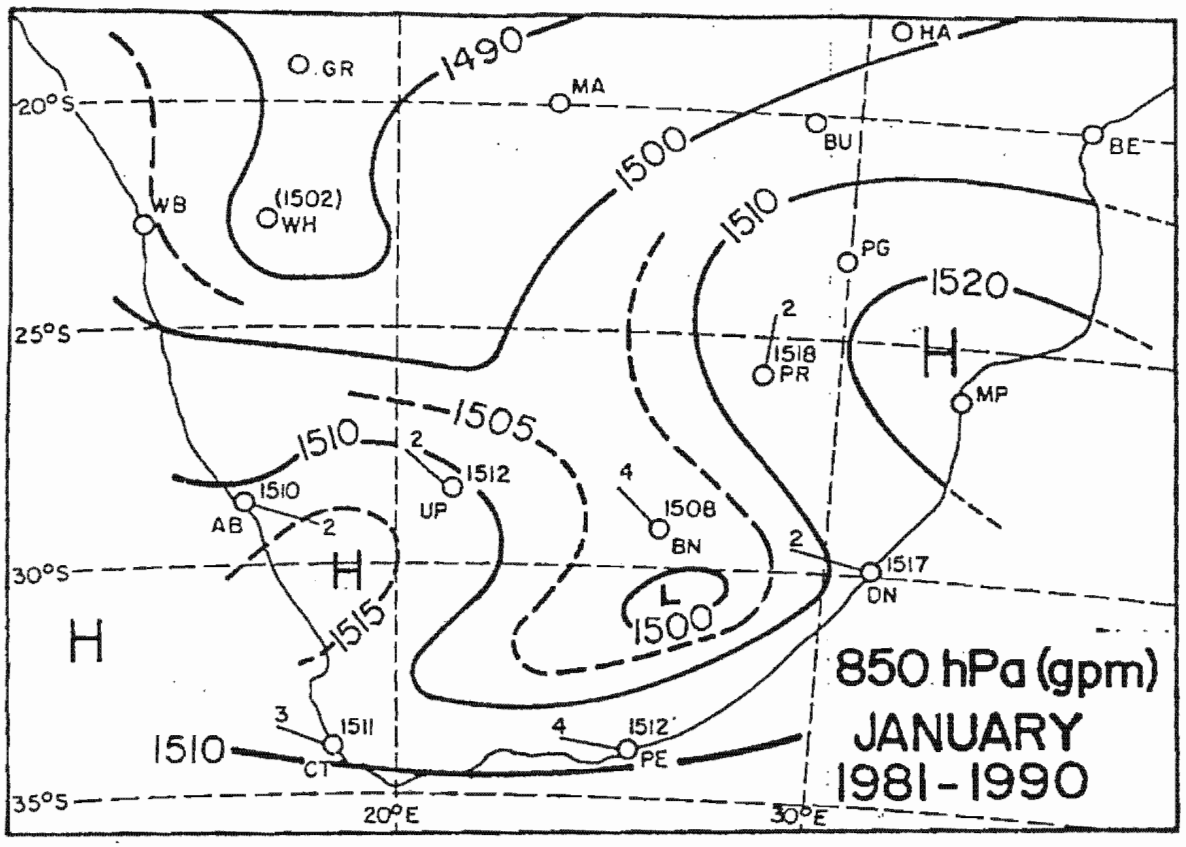

Figure 1.2. Mean 850 hPa contour charts for January for the period 1981 to 1990, based on daily grid point values (in gpm) of the 14:00 SAST synoptic maps of the South African Weather Bureau (Taljaard, 1995).

The semi-permanent ridge over the Maputo region steers the flow of moist tropical air from the Mozambique Channel westwards and then southwards towards the trough situated from the northwest to the southeast. Over the west coast the Atlantic ridge mostly imports very dry subsided air to the regions west of the trough. This is probably the main reason for high summer rainfall in the east compared to lower rainfall west of the trough. The mean 850 hPa contour patterns for each January from 1981 to 1984 were constructed (Figure 1.3.). They all have the same general circulation pattern in common but significant differences are evident. For example, in January 1981, which was a wet month, the 850 hPa heights were 20 to 25 gpm lower all over the plateau than in January 1983, when it was extremely dry. It is thus inferred that the higher 850 hPa gpm heights in general might

model is associated with ENSO and will be further discussed in section 1.3. Miron and Lindesay (1983) showed that differences in the airflow patterns between the 1971/2 to 1978/9 wet spell and 1963/4 to 1970/1 dry spell can be related to atmospheric circulation changes. High rainfall over the northern parts and interior of the country resulted from the predominance of easterly waves and development of cyclonic circulations at lower and upper levels. Dry conditions were associated with the development of high pressure cells at upper levels. Considering the period 1963 to 1979, Miron and Tyson (1984) showed that wet conditions are associated with negative anomalies of geopotential height over the continent and positive anomalies over the oceans to the southwest and south for monthly, seasonal and near-decadal scales, and vice versa during dry conditions. These changes in the pressure anomaly fields were shown to produce adjustments in the atmospheric fields of motion responsible for rain-producing conditions. Tyson (1984) showed that it is primarily variations in the atmospheric field of motion at the 500 hPa level that are responsible for year-to-year fluctuations in annual rainfall totals. Taljaard (1986a) stated that during a rainy spell, more and stronger anticyclones are present in the zone 35 to 50°S than during a dry spell. During the latter situation more than the normal number of cold fronts and low-pressure systems move along the same zone. Thus, the meridional pressure and temperature gradients, and thus the average westerly winds, are relatively weak during rainy spells and relatively strong during dry periods over the southernmost part of the subcontinent and over the zone 35 to 50°S.

Mason and Jury (1997) give a broad overview of studies on relationships between atmospheric circulation patterns and wet and dry conditions over the subcontinent. Features identifiable on average seasonal circulation maps are firstly, apart from below- or above-normal geopotential heights, latitudinal displacement of systems (Torrance, 1979; Lindesay and Jury, 1991; van den Heever, 1994; Shinoda and Kawamura, 1996). It is recognised that when the tropical convergence zones lie further north and weaken, rainfall over much of the subcontinent decreases. A second factor is the Indian Ocean Anticyclone. During dry years, the Indian Ocean Anticyclone is typically weaker than normal so that the northeasterly inflow over the east coast diminishes (Matarira, 1990; Matarira and Jury, 1992; Jury and Pathack, 1993; Hatenrath *et. al.*, 1995; Jury *et. al.*, 1992; 1995; Jury, 1996). The northeasterly inflow is an important source of atmospheric moisture throughout the summer rainfall season (D'Abreton and Lindesay, 1993; D'Abreton and Tyson, 1995). A third factor is the location

of a northwest to southeast aligned trough over the subcontinent (D'Abreton and Lindesay, 1993; van den Heever, 1994; D'Abreton and Tyson, 1995; 1996; Jury, 1996). Also, a displacement or weakening of the trough cause reduced rainfall over the subcontinent (Lyons, 1991).

1.3. An overview of the relationship between ENSO, summer rainfall in South Africa, and atmospheric circulation patterns over the subcontinent.

The relationship between summer rainfall and the Southern Oscillation was found as early as 1930 (Walker and Bliss, 1930). But only after about 50 years South Africa's full attention was captured. After the 1982/83 El Niño the importance of studying this relationship was realised. It led to increased interest in this matter (Erskine, 1983; Schulze, 1984; Alexander, 1984; Hattle and Webster, 1984; Bhalatra, 1985; Dent *et. al.*, 1987). In Schulze (1984), atmospheric circulation anomalies over South Africa during the 1982/83 rainfall season were highlighted. The summer of 1982/83 was characterised by large, negative rainfall anomalies, a severe fall in the Southern Oscillation Index (SOI) and positive sea-surface temperature anomalies in the equatorial Pacific Ocean. The eastward moving westerly disturbances to the south of the subcontinent, alternating with weak high-pressure systems, occurred further north than usual.

By comparing the month of October 1982 with those of previous years a weakening in high-pressure systems over the Pacific as well as in the trade winds over the tropical Pacific was found. Positive pressure anomalies south of the subcontinent with negative anomalies over the western parts of the Atlantic were also evident. These anomalies were caused by the fast moving lows that moved further north than usual. Van Loon and Madden (1981) found that during the low phase of the SOI, the westerlies are stronger north and weaker south of 45-50°S. The summer of 1982/83 showed the same tendency.

Previous to these studies, research on variations in South African rainfall concentrated mainly on the temporal aspects of these variations (Tyson *et al.*, 1975; Dyer and Tyson, 1978; Tyson and Dyer, 1978; Tyson, 1980), and on their spatial characteristics (Gillooly and Dyer, 1979; Lindesay, 1984). Prior to 1984, most studies to relate rainfall variability to atmospheric

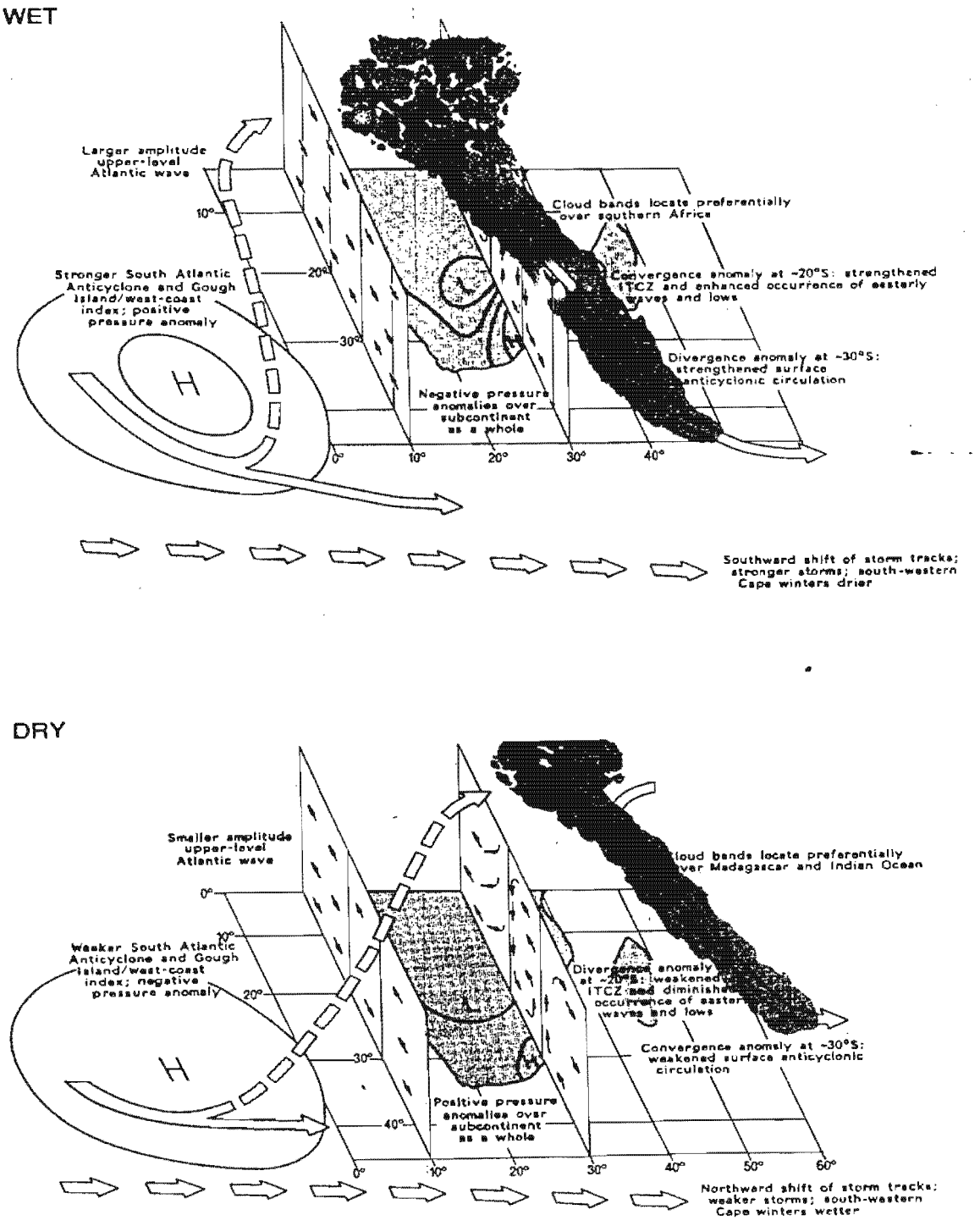

Figure 1.4. A model of the anomalous meridional circulations over southern Africa during spells of years of predominantly wet or dry conditions. The relative positions of the upper-tropospheric Atlantic wave, preferred zones for cloud-band formation, the surface manifestations of the South Atlantic Anticyclone and location of storm tracks are also shown. (Tyson, 1986)

circulation adjustments have considered circulation parameters only in the immediate vicinity of South Africa (Tyson, 1981, 1984; Miron and Lindesay, 1983; Miron and Tyson, 1984; Taljaard, 1986a; 1986b). The work of Dyer (1976, 1979) is an exception. In his work he relates the index of the latitude of the Southern Hemisphere high-pressure belt off the Australian east coast (Pittock's L index) to South African rainfall. In his research unit of 1978, 18 rainfall series of stations within a latitude belt 28°08'S to 30°25'S were investigated for relationships with Pittock's L index for the latitude of the subtropical high pressure belt and the SOI. Positive rainfall anomalies in the south were associated with negative anomalies in the north. This is meaningful since a compensatory system is likely to prevail as a result of the fluctuating movement of the Indian Ocean anticyclone. It was found that useful relationships exist between rainfall and Pittock's L index but there was no evidence to suggest that the same situation applies for the SOI.

Another exception is the work of Dyer and Tyson (1978) in which associations between inter-annual changes in the positions of the South Atlantic and South Indian Ocean anticyclones and other major components of the general circulation are shown. Both the South Atlantic and Indian Ocean anticyclones have been shown to exhibit major year-to-year variations in latitudinal position. This finding, while in itself offering no explanation of the quasi-periodic 20-year fluctuation in summer rainfall over South Africa, does suggest that detailed analysis of co-spectral changes in rainfall and annual variations in anticyclones would be worthwhile. These works, together with the work of Vines (1982), in which similarities between South American and South African rainfall spectra are shown, suggest the importance of Southern Hemisphere circulation influences on rainfall over South Africa.

Only recently has attention been given to the effects of adjustments in the Southern Hemisphere circulation on southern African rainfall and circulation parameters (Harrison, 1983, 1986; Nicholson, 1986a, 1986b, 1986c; Nicholson and Entekhabi, 1986; 1987; Tyson, 1986). The most important of these adjustments is the Southern Oscillation. Lindesay (1988) established that rainfall in the north-west to south-east aligned zone across the central summer rainfall region of South Africa is directly related to the SOI. The semi-annual cycle in the rainfall-SOI correlations is in phase with the November and February turning points of a semi-annual cycle in the atmospheric circulation patterns of South Africa. Referring again to Figure 1.4, Tyson (1986) shows that, during the high phase of the Southern Oscillation,

upper-tropospheric flow over tropical southern Africa at about 20°S becomes anomalously easterly and produces conditions conducive to cumulus convection and release of heat into easterly flow, and subsequently to the occurrence of increased rainfall over central South Africa. Other aspects of the high and low phases of the Southern Oscillation are also indicated. The low phase, in contrast to the high phase, is characterised over the subcontinent by reduced convection. This is mainly brought about by the eastward movement of the region of maximum convective activity so that cloud bands form preferentially over the Madagascar region while most of central southern Africa experiences the opposite. The effect is drier conditions over large areas of the subcontinent. Atmospheric conditions representing an eastward shift in the location of summer convection are also discussed by Harangozo and Harrison (1983), Jury and Pathack (1991,1993), Jury *et al.* (1992, 1994) and Jury (1992, 1996).

Van Heerden *et al.* (1988) emphasized that there is a strong association between warm events and negative rainfall anomalies, and between cold events and positive anomalies. During December to March a positive SOI normally coincides with negative deviations over and to the north of South Africa, with positive correlations to the south resulting in a decrease in the upper-air westerlies. The reverse is true during the negative phase of the SOI. The relationships between the SOI and December-March rainfall remained persistent since at least 1882.

Schulze (1989) reiterated the strong association between ENSO and rainfall. ENSO relates to a reinforcement or weakening in the seasonal cycle of several weather elements. This connection between ENSO and rainfall is only linear for some regions. The orientation of a region with a strong connection may differ from event to event but also between the two extreme phases of ENSO.

Mason and Lindesay (1993) found that the association between the SOI and South African rainfall variability is not stable. The SOI-South African rainfall association is modulated with the phase of the quasi-biennal oscillation in tropical stratospheric zonal winds such that high phase (low phase), wet (dry) conditions occur over the summer rainfall region in January-March. The quasi-biennal oscillation modulation only occurs when the prevalent synoptic systems over the country are of tropical origin. During the dry winter season (July-

September), this modulation and the SOI-rainfall association are inverse to the relationships in the rainfall season. Thus a wetter or drier season occurs after the SOI has been in low or high phase.

Nicholson and Kim (1996) found the strongest signs where ENSO appears to modulate rainfall are in the eastern equatorial and south-eastern Africa. The ENSO signal in the rainfall commences far to the south and propagates northward. A strong tendency exists for positive rainfall anomalies to exist during the first half of an El Niño season and negative anomalies during the second half. This agrees with cold and warm phases in the Atlantic and Indian oceans where the cold phase brings rain and the warm phase reduces rainfall. It seems that the Atlantic Ocean controls rainfall during the cold phase and the Indian Ocean controls it during the warm phase. The ENSO episodes that influence rainfall over Africa are manifested as SST fluctuations in the low-latitude Atlantic and Indian Oceans.

Other studies of note relating ENSO warm events with drought over large parts of southern Africa are Stoeckenius (1981), Mo and White (1985), Janowiak (1988), Ropelewski and Halpert (1987, 1989), Halpert and Ropelewski (1992), Main and Hewitson (1995), Moron *et. al.* (1995) and Rocha and Simmonds (1997). However, El Niño (La Niña) years are not always synchronous with dry (wet) conditions over the subcontinent, as shown by Mason and Mimmack (1992).

1.4. Aims of the study

The main emphasis of this study is to identify general relationships that possibly exist between ENSO events, atmospheric circulation anomalies and rainfall in the summer rainfall region of southern Africa. The study itself is subdivided into five sections according to chapter. In Chapter 2 the relationship between equatorial Pacific sea-surface temperatures and summer rainfall over South Africa is confirmed, but with a much larger amount of rainfall data than used in previous studies. The spatial extent of this data is sufficient to isolate regions of some relationship between the sea-surface temperatures and summer-rainfall. In Chapter 3 the first aim is to identify the main rainfall cycles existing in the summer-rainfall region, and then to compare the impacts of ENSO events on summer-rainfall during epochs of below-normal and above-normal rainfall. The associations between equatorial Pacific sea-

surface temperatures and circulation patterns over southern Africa are investigated with canonical correlation analysis in Chapter 4. The results are then also compared to general circulation model runs with observed equatorial Pacific sea-surface temperatures as boundary conditions. Further interpretation of the results of Chapter 4 is conducted in Chapter 5, with the aid of average circulation maps for different combinations of years. Chapter 6 summarises the results and reviews the value of the study.

CHAPTER 2

THE RELATIONSHIP BETWEEN EQUATORIAL PACIFIC SEA-SURFACE TEMPERATURES AND SUMMER RAINFALL

2.1. Introduction

Van Heerden *et al.* (1988) established that there is a strong association between warm events, i.e. seasons where the equatorial Pacific sea-surface temperatures are anomalously high, and negative rainfall anomalies over the summer rainfall region of South Africa. This relationship remained persistent since at least 1882. Lindesay (1988) found that rainfall in a north-west to south-east aligned zone across the central summer rainfall region of South Africa is directly related to the SOI. In the above study it was also inferred from statistical results, that there are much more significant and spatially coherent correlations between El Niño-Southern Oscillation and South African rainfall for the late-summer season (January to March) than for the early-summer season (October to November). It is attempted, with a much larger previously unavailable data set, to shed more clarity on this issue, by finding more exact regions of correlation between South African early- and late-summer rainfall and equatorial Pacific sea-surface temperatures.

2.2. Data

To investigate the correlation between equatorial Pacific sea-surface temperatures and summer rainfall over South Africa, two data-sets are needed. The first data set acquired is monthly time series of 510 rainfall stations, spatially well distributed throughout South Africa. The spatial distribution of these stations are depicted in Figure 2.1. This data-set, consisting of a climate period from 1930 to 1995, i.e. a total of 66 years, is described by Kruger (1996).

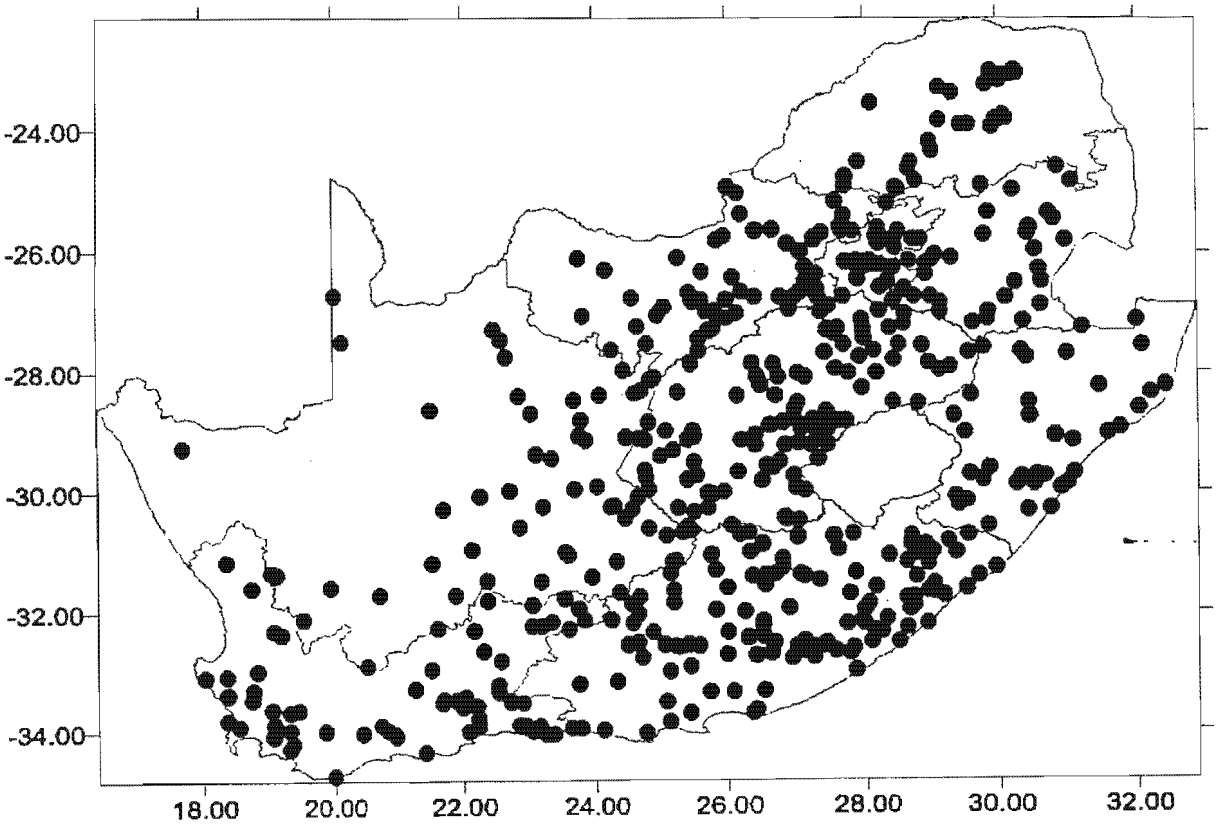

Figure 2.1. Spatial distribution of rainfall stations used in the test for correlation between NINO3 SST's and summer rainfall in South Africa.

The second data-set required, that for equatorial Pacific sea-surface temperatures, was obtained from the Climate Prediction Center (CPC) at the National Oceanic and Atmospheric Administration (NOAA). This data-set consists of average monthly observed sea-surface temperatures for the NINO3 region, an area in the Pacific Ocean between longitudes 150 and 90°W, and latitudes 5°N and 5°S, shown in Figure 2.2.

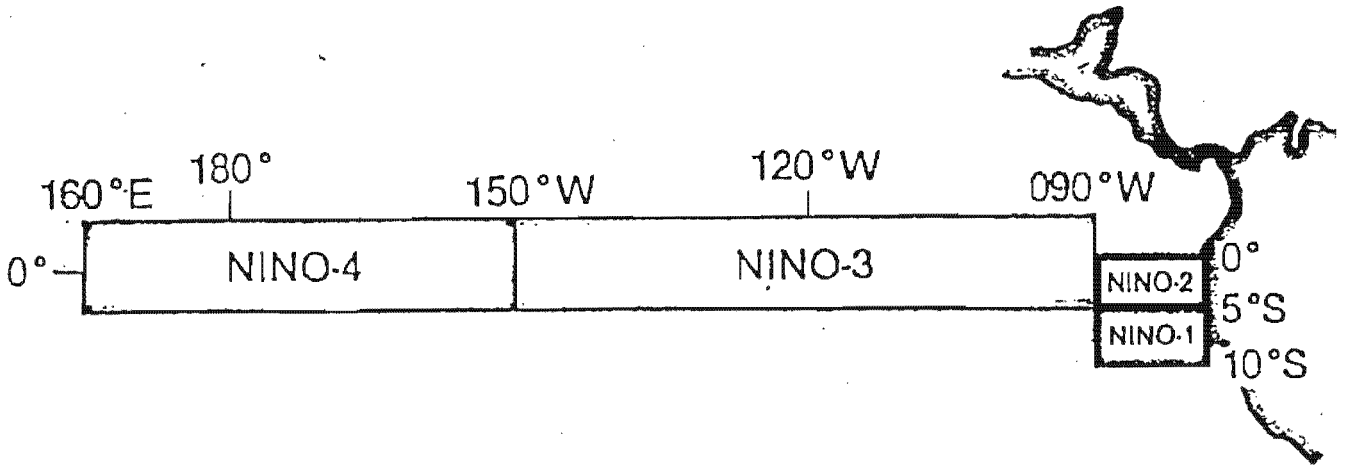

Figure 2.2. The extent of the NINO1 to NINO4 regions in the equatorial Pacific Ocean (Reynolds, 1988).

2.3. Methods

From each time series of the 510 rainfall stations, two series were constructed, for the total rainfall for October to December (OND) and the total rainfall for January to March (JFM), which then represents rainfall time series for the early and late rainfall season respectively. By the use of a much larger data set than Lindesay (1988) (510 compared to 60 rainfall stations), it is thought that more exact regions of correlation than the mentioned study can be found.

The OND- and JFM-rainfall time series were then separately tested for correlation with the sea-surface temperature (SST) time-series in the NINO3 region of the Pacific Ocean at zero lag. A test for no correlation was applied to the data. To briefly explain the test, let (X_i,Y_i), $i=1,...,n$ be a sample of size n from a bivariate normal distribution, and let R be the correlation coefficient between the two samples. If $\rho=0$, then the statistic

$$T = \frac{\sqrt{(n-2)}}{\sqrt{(1-R^2)}} * R$$

is distributed as Student's t-distribution with (n-2) degrees of freedom. We use this result to test the hypothesis

H_0: $\rho=0$ against

H_1: $\rho\neq 0$

If $t=t_{½\alpha\ ;n-2}$ then it can be proven with simple mathematical manipulation that we can accept H_0 if

$$|R| < \frac{t}{\sqrt{n-2+t^2}}$$

In this case, the test was modified by using $t=t_{\alpha;n-2}$, using the statistic

$$|R| < -\frac{t}{\sqrt{n-2+t^2}}$$

to test for negative correlation and the statistic

$$|R| > \frac{t}{\sqrt{n-2+t^2}}$$

to test for positive correlation. The test was performed at a 95 % level of confidence to isolate areas with no correlation, positive correlation, or negative correlation between NINO3 SST's and early- or late-summer rainfall.

2.4. Analyses and results

The above tests were applied to all 510 stations, and the results transformed to a grid using the kriging method, and then analysed. The analyses for early-season and late-season are shown in Figure 2.3(a) and (b) respectively, which shows areas of correlation between the NINO3 sea-surface temperatures and the rainfall for the specific season, positive or negative.

From figure 2.3(a) it can be seen that, for the major part of South Africa, only coherent patterns

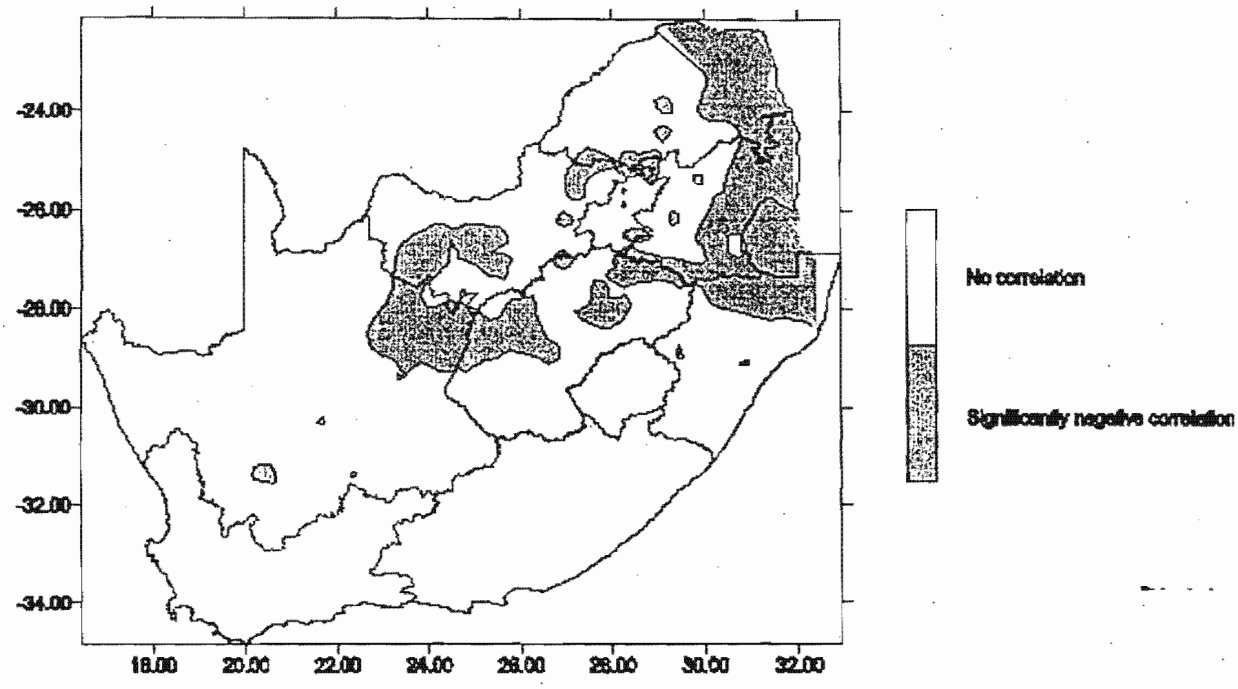

Figure 2.3(a). Analysis of correlations between NINO3 sea-surface temperatures and total rainfall for the period October to December (5% level).

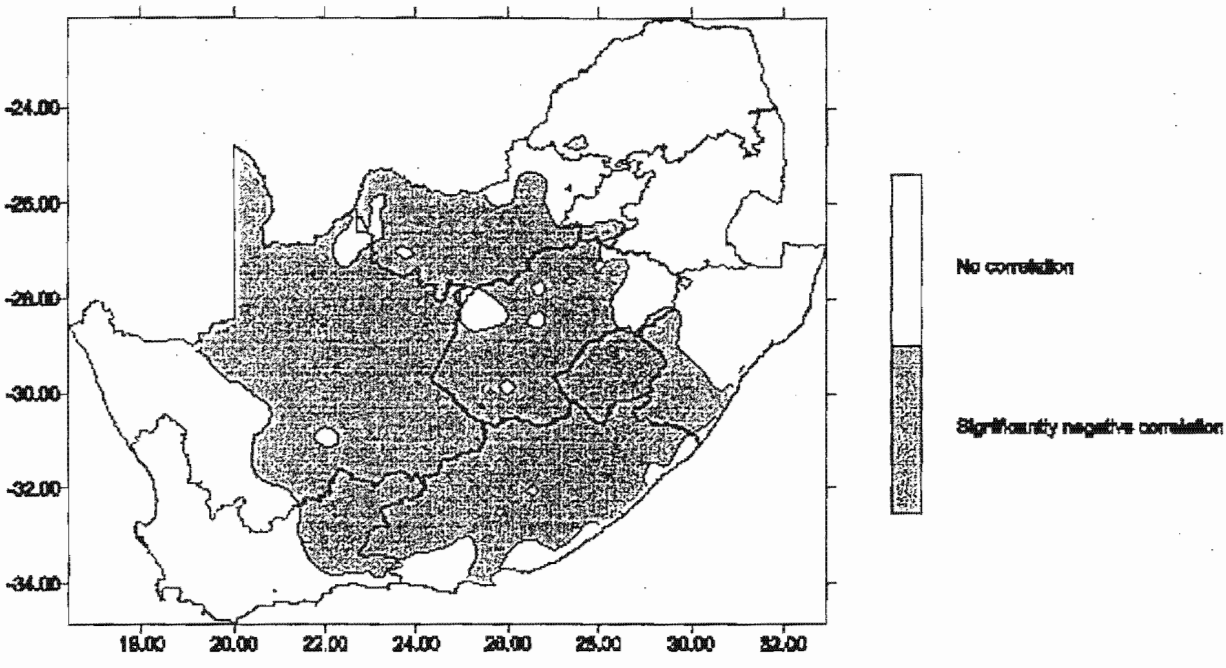

Figure 2.3(b). The same as (a), except for the period January to March

of negative correlation, i.e. positive sea-surface temperature anomalies correlate with negative rainfall anomalies and vice versa, exists in the far north-eastern regions between the NINO3 sea-surface temperatures and early-summer rainfall, but this is probably only a result of the kriging procedure, as there are no stations over most of the area (see Figure 2.1).

In contrast with the findings in Figure 2.3(a), Figure 2.3(b) shows that, for late-summer rainfall, the area of correlation is spatially more coherent and therefore more realistic. This area covers almost the whole of South Africa, except for the winter-rainfall and all-year rainfall regions in the west, as well as the north-eastern regions. From the figure it is interesting to note that there exists almost no correlation between NINO3 sea-surface temperatures and late -summer rainfall over the Northern Province, northern Gauteng, Mpumalanga and northern KwaZulu-Natal provinces, although the regions receive predominantly summer rainfall.

To simplify the study, only the late-summer rainfall season will further be considered and only regions with areas which correlate with NINO3 sea-surface temperatures (and thus directly with ENSO), as depicted in Figure 2.3(b).

CHAPTER 3

THE INFLUENCE OF THE INTER-DECADAL VARIABILITY OF LATE-SUMMER RAINFALL ON THE IMPACT OF EL NIÑO AND LA NIÑA EVENTS

3.1. Introduction

In Chapter 2 it was confirmed that late-summer rainfall over a large area is associated with ENSO. This chapter attempts to shed more clarity on the question of the variability of the impact of El Niño and La Niña events on the late-summer rainfall of South Africa.

Although the El Niño phenomenon is associated with below-normal late-summer rainfall over the summer rainfall region of South Africa in the majority of events, it is also apparent that it cannot be assumed that the summer rainfall region of South Africa will always experience below-normal rainfall during an El Niño event and vice versa during a La Niña event. Historically, seasonal amounts for a specific region differed considerably from one event to the other. The 1997/98 rainfall season is a good example where even above normal rainfall was experienced over certain regions of the summer-rainfall region of South Africa during an El Niño event, opposite to the general tendency.

Another aspect to recognise, for which there are no explanations in terms of the general rainfall tendency during El Niño and La Niña events, is that there are seasons where an El Niño event has not occurred, where much below normal rainfall was experienced over the summer rainfall region, and also seasons with much above normal rainfall, without the simultaneous occurrence of a La Niña event. This reiterates the fact that the occurrence of anomalously high or low late summer rainfall is not solely dependent on occurrences of El Niño or La Niña events.

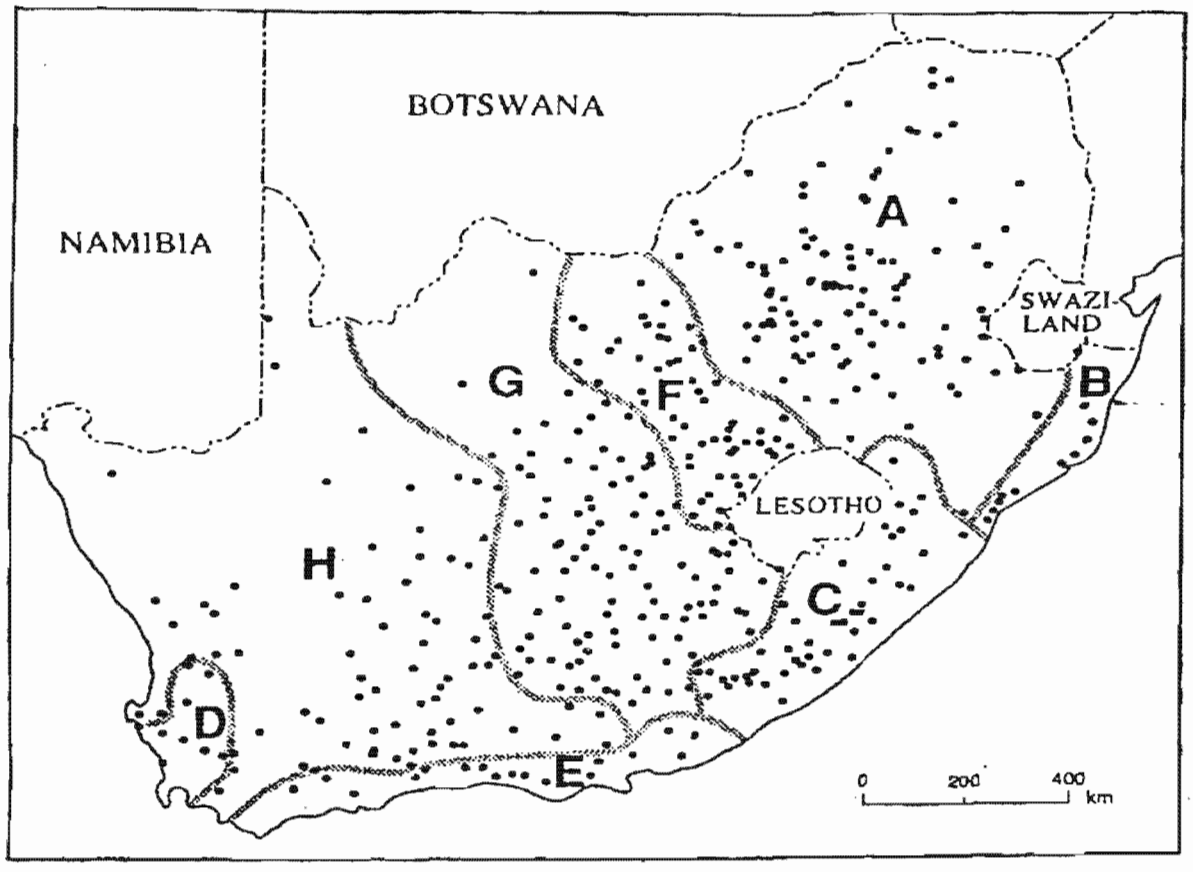

Figure 3.1. Geographical distribution of stations used and the eight homogeneous rainfall regions (Landman and Mason, 1999).

3.2. Data

A monthly rainfall data set, consisting of data for 418 stations for the period 1950 to 1996, was used to obtain a single time series for eight homogeneous rainfall regions in South Africa The methods to obtain this data set are described by Landman and Mason (1999). Figure3.1, obtained from Landman and Mason (1999), shows the geographical distribution of the rainfall stations and the eight homogeneous rainfall regions.

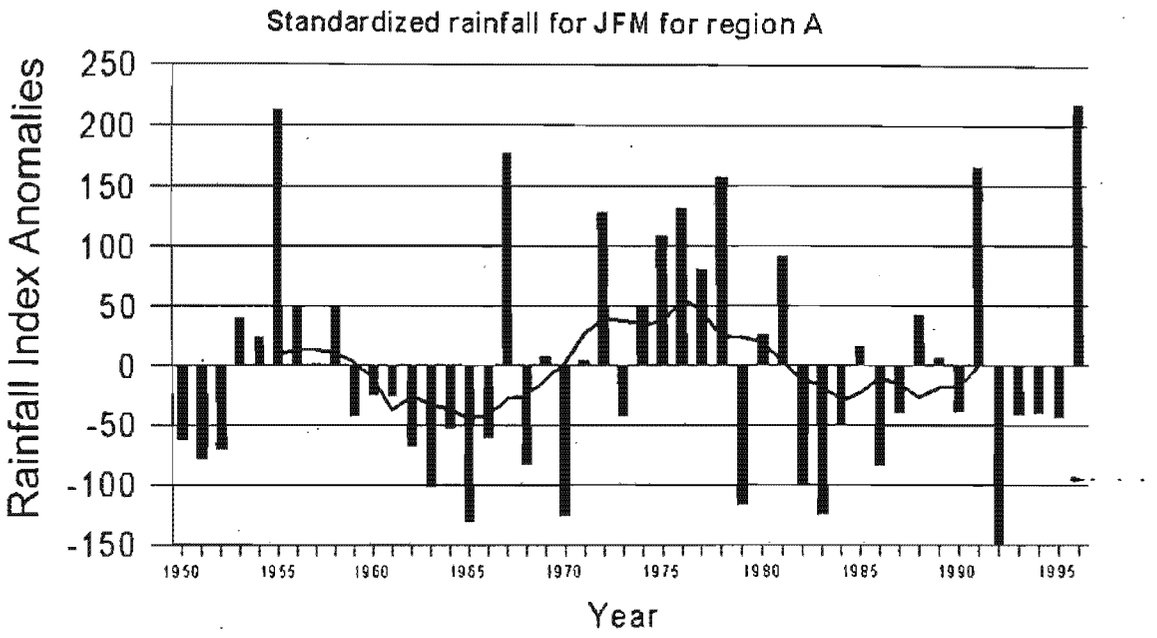

Figure 3.2(a). Standardized total rainfall for January to March for region A (Figure 3.1). The solid line depicts the 11-year running mean for the time series.

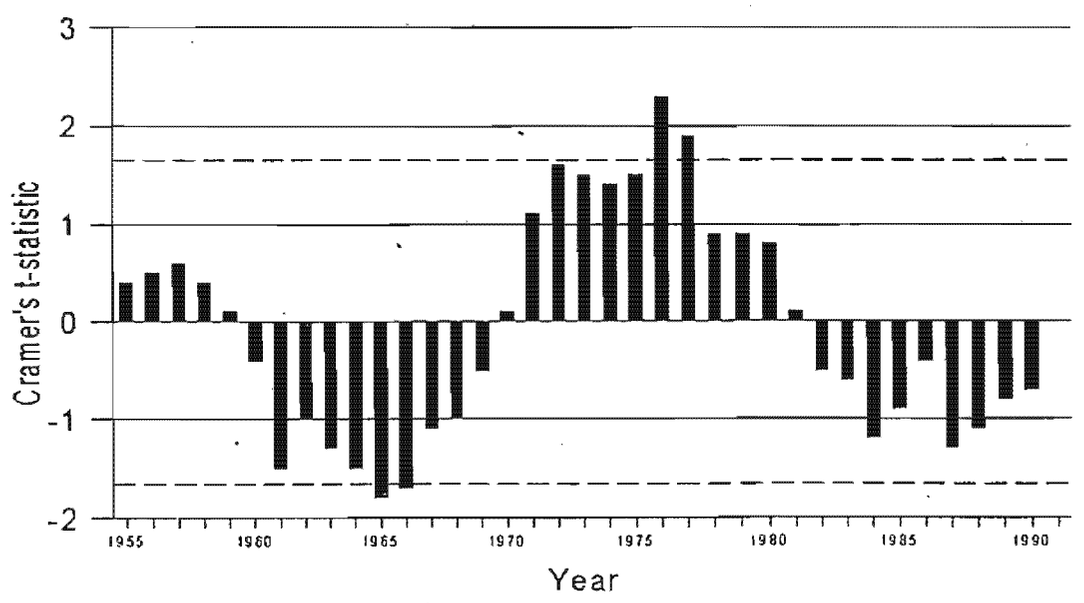

Figure 3.2(b). Cramer's t-statistic (11-year mean) for region A in Figure 1. The year indicates the centre year used in the statistical analysis.

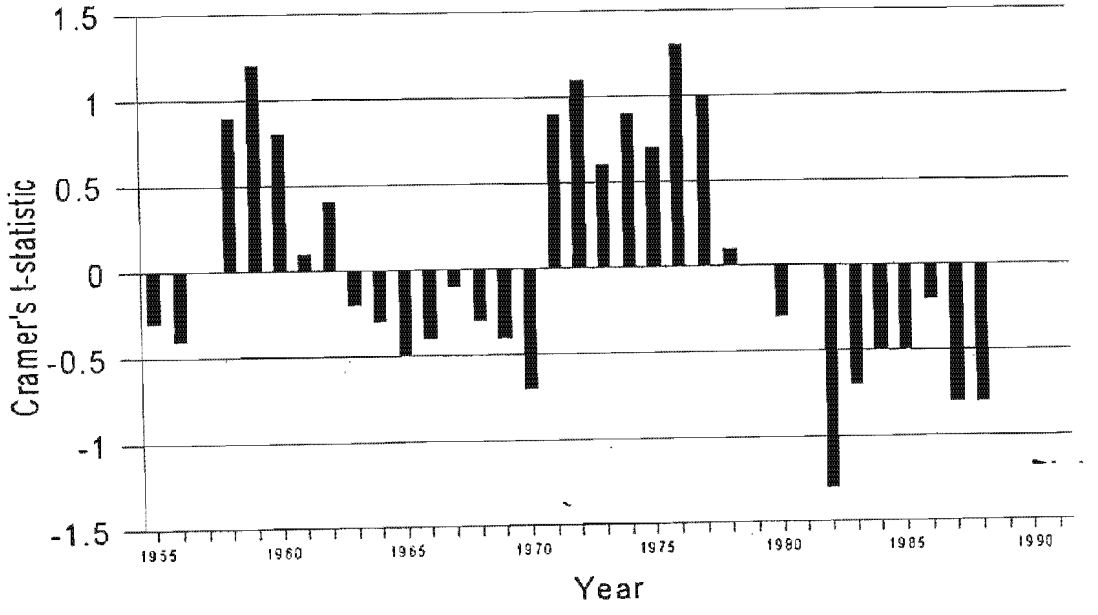

Figure 3.3. The same as Figure 3.2(b), but for region C.

the period 1955 to 1991, are depicted in Figure 3.2(b). Easily recognizable are the epochs of above- and below-normal rainfall with a period of about 20 years. The same test was applied to regions which show some correlation with the NINO3 SST time-series, namely C, F, G and H in Figure 3.1. The results, which are similar to that of region A, are shown in Figures 3.3 to 3.6.

By inspecting Figures 3.2(b) to 3.6, it is clear that the 1960's and 1980's are characterized by below normal rainfall, and the 1970's by above normal rainfall. The part of the 1950's that was part of the calculation also shows signs of above-normal rainfall. By applying the method of cumulative deviations, turning points between epochs of above-normal and below-normal rainfall, and vice versa, are found to be around 1959/1960, 1969/70, 1981/82 for regions A and H, 1980/81 for regions C, F and G, and 1991/1992. For conformity 1959/60,1969/70, 1980/81 and 1991/92 are chosen as the turning points.

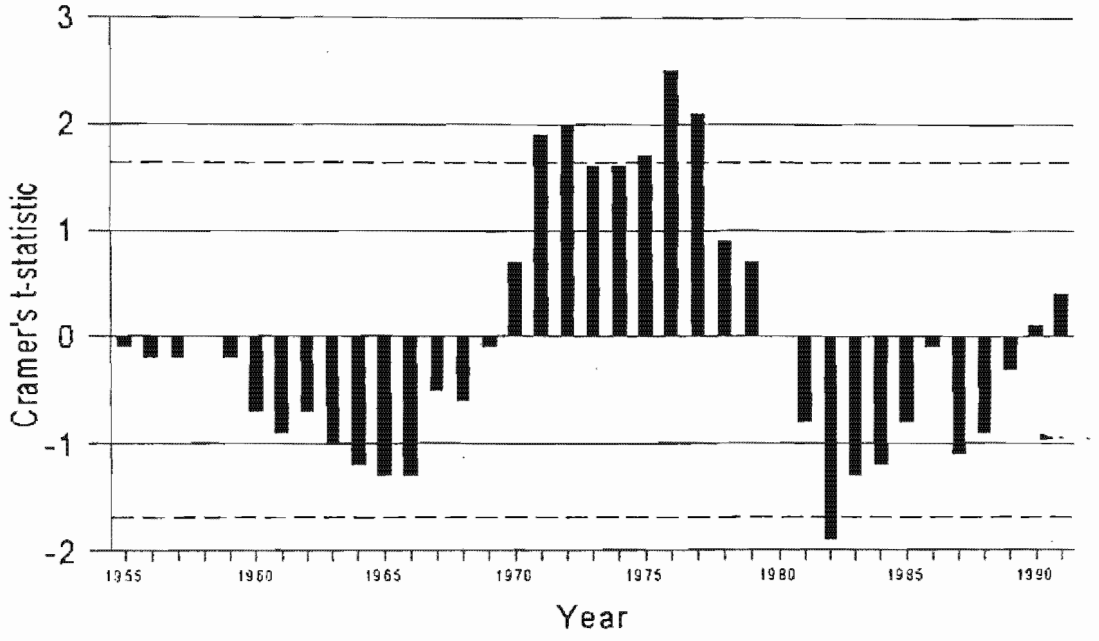

Figure 3.4. The same as Figure 3.2 (b), but for region F.

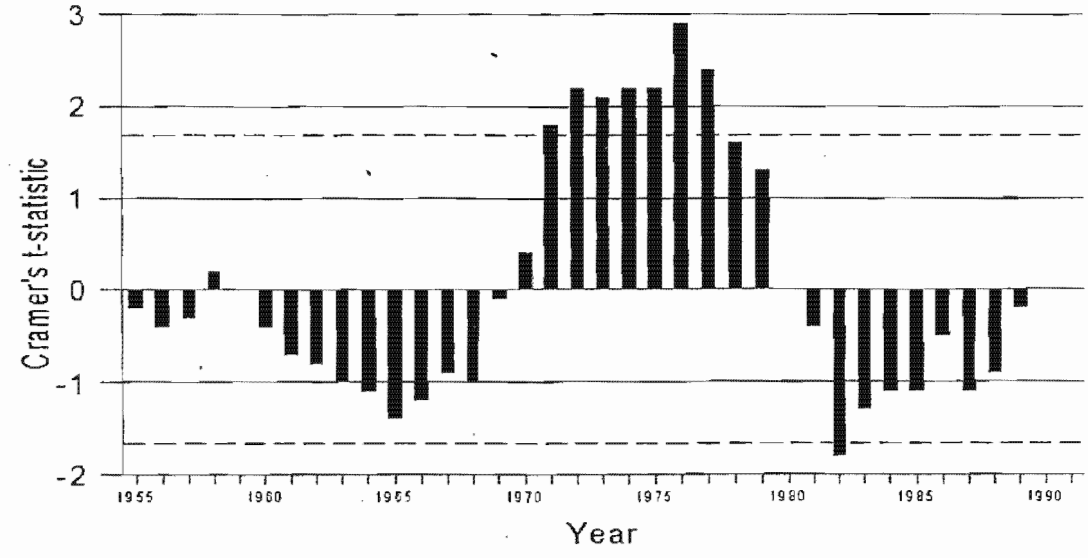

Figure 3.5. The same as Figure 3.2(b), but for region G.

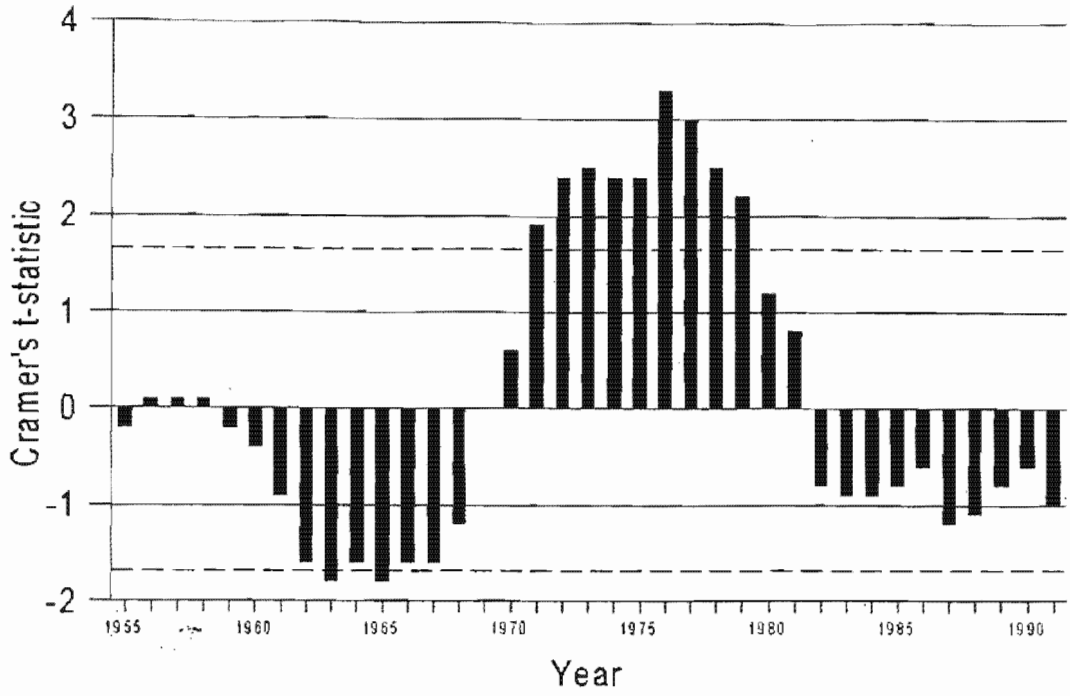

Figure 3.6. The same as Figure 3.2(b), but for region H.

3.3.2. El Niño/La Niña events and late summer rainfall

During the period 1950 to 1997, a total of 11 El Niño events and 10 La Niña events occurred, according to the index of the Japan Meteorological Agency, which is based on a five-month running mean of spatially averaged SST anomalies over the tropical Pacific Ocean: 4°S to 4°N, 150°W to 90°W. If index values are 0.5°C or greater for six consecutive months, the year of October through the following September is categorized as El Niño (with index values equal or exceeding 0.5°C), La Niña (index values equal or lower than –0.5°C), or neutral. The late summer rainfall anomalies associated with each of these events for regions A, C, F, G and H, which are affected in some degree by El Niño/La Niña, is given in Table 3.1(a) and (b). The average values of the average figures in Table 3.1(a) and (b) are –38.7 and 51.9 respectively, which differ significantly from each other at the 95 % confidence level. The method of determining this is fully described by Panofsky and Brier (1958). To test

whether the inter-decadal behaviour, described previously, is forced partly by El Niño/La Niña events, regression analysis was performed using average late summer NINO3 SST's and late summer rainfall for each of the above regions. Differences were taken between the predicted and observed rainfall values, which gave an estimation of the rainfall time series excluding the linear influence of NINO3 SST's. An example is given for region F in Figure 3.7. By calculating 11-year running means, similar periods of above- and below-normal rainfall that was observed before the exclusion of the NINO3 influences were still clear.

Table 3.1(a). Seasons of El Niño and associated rainfall index anomalies over regions A, C, F, G and H during the late summer rainfall season.

	Year										
Region	1952	1958	1964	1966	1970	1973	1977	1983	1987	1988	1992
A	-70.4	10.3	-52.4	-60.5	-125.9	-42.1	80.2	-124.1	-39.2	41.7	-148.6
C	-22.5	14.9	20.9	-66.8	-100.0	-2.5	-23.5	-151.7	-49.0	118.7	-93.0
F	-31.5	-5.8	-73.2	4.7	-90.6	-57.0	40.3	-135.3	-73.2	186.0	-163.0
G	-32.1	3.5	-99.1	-27.4	-103.9	-11.3	45.9	-107.6	-83.8	149.0	-102.9
H	-7.7	-71.8	-94.2	-72.6	-92.4	10.4	34.8	-28.8	-103.8	11.8	-60.1
Average	-32.8	-9.8	-59.6	-44.5	-102.6	-20.5	35.5	-109.5	-69.8	101.4	-113.5

Table 3.1(b). Seasons of La Niña and associated rainfall index anomalies over regions A, C, F, G and H during the late summer rainfall season.

	Year									
Region	1955	1956	1957	1965	1968	1971	1972	1974	1976	1989
A	212.6	49.6	0.8	-130.5	-82.4	3.7	127.4	50.0	130.9	5.8
C	85.4	0.9	17.2	-103.9	-118.7	-9.7	62.2	164.9	251.8	-5.6
F	61.4	97.2	-22.2	-95.2	-83.4	-11.7	153.8	152.2	190.3	66.9
G	59.2	20.4	-28.9	-95.0	-76.2	1.4	65.0	309.6	235.4	44.9
H	58.2	136.6	2.4	-13.0	-40.6	-25.9	83.2	313.4	298.3	22.5
Average	95.4	60.9	-6.1	-87.5	-80.3	-8.4	98.3	198.0	221.3	26.9

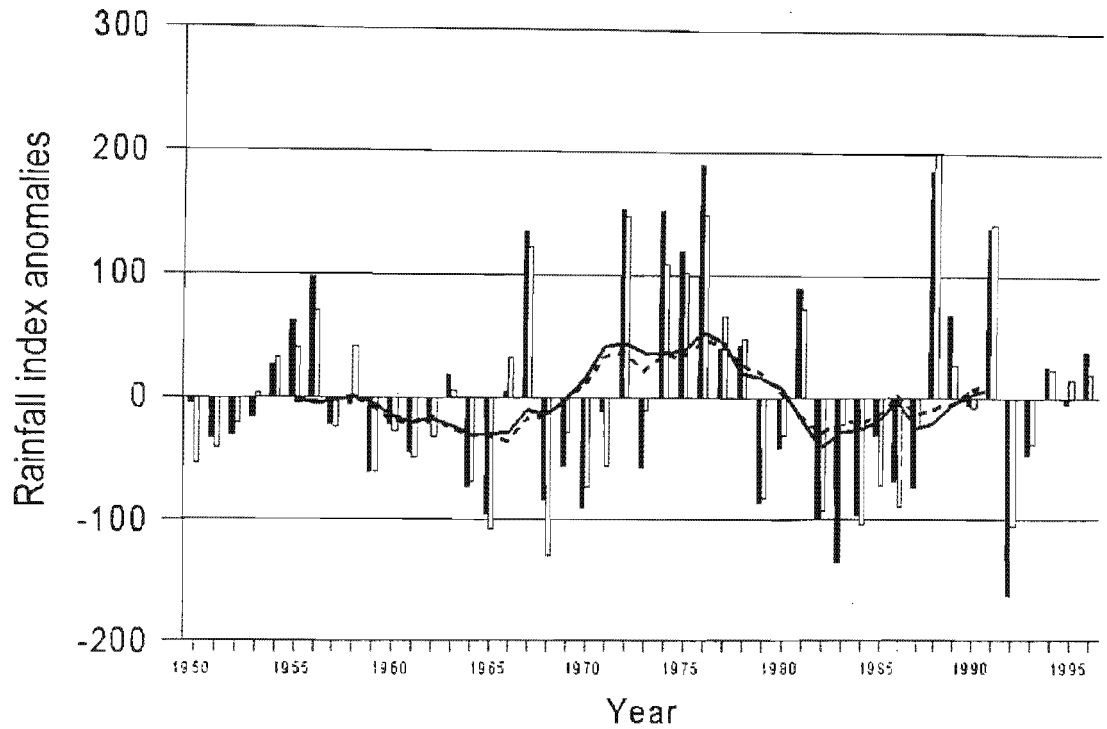

Figure 3.7. Late summer rainfall anomalies for region F (black bars) and anomalies with the effects of NINO3 SST's removed (white bars). The solid line depicts the 5-year running mean for the standardized late-summer rainfall anomalies and the broken line depicts the 5-year running mean for the anomalies with the effects of NINO3 SST's removed.

3.3.3. Epochal variability and the impact of El Niño/La Niña

To assess whether the impact of El Niño/La Niña events on late summer rainfall was influenced by the epochal variability of the rainfall, the late summer rainfall totals of regions A, C, F, G and H were compared with high and low epochs in rainfall for the nine El Niño seasons as well as the 10 La Niña seasons during the period 1955 to 1991, for which

Cramer's t-statistic and turning points could be calculated. The results are shown in Table 3.2(a) and (b) for the El Niño and La Niña seasons respectively.

Table 3.2(a). Seasons of El Niño events and associated rainfall over regions A, C, F, G and H during the late summer rainfall season. R indicates rainfall, E epoch, A above the normal value, B below the normal value, - below normal epoch, and + above normal epoch.

	Year								
Region	1958	1964	1966	1970	1973	1977	1983	1987	1988
	R/E	R/E	R/E	R/E	R/E	R/E	R/E	R/E	R/E
A	A/+	B/-	B/-	B/-	B/+	A/+	B/-	B/-	A/-
C	A/+	A/-	B/-	B/-	B/+	B/+	B/-	B/-	A/-
F	B/+	B/-	A/-	B/-	B/+	A/+	B/-	B/-	A/-
G	A/+	B/-	B/-	B/-	B/+	A/+	B/-	B/-	A/-
H	B/+	B/-	B/-	B/-	A/+	A/+	B/-	B/-	A/-

Table 3.2(b). The same as Table 3.2(a), but only for seasons of La Niña events.

	Year									
Region	1955	1956	1957	1965	1968	1971	1972	1974	1976	1989
	R/E	R/E	R/E	R/E	R/E	R/E	R/E	R/E	R/E	R/E
A	A/+	A/+	A/+	B/-	B/-	A/+	A/+	A/+	A/+	A/-
C	A/+	A/+	A/+	B/-	B/-	B/+	A/+	A/+	A/+	B/-
F	A/+	A/+	B/+	B/-	B/-	B/+	A/+	A/+	A/+	A/-
G	A/+	A/+	B/+	B/-	B/-	A/+	A/+	A/+	A/+	A/-
H	A/+	A/+	A/+	B/-	B/-	B/+	A/+	A/+	A/+	A/-

From Table 3.2(a) it is evident that there is a remarkable association between rainfall and type of epoch regardless of the fact that only El Niño events were taken in consideration. Below normal rainfall was experienced during epochs of below normal rainfall and vice versa except for a minority of cases; i. e. 14 out of 45 cases. A peculiar season in this regard is the 1988 season, with above-normal rainfall in all the regions, regardless of the fact that 1988 fell in the below-normal epoch from 1980/81 to 1991/92. Table 3.2(b) shows similar results with below-normal rainfall during epochs of below-normal rainfall and vice versa. On the whole, only nine out of 50 cases did not show this association.

To conclude the analysis, the average rainfall anomalies for late summer was calculated separately for the El Niño and La Niña seasons during above- and below-normal epochs during the period 1950 to 1996 respectively for regions A, C, F, G and H. The results are shown in Table 3.3, from which we can see that during an El Niño season during a below-normal epoch, the lowest average rainfall was experienced and when a La Niña season during an above normal epoch occurred, the highest average rainfall was experienced in general. The difference between the averages of El Niños during above-normal epochs to El Niños during below-normal epochs is significant at the 99 % confidence level. The same level of significance was found in the difference between the averages of La Niñas during above-normal epochs and La Niñas during below-normal epochs. Regardless of an El Niño or La Niña season, on average, rainfall above the normal value was experienced during epochs of above-normal rainfall and rainfall below the normal value was experienced during epochs of below-normal rainfall.

Table 3.3. Average late summer rainfall index anomalies, calculated separately for El Niño and La Niña seasons during epochs of above and below normal rainfall for regions A, C, F, G and H.

Region	El Niño-above normal epoch	El Niño-below normal epoch	La Niña-above normal epoch	La Niña-below normal epoch
A	16.0	-60.1	82.1	-69.0
C	-3.7	-38.0	81.8	-76.1
F	-7.5	-30.3	88.7	-37.2
G	12.7	-45.5	94.6	-42.1
H	-8.9	-63.3	123.7	-10.4
Average	1.7	-47.4	94.2	-47.0

3.4. Conclusions

In this chapter, it was acknowledged and further confirmed that there are non-random epochs of above- and below-normal rainfall. These epochs of above and below-normal rainfall between 1955 and 1991 as well as the turning points between epochs were established using Cramer's t-statistic for an 11-year moving average, as well as cumulative deviations. It seems that the epochal behaviour is not forced by the frequencies of El Niño and La Niña events. This was also concluded by Kripalani and Kulkarni (1997a, 1997b), in their study of Indian monsoon rainfall. The epochs in turn influence the impact of El Niño and La Niña events in such a way that during an epoch of above-normal rainfall a moderating influence is evident on the severity of El Niño events so that even rainfall above the normal value is experienced during such events. The opposite is also true in that an epoch of below-normal rainfall will have a negative effect on the enhancement of rainfall usually experienced during a La Niña event.

It also seems that extreme events of rainfall usually occur when an El Niño occurs during an epoch of below-normal rainfall, e. g. the 1982/83 season, and also when a La Niña occurs during an epoch of above-normal rainfall, e. g. the 1975/76 season. See Figure 3.7 in the case for region F.

During the 1990's, it was evident that seasons associated with El Niño, except for 1992, were not as severe as during the 1980's. The impacts of further El Niño events during the 1990's, e. g. during the 1997/98 season, could thus be moderated, as was the case. If 1991/92 is assumed to be a turning point from below- to above-normal rainfall, and that an epoch of above- or below-normal rainfall persists for more or less a decade. It is, however, uncertain when the next turning point will be. These findings will be utilised in further chapters.

CHAPTER 4

ASSOCIATIONS BETWEEN EQUATORIAL PACIFIC SEA-SURFACE TEMPERATURES AND CIRCULATION PATTERNS OVER SOUTHERN AFRICA

4.1. Introduction

In this chapter it is attempted to identify relationships between equatorial Pacific SST's and circulation patterns over Southern Africa. The effect of these relationships on the average circulation will then be discussed in Chapter 5. In the light of the inter-decadal variability in the strength of the association between ENSO and South African summer rainfall, this study cannot be approached in a simplistic manner. It will rather be assumed that the relationship studied is of the same complexity as the relationship between the equatorial Pacific SST's and rainfall, although some general relationships might also exist.

Different statistical methods are available to investigate such a potential relationship. Because of the probable complexity of such a relationship, it was decided that canonical correlation analysis is the most appropriate method. Canonical correlation analysis (CCA) is at the top of the hierarchy of regression modelling approaches (Barnett and Preisendorfer, 1987), as it is the generalization of the approaches of simple regression, multiple regression and stepwise multiple regression. CCA was applied to different combinations of data-sets, some based on the findings in Chapter 3, to find the most possible relationships that might exist between equatorial Pacific SST's and atmospheric circulation over Southern Africa. In section 4.5, comparisons are made between the CCA results and available climate model runs.

4.2. Data

Following the approach of Barnett and Preisendorfer (1987), predictor data are first defined, in this case data representing equatorial SST's. Global Ocean Global Atmosphere (GOGA)

SST data (Pan and Oort, 1990, Lau and Nath, 1994) of the region 120°E to 80° W and 15°S to 15°N, in the equatorial Pacific Ocean were used. This data set has a resolution of 4.5° by 7.5° latitude-longitude, and was obtained for the period 1958 to 1985. Blended (Reynolds, 1988) and Optimum Interpolation (OI) SST data (Reynolds and Smith, 1994) have been obtained for the period 1985 to 1997. Both the blended (2° latitude-longitude) and the OI data (1° latitude-longitude) are interpolated to the GOGA grid, using cubic interpolation.

The predictand data should be data with which it is possible to detect deviations from the average atmospheric circulation patterns at significant pressure levels. Here it is thought that geopotential height fields for 1000hPa and 500hPa respectively for the region from the Greenwich meridian to 50°E, and from 45°S to 15°S latitude are sufficient to detect possible general relationships between equatorial Pacific SST's and atmospheric circulation patterns over Southern Africa. South Africa is situated in the subtropical high pressure belt, and the strength and movement of these anticyclones at the surface, more or less the 1000 hPa level, are a major control of the weather over the subcontinent (Taljaard, 1994). In the upper-air, the position and strength of troughs at the 500 hPa level also account for the favourability of rainfall or not, particularly when there is a simultaneous supply of moisture in the lower levels (Taljaard, 1986b). Because it was previously decided in Chapter 2 that the study will only focus on the latter half of the rainfall season, only three-monthly averaged (January to March) NCEP reanalysis data for the period 1958 to 1997 (40 years) were obtained for analysis. The data thus chosen covered the above region on a 2.5° × 2.5° grid. i. e. 273 grid points in the region studied.

4.3. Methods

With SST data the predictor data and the geopotential height fields the predictand data, CCA finds the optimum linear combination between the predictor and predictand fields. Both predictor and predictands are full multidimensional vectors of information. Coordinate systems are defined that optimally describe the cross covariance between two different data sets. This is expressed as an eigenvalue problem. Eigenstructure is obtained from the cross product of the cross covariance matrix between two data sets and its transpose. Since this product matrix describes the hindcast skill, its

eigenstructure maximises the skill. The resulting eigenvalues are called canonical correlation coefficients and represent the levels of correlation between patterns of predictor variables and patterns of predictand variables.

The predictor and predictand fields, **Y** and **T** respectively, can now be represented by linear combinations of their canonical component vectors:

$$Y(x,t) = \sum_{j=1}^{p} u_j(t) g_j(x)$$

and

$$T(x',t) = \sum_{k=1}^{q} v_k(t) h_k(x')$$

where u_j and v_k are the desired canonical component vectors. We define

$$h_k(x') = \langle Y(x',t) v_k(t) \rangle_t$$

$$g_j(x) = \langle Y(x,t) u_j(t) \rangle_t$$

where h_k and g_j are the canonical maps which are vectors whose components show the correlation at a specific location (x or x') between **Y** or **T** and their respective canonical component time series (j or k).

Six different combinations of years of the data-fields, at both 1000 hPa and 500 hPa respectively, were used as predictand data sets. Thus, a total of 12 different predictand data sets were constructed for the analysis. The years used for the different combinations, taking into account the results of Chapter 3 of the below- and above-normal rainfall cycle, are as follows:

a) All (40 years)
b) ENSO (17 years)
c) El Niño (10 years)
d) La Niña (7 years)
e) ENSO occurring during above normal years in the rainfall cycle (see Chapter 3) (8 years)
f) ENSO occurring during below normal years in the rainfall cycle (see Chapter 3) (9 years)

Associations between equatorial Pacific SST's and circulation patterns for only El Niño seasons (c) can, for example, be used to make intercomparisons between these seasons on the basis of anomalous SST's in the equatorial Pacific Ocean. Relatively higher or lower SST's

during El Niño seasons can then be associated with different circulation patterns over the subcontinent. The same applies to (d) in the case of La Niña years.

Referring to Chapter 3, the existence of an inter-decadal rainfall cycle in the summer rainfall region of South Africa was identified. In sections 4.4.9 and 4.4.10, possible associations between extreme equatorial Pacific SST's, only during ENSO years, and 1000 or 500 hPa heights during the above-normal part of the rainfall cycle are investigated. In sections 4.4.11 and 4.4.12, the same is done, but for the below-normal part of the decadal rainfall cycle.

4.4. Results

The results of the analyses are given in the same order ((a) to (f)) as above; first the 1000 hPa level and then the 500 hPa level for each combination of years, e. g. only ENSO years. Graphs of the predictor and predictand vectors on the same coordinate system with accompanying G-maps and H-maps are shown for modes of each combination, depending whether the correlation between the predictor and predictand vectors are significant (see Table 4.1.), and meaningful. By investigating the temporal variability of the canonical coefficients and the spatial patterns, inferences about the nature of ocean-atmosphere interactions that contribute to anomalous atmospheric circulation conditions over the subcontinent can be drawn.

4.4.1. All years (1000 hPa)

The correlation obtained between the first canonical vectors was significant at the 95% level of confidence. By investigating the temporal variability of the canonical coefficients (Figure 4.1.) and the spatial patterns (Figures 4.2. and 4.3.), we see that if SST's in the equatorial Pacific Ocean are anomalously high (low), it can be associated with anomalously high (low) 1000 hPa heights over the whole subcontinent and surrounding oceans. A similar association can be inferred from the second mode (Figures 4.4. to 4.6.), which also has a significant correlation between the predictor and predictand vectors. Here it can be seen that anomalously high (low) SST's are associated with anomalously high (low) 1000 hPa heights over the western half of the subcontinent with a maximum over the adjacent ocean. The opposite association is found over the southern and especially the south-eastern ocean areas.

The above indicates a strengthening (weakening) of high-pressure synoptic systems in the west (east) and vice versa for low-pressure synoptic systems at the surface, e. g. high pressure systems west of the subcontinent will be stronger than usual, and will ridge in stronger from the west or south-west.

Table 4.1. Least values for correlation coefficients to be significant at the 5 % level of confidence for different data series lengths N (n = N-2, the degrees of freedom).

n	r
5	0.830
6	0.775
7	0.727
8	0.686
9	0.650
10	0.619
12	0.568
14	0.527
16	0.493
18	0.466
20	0.442
22	0.421
24	0.403
26	0.387
30	0.361
40	0.312

4.4.2. All years (500 hPa)

The correlations between the canonical vectors were significant for both the first mode and the second mode. From the graphs and maps for the first mode (Figures 4.7 to 4.9) it can be seen that there is, similar to the 1000 hPa level, an association between anomalously high

(low) SST's and anomalously high (low) 500 hPa heights over the whole subcontinent. The same association is inferred from the graphs and figures for the second mode (Figures 4.10 to 4.12), but with an opposite tendency, i.e. 500 hPa heights decreasing (increasing) towards normal to the north of the subcontinent, so that there exists a negative correlation between equatorial Pacific SST's and 500 hPa heights to the south of the subcontinent.

From the above it can be inferred that a high pressure system over the subcontinent will be more defined, while low-pressure systems to the south will be deeper (more shallow) with anomalously positive (negative) equatorial Pacific SST's in general. The same association was found by Lindesay (1988).

4.4.3. Only ENSO years (1000 hPa)

To investigate possibly stronger associations only during extreme equatorial Pacific SST deviations during late summer, only ENSO years were used in this combination of years. From 1958 to 1997 a total of 17 El Niño and La Niña years are identified by the Japan Meteorological Agency (see Chapter 3). For only these years, the association between the first canonical vectors was even stronger than for all years, as anticipated. For this mode it is seen, from Figures 4.13 to 4.15, that there is a close association between anomalously warm (cold) SST's and anomalously high (low) 1000 hPa heights over the subcontinent, especially over the far western to northern parts, as well as an area south-east of Madagascar, decreasing (increasing) southwards.

It is inferred from this case, that there is a positive association between 1000 hPa heights to the west of the subcontinent as well as south of Madagascar, and equatorial Pacific SST's. An opposite association exists over the south-eastern interior and south of the subcontinent. Thus during El Niño (La Niña) a strengthening (weakening) of high pressure systems west of the subcontinent as well as over southern Madagascar is evident, while a deepening (weakening) of low-pressure systems are inferred for the south-eastern interior as well as the southern oceanic areas.

4.4.4. Only ENSO years (500 hPa)

Years were chosen on a similar basis as for 4.4.3, but only for 500 hPa heights. Both modes proved to have significant associations between canonical vectors. Similar to the findings in 4.4.2, it can be inferred from the first mode (Figure 4.16 to 4.18), that there is a close association between anomalously warm SST's and anomalously high 500 hPa heights over the whole subcontinent, especially in the north.

With similar results as with the case where all years were taken into account, El Niño (La Niña) is associated with stronger (weaker) possible high pressure systems over the interior at the surface and vice versa for possible low pressure systems. The opposite association to the above is evident for the oceanic areas south of the subcontinent.

4.4.5. Only El Niño years (1000 hPa)

An attempt is made to find associations between SST's and pressure level heights, but only during El Niño years. A total of 10 El Niño years were identified from 1958 to 1997 and were subsequently used in the analysis. For the first mode, from Figures 4.19 to 4.21, it can be seen that there is a close relationship between anomalously high (low) SST's over the equatorial Pacific region, and anomalously high (low) 1000 hPa heights over the entire subcontinent, decreasing (increasing) southwestwards towards an opposite association over the ocean.

In general for El Niño seasons, it can be inferred that during strong (weak) El Niño seasons, high pressure systems are stronger (weaker) over the interior and west of the subcontinent at the surface, but vice versa for low pressure systems. Southwards, the opposite applies. The result is that high pressure systems to the west and over the interior of the subcontinent will be stronger in relation to the strength of an El Niño. The opposite applies for low pressure systems, which can have a negative bearing on the favourability of rainfall over the interior of the subcontinent.

4.4.6. Only El Niño years (500 hPa)

From the first mode (Figures 4.22 to 4.24), similar to section 4.4.5, an association is again found between anomalously high (low) SST's, and anomalously high (low) 500 hPa heights over the whole subcontinent.

It is inferred that possible high-pressure systems at the 500 hPa level will be stronger (weaker) for stronger (weaker) El Niño seasons, having a direct effect on the favourability of rainfall. Well-defined high-pressure systems in the upper-air are unfavourable for the occurrence of rainfall over the subcontinent.

4.4.7. Only La Niña years (1000 hPa)

For this combination of years, a total of 7 La Niña years were available. From Figures 4.25 to 4.27 it can be seen that there is a very strong association between anomalously high (low) SST's in the NINO3 and NINO4 regions and anomalously high (low) 1000 hPa heights over the West Coast and adjacent ocean. The opposite association applies for the rest of the subcontinent and surrounding oceans.

From the above an association between stronger (weaker) La Niña seasons and a weakening (strengthening) and probable southward (northward) displacements of high-pressure systems to the west of the subcontinent, as well as a deepening (weakening) of surface troughs over the interior can be deduced. This infers a positive association between moisture influx over the interior from the tropics and the strength of La Niña.

4.4.8. Only La Niña years (500 hPa)

For the first mode, from Figures 4.28 to 4.30, it can be seen that there is an association between anomalously high (low) SST's and anomalously low (high) 500 hPa heights over the whole subcontinent and surrounding oceans.

It is clear that no simple associations between the strength of La Niña and 500 hPa geopotential heights over the region can be made.

4.4.9. Only ENSO years occurring during the above-normal part of the decadal rainfall cycle (1000 hPa)

A total of 8 ENSO years were identified to have occurred during the above normal part of the decadal rainfall cycle. Only the correlations between the canonical vectors for the first mode proved to be significant at the 95 % level of confidence. Investigating Figures 4.31 to 4.33, an association is found between anomalously high (low) SST's and anomalously low (high) 1000 hPa heights in a band from northern Namibia south-eastwards over the subcontinent, as well as the far southern ocean areas. The opposite association exists over the western coast of the subcontinent and adjacent ocean area and the north-eastern part of the subcontinent eastwards over Madagascar.

A discussion on the effects of the above associations on the circulation over the subcontinent is best given keeping the average circulation over the subcontinent in mind. It will thus be further discussed in Chapter 5. This applies for section 4.4.10 to 4.4.12 as well, where the effects of the associations in those cases will also be discussed in the following chapter, with the aid of average circulation charts during those combinations of years.

4.4.10. Only ENSO years occurring during the above-normal part of the decadal rainfall cycle (500 hPa)

Here correlations between the canonical vectors for both the first and second mode proved to be significant at the 95% level of confidence. For the first mode (Figures 4.34 to 4.36) it can be deduced that El Niño (La Niña) is associated with anomalously high (low) 500 hPa heights over the subcontinent excluding the southern part and ocean areas south of about 33°S. For the second mode (Figures 4.37 to 4.39) an association between El Niño (La Niña) and anomalously high (low) 500 hPa heights over the whole subcontinent and surrounding oceans can be inferred, but especially over the central to southern parts of the subcontinent.

4.4.11. Only ENSO years occurring during the below-normal part of the decadal rainfall cycle (1000 hPa)

From Figures 4.40 to 4.42, for the first mode, an association is found between anomalously high (low) SST's in the NINO4 region and anomalously low (high) SST's in the NINO1 to NINO3 regions; and anomalously high (low) 1000 hPa heights west of the subcontinent and anomalously low (high) 1000 hPa heights over the whole subcontinent and the remainder of the surrounding oceans.

4.4.12. Only ENSO years occurring during the below-normal part of the decadal rainfall cycle (500 hPa)

From Figures 4.43 to 4.45, for the first mode, an association is found between El Niño (La Niña) and anomalously high (low) 500 hPa heights over the whole subcontinent and surrounding oceans. This association is very similar to that found in section 4.4.10.

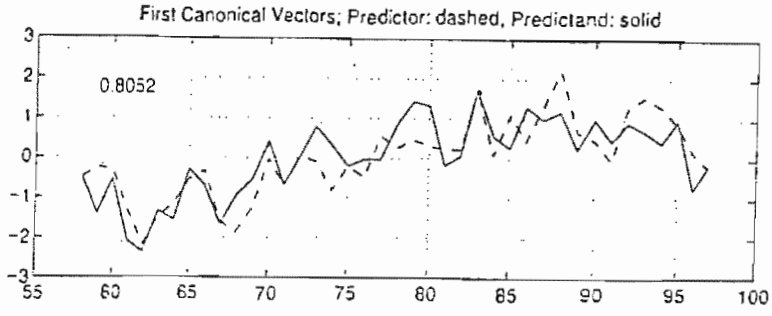

Figure 4.1. First canonical vectors for all years for the 1000 hPa level (predictor dashed, predictand solid). The value in the graph indicates the correlation between the vectors.

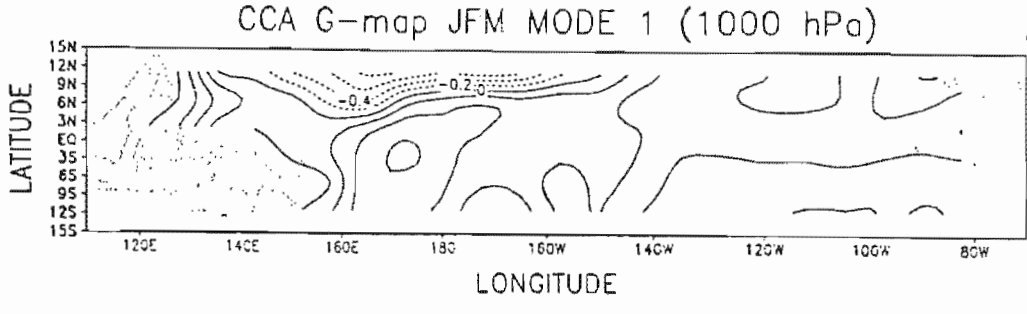

Figure 4.2. Canonical map of first canonical vectors for the predictor field for all years for the 1000 hPa level.

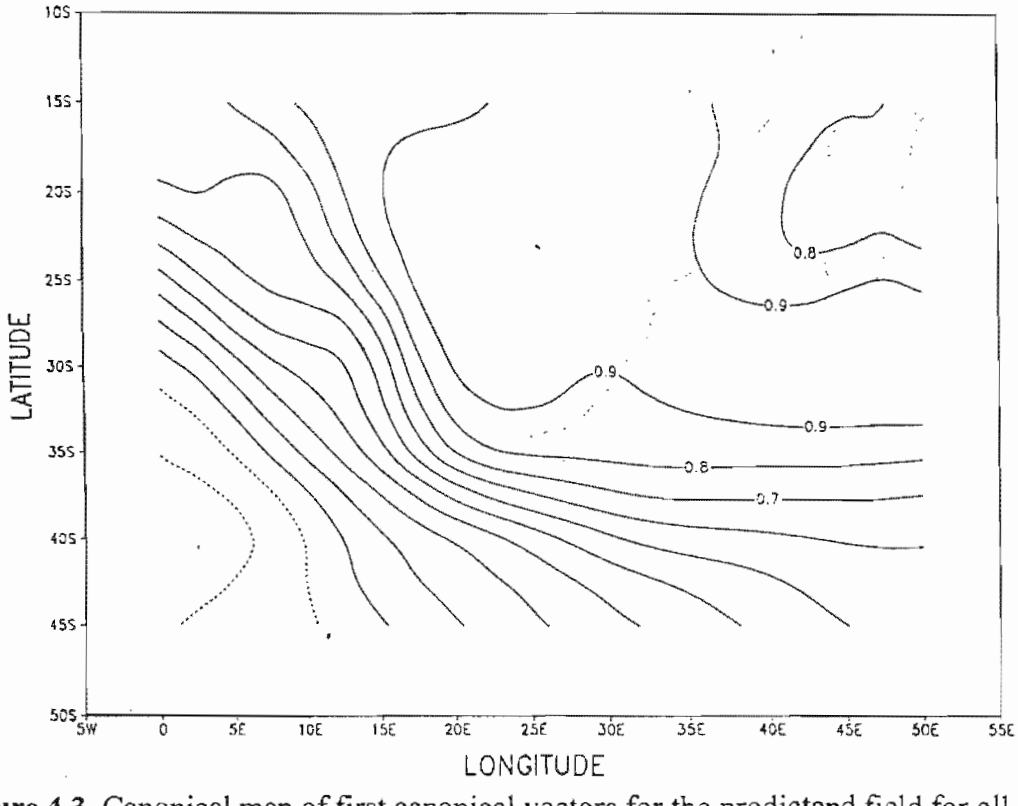

Figure 4.3. Canonical map of first canonical vectors for the predictand field for all years for the 1000 hPa level (solid lines positive, broken lines negative)

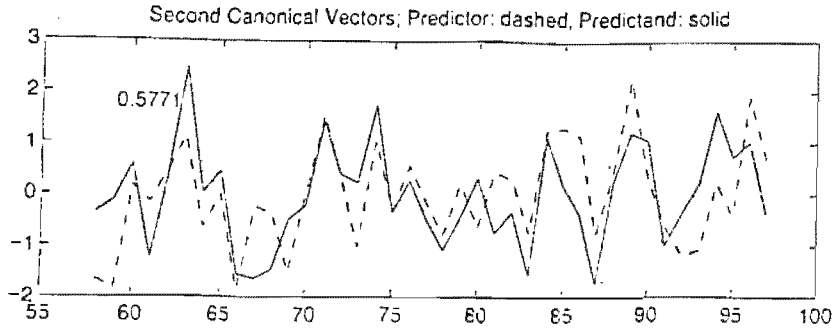

Figure 4.4. Second canonical vectors for all years for the 1000 hPa level (predictor dashed, predictand solid). The value in the graph indicates the correlation between the vectors.

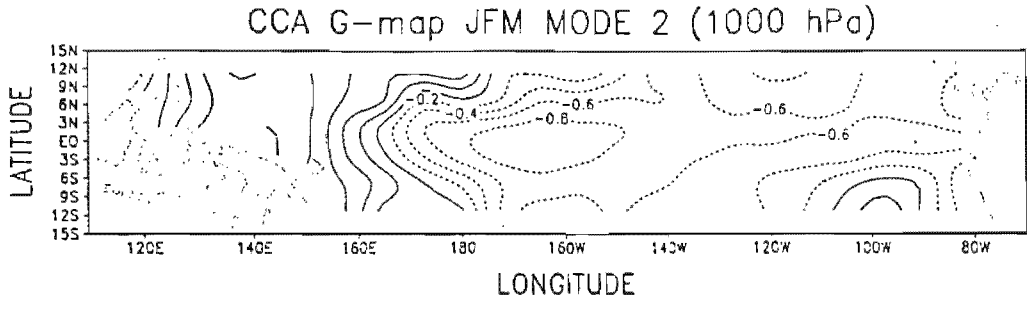

Figure 4.5. Canonical map of second canonical vectors for the predictor field for all years for the 1000 hPa level.

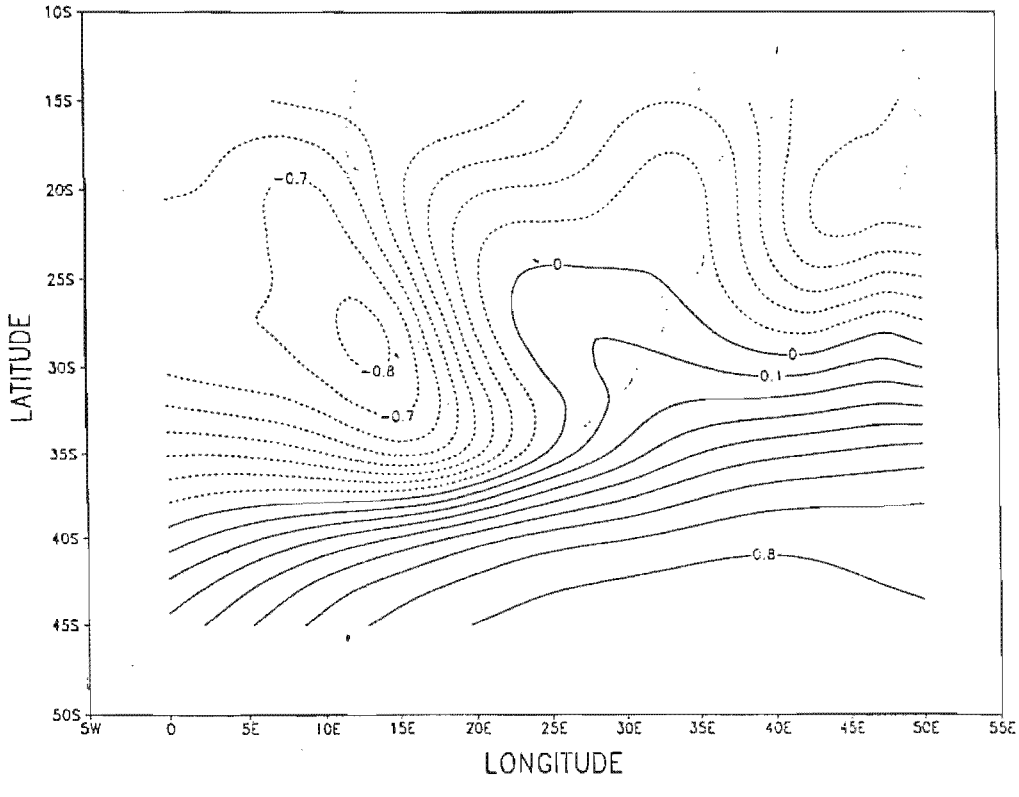

Figure 4.6. Canonical map of first canonical vectors for the predictand field for all years for the 1000 hPa level (solid lines positive, broken lines negative)

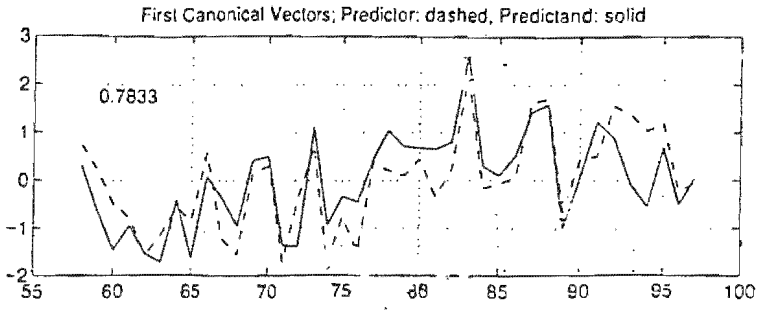

Figure 4.7. First canonical vectors for all years for the 500 hPa level (predictor dashed, predictand solid). The value in the graph indicates the correlation between the vectors.

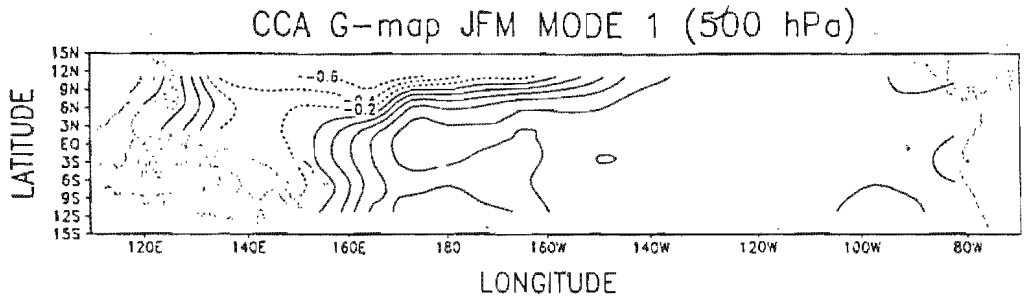

Figure 4.8. Canonical map of first canonical vectors for the predictor field for all years for the 500 hPa level.

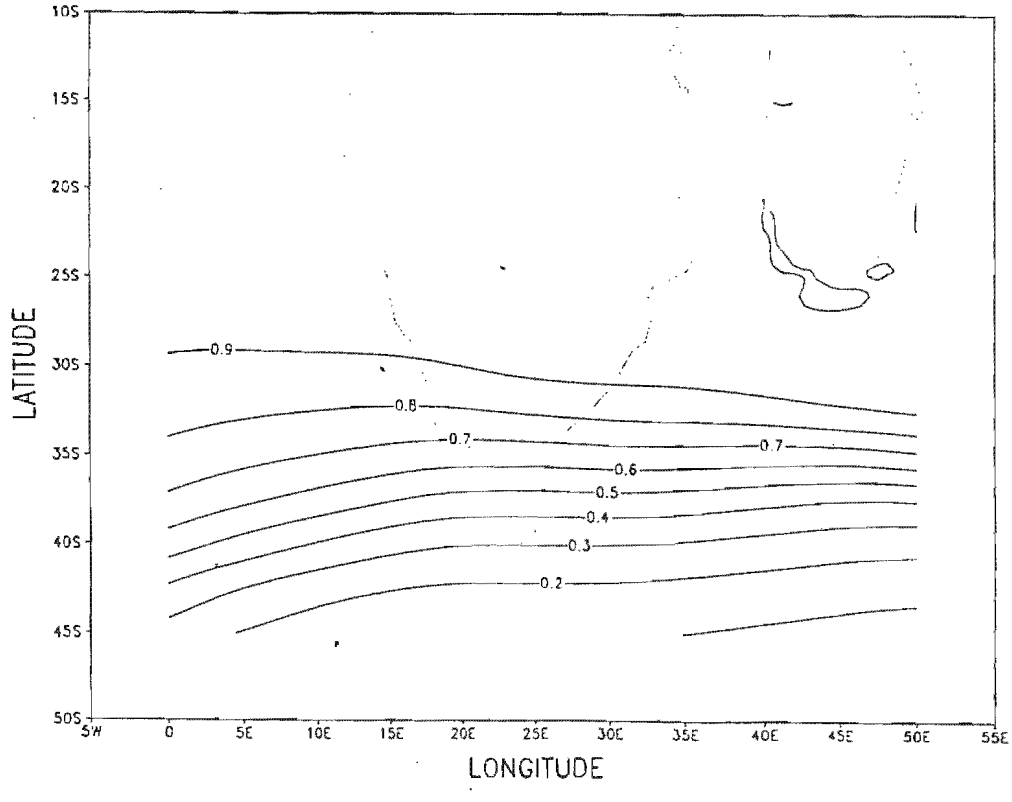

Figure 4.9. Canonical map of first canonical vectors for the predictand field for all years for the 500 hPa level (solid lines positive, broken lines negative)

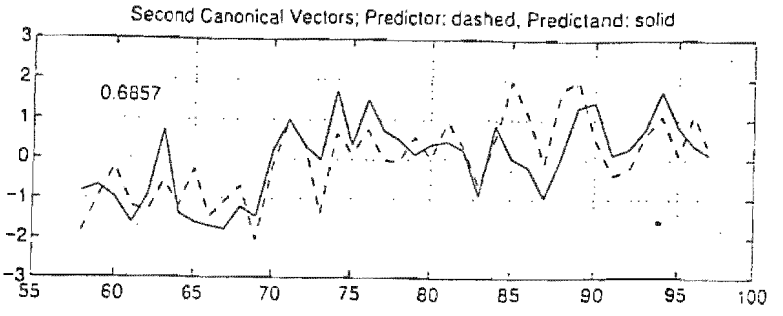

Figure 4.10. Second canonical vectors for all years for the 500 hPa level (predictor dashed, predictand solid). The value in the graph indicates the correlation between the vectors.

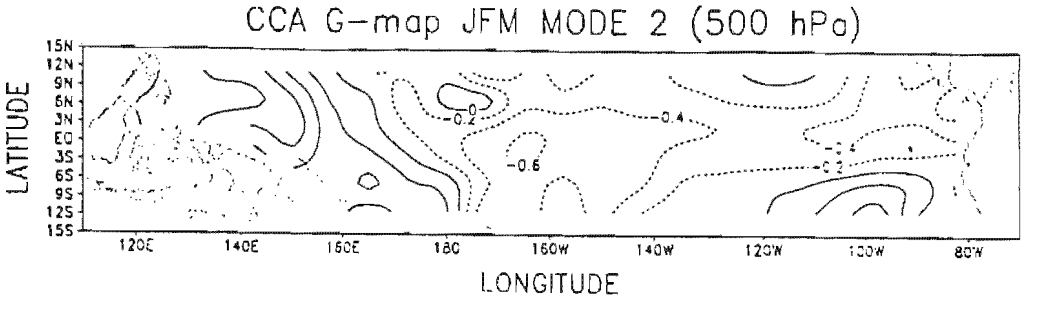

Figure 4.11. Canonical map of the second canonical vectors for the predictor field for all years for the 500 hPa level.

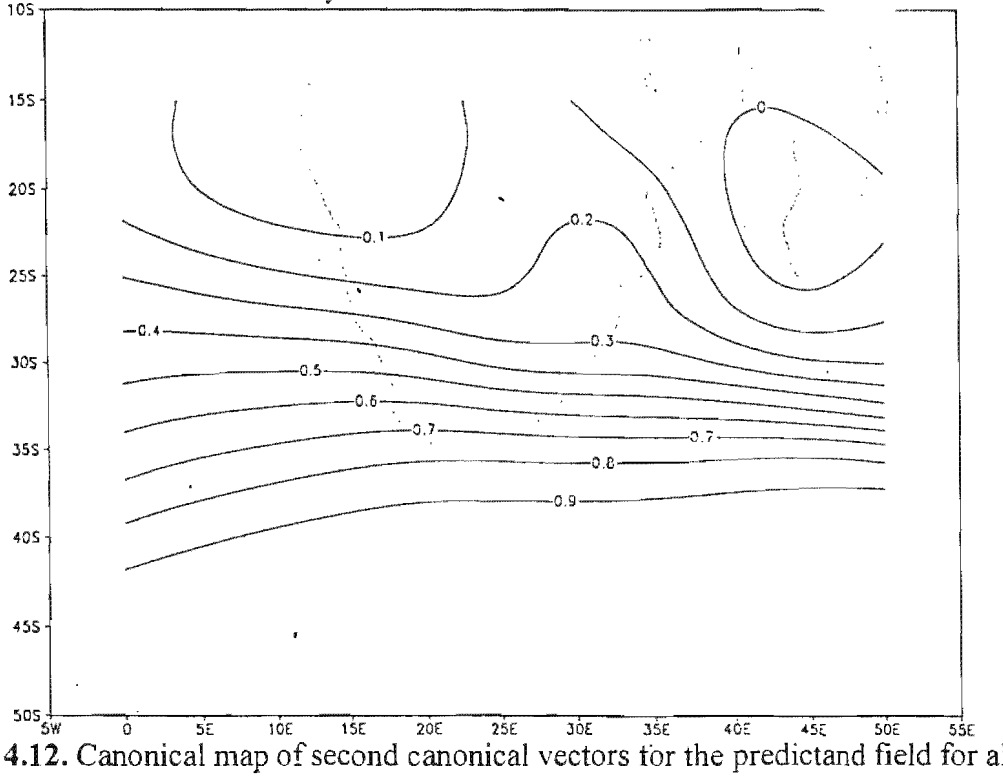

Figure 4.12. Canonical map of second canonical vectors for the predictand field for all years for the 500 hPa level (solid lines positive, broken lines negative)

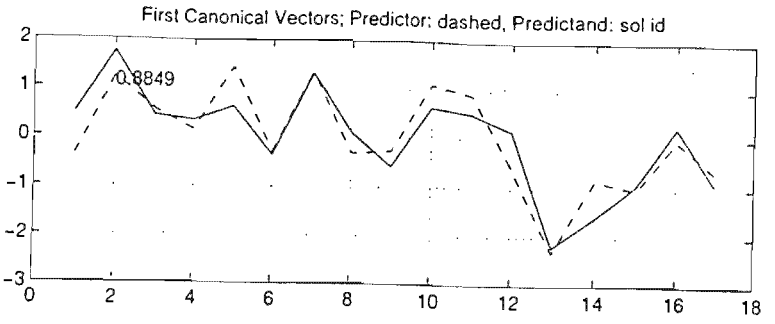

Figure 4.13. The same as Figure 4.1, but for ENSO years only. (Years in the same order as occurrence)

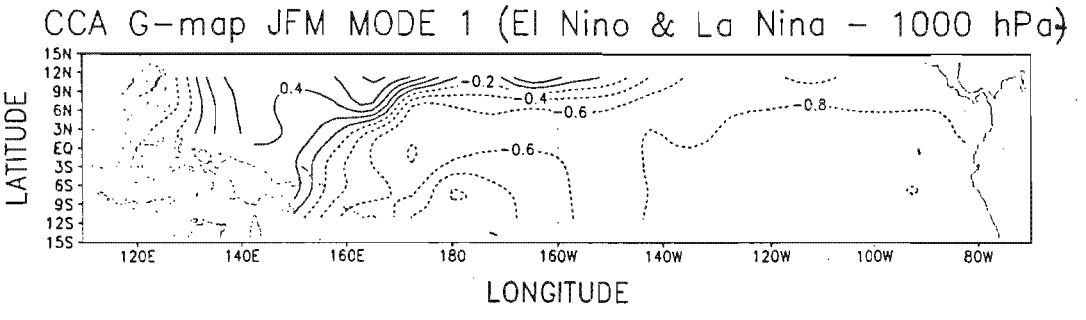

Figure 4.14. The same as Figure 4.2, but for ENSO years only.

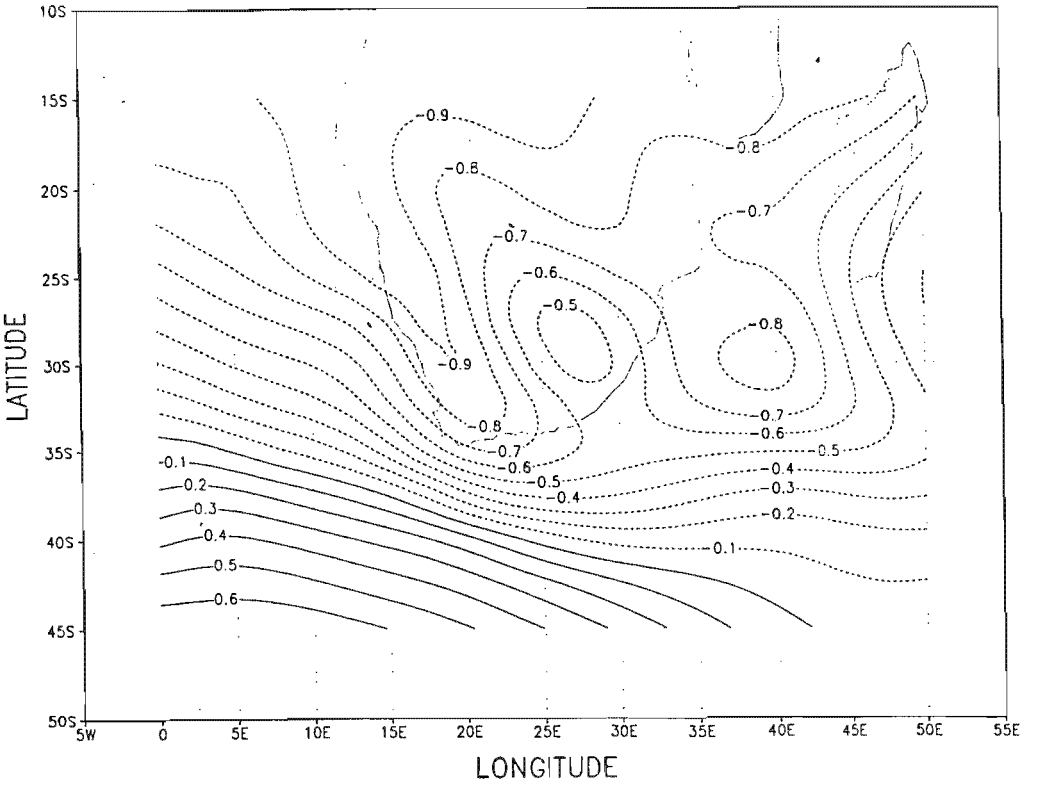

Figure 4.15. The same as Figure 4.3, but for ENSO years only.

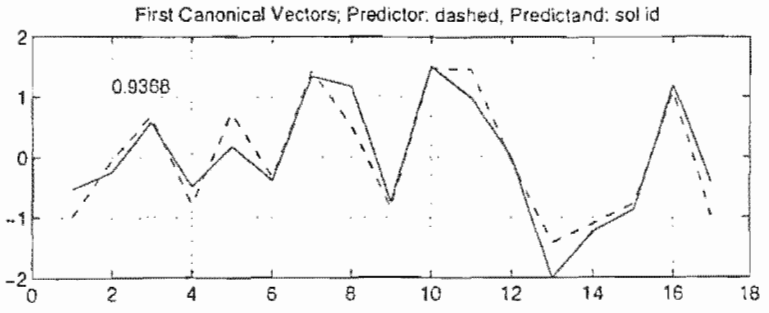

Figure 4.16. The same as Figure 4.7, but for ENSO years only.

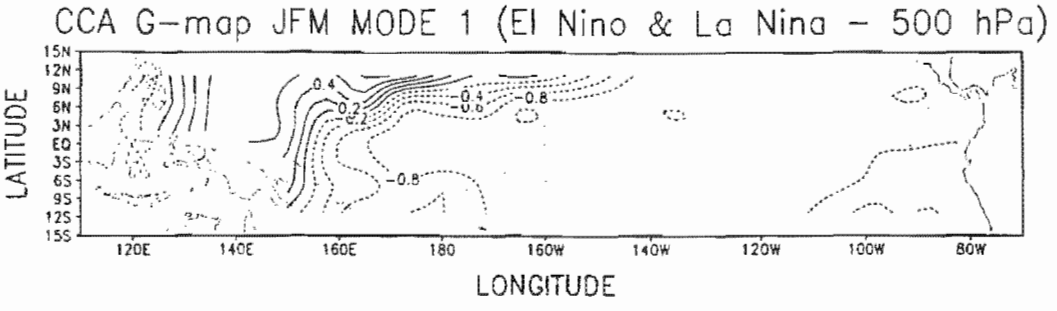

Figure 4.17. The same as Figure 4.8, but for ENSO years only.

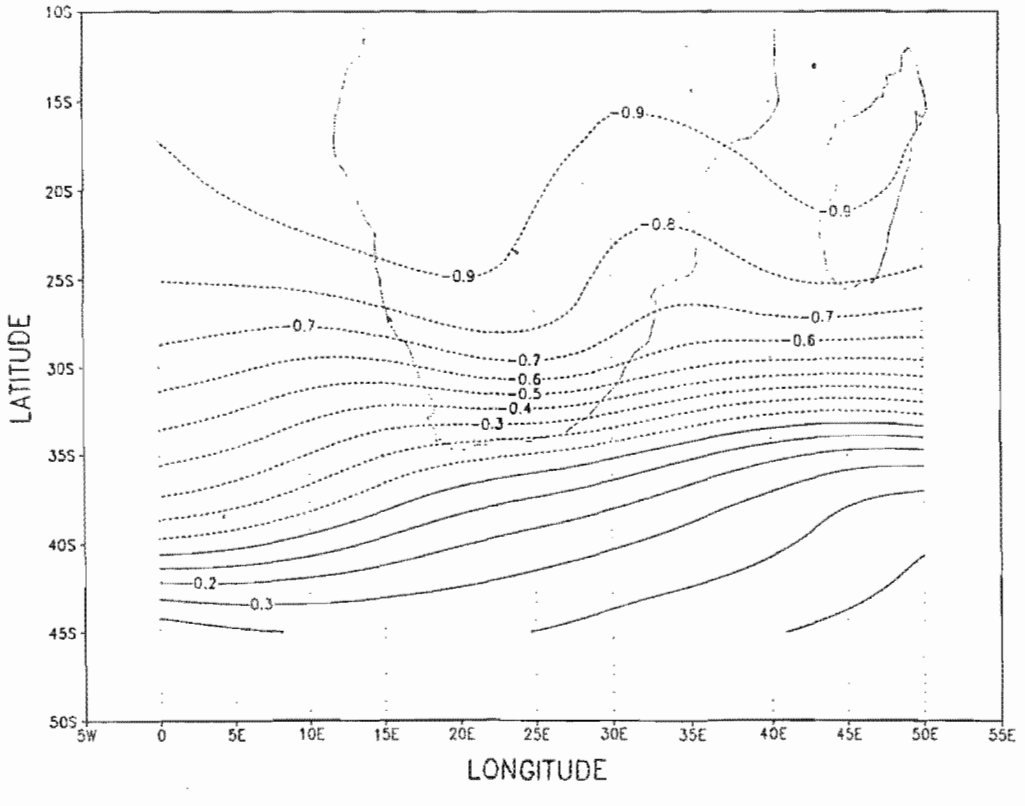

Figure 4.18. The same as Figure 4.9, but for ENSO years only.

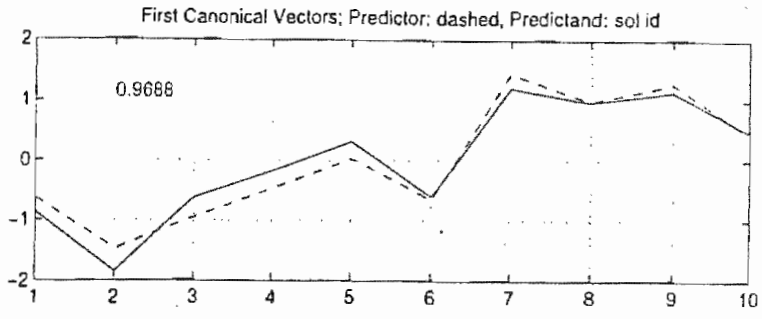

Figure 4.19. The same as Figure 4.1, but for El Niño years only.

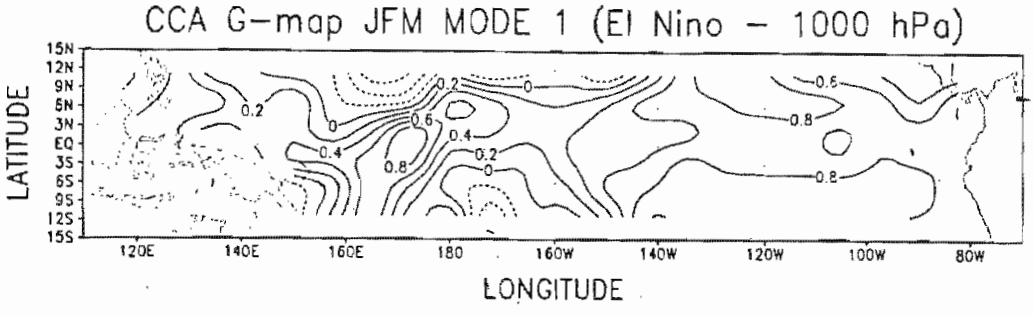

Figure 4.20. The same as Figure 4.2, but for El Niño years only.

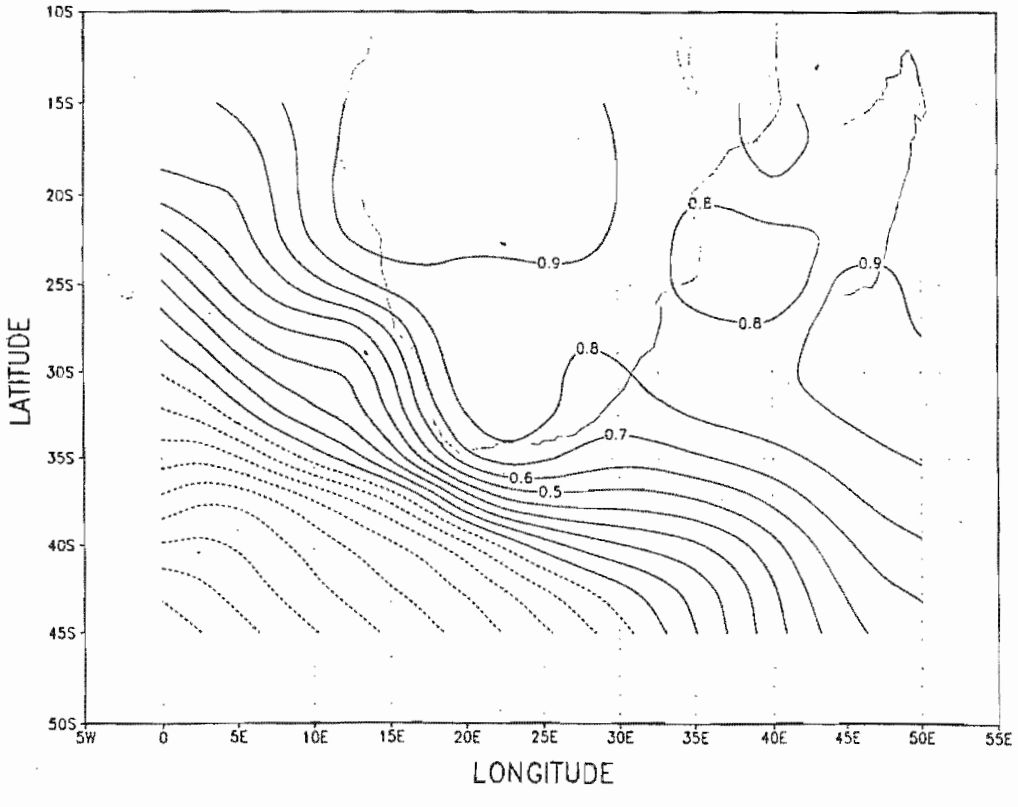

Figure 4.21. The same as Figure 4.3, but for El Niño years only.

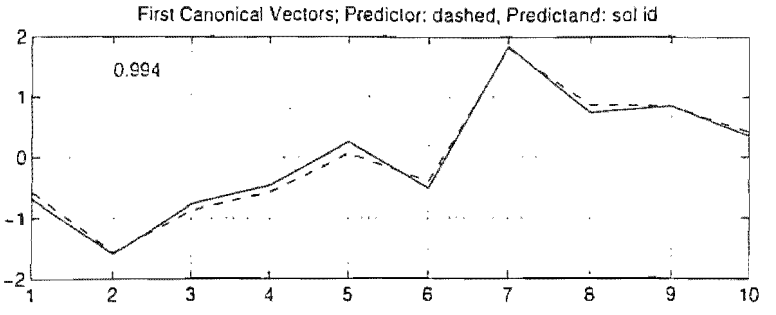

Figure 4.22. The same as Figure 4.7, but for El Niño years only.

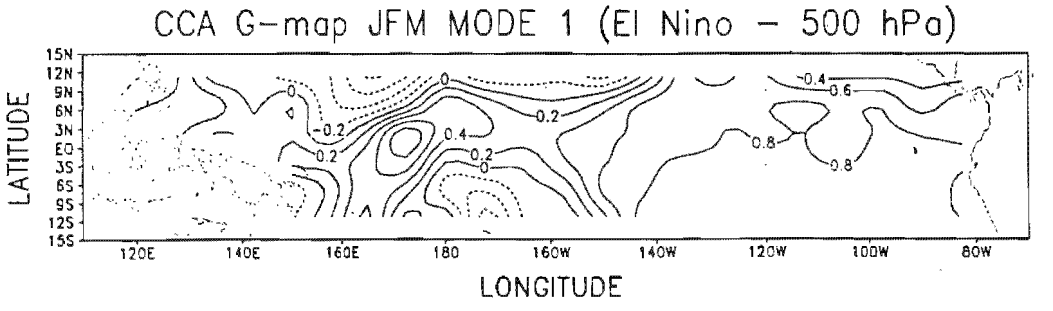

Figure 4.23. The same as Figure 4.8, but for El Niño years only.

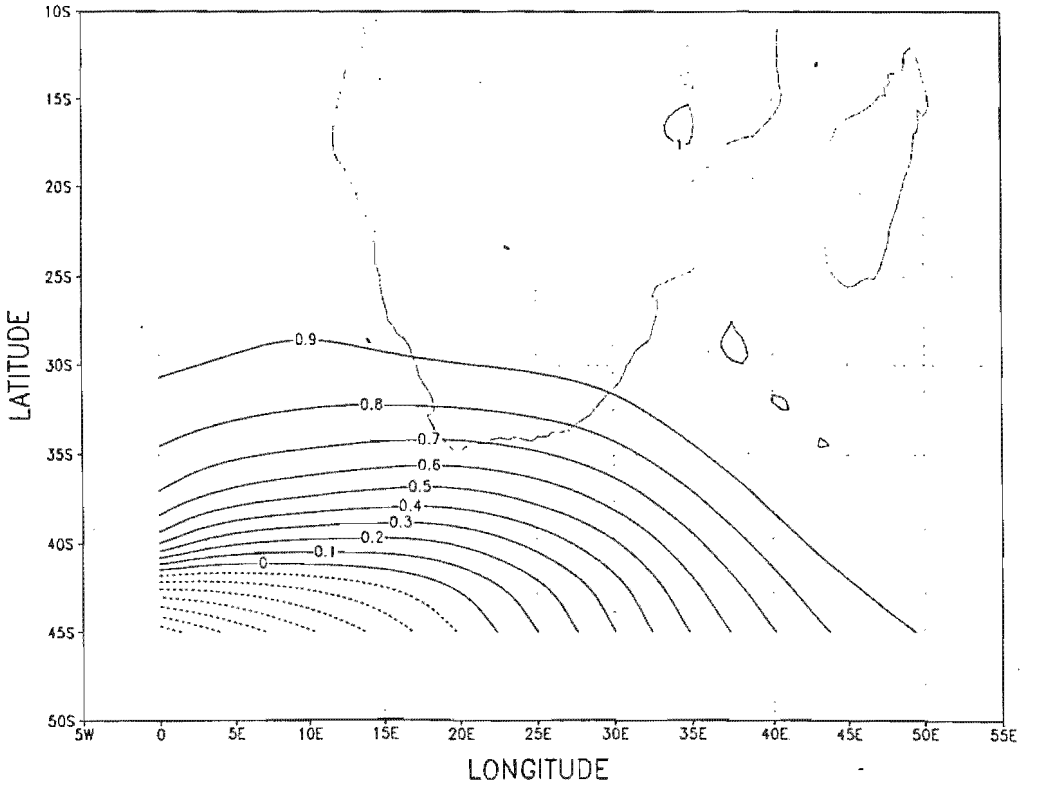

Figure 4.24. The same as Figure 4.9, but for El Niño years only.

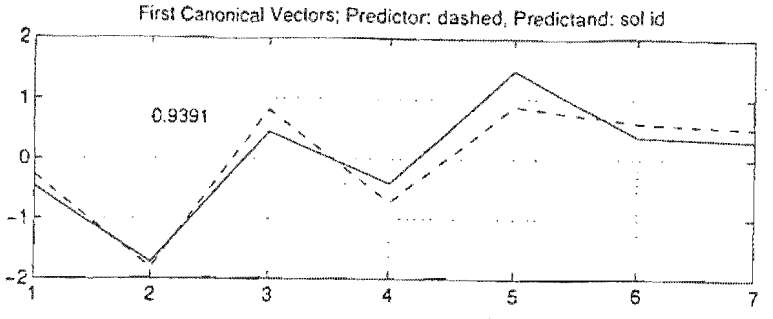

Figure 4.25. The same as Figure 4.1, but for La Niña years only.

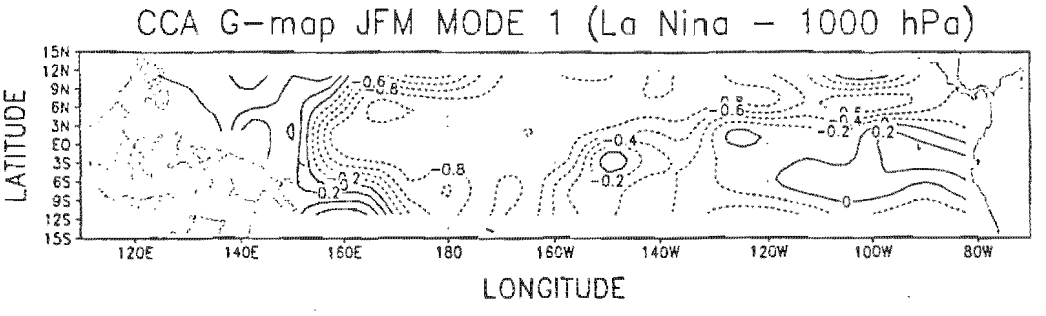

Figure 4.26. The same as Figure 4.2, but for La Niña years only.

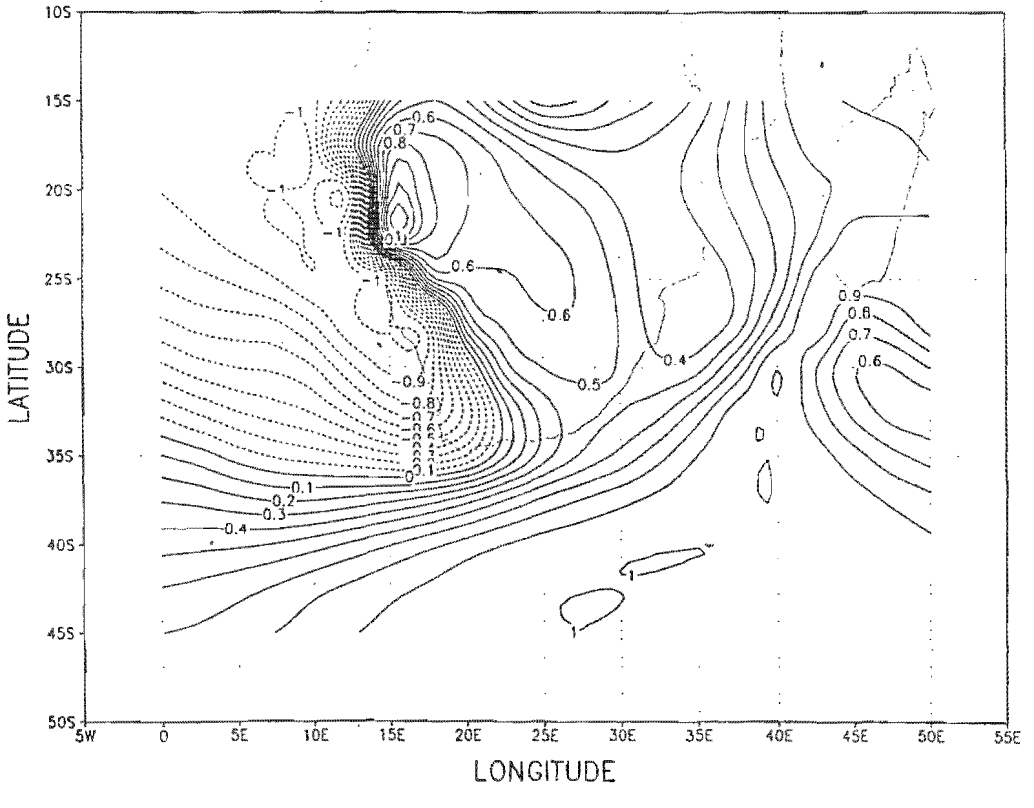

Figure 4.27. The same as Figure 4.3, but for La Niña years only.

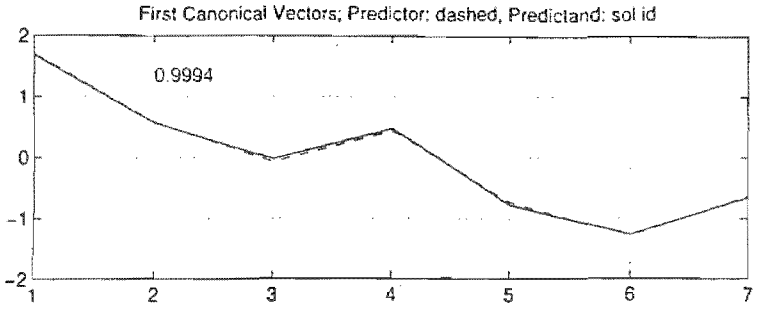

Figure 4.28. The same as Figure 4.7, but for La Niña years only.

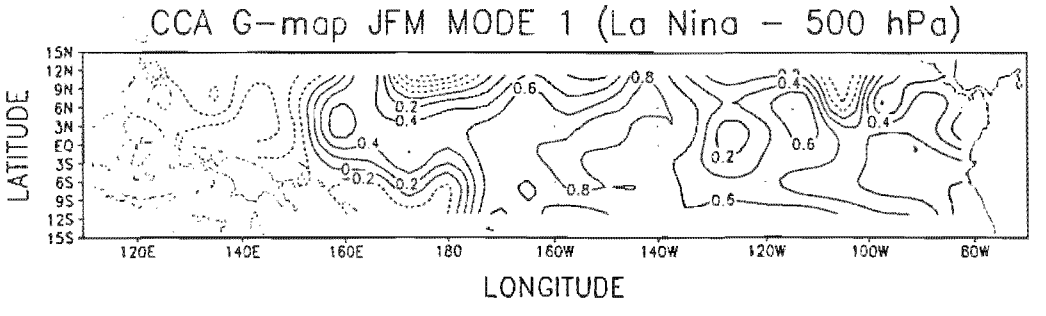

Figure 4.29. The same as Figure 4.8, but for La Niña years only.

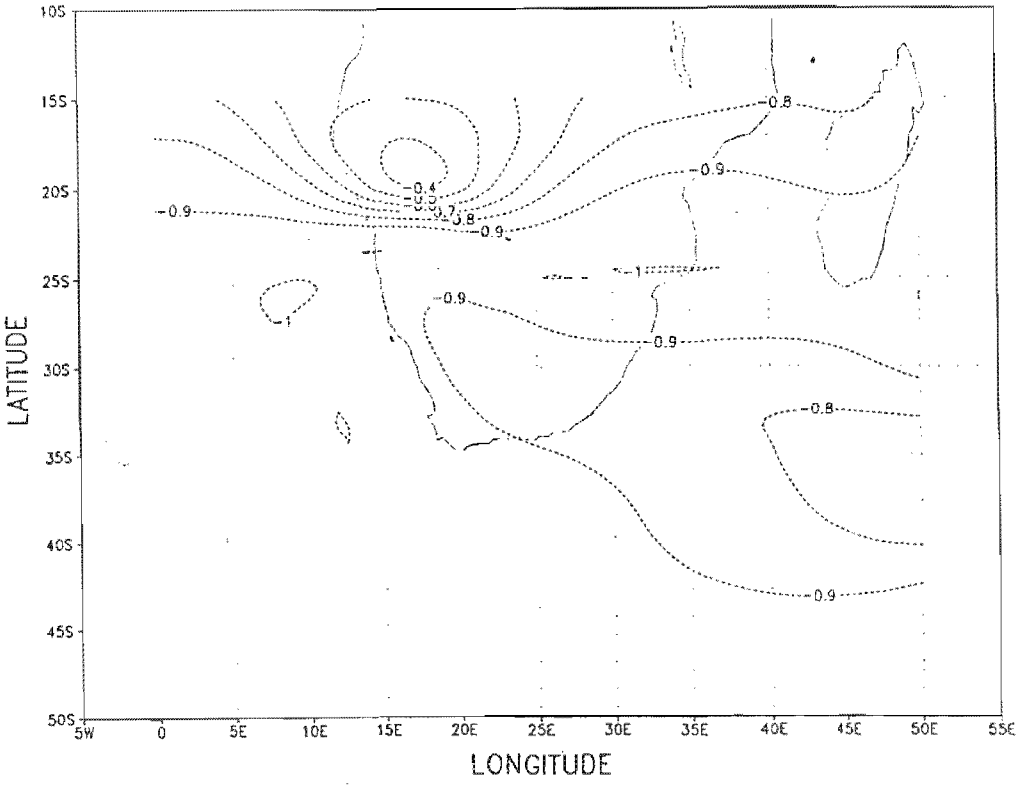

Figure 4.30. The same as Figure 4.9, but for La Niña years only.

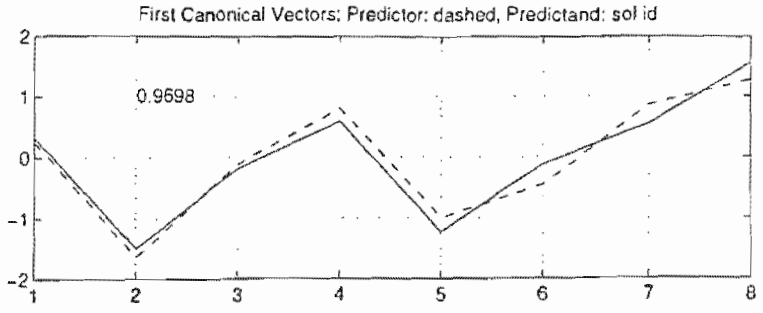

Figure 4.31. The same as Figure 4.1, but for ENSO years during the above-normal part of the decadal cycle only.

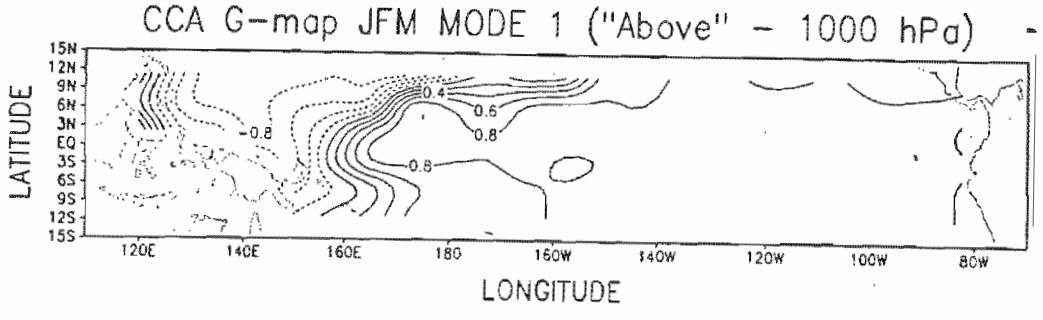

Figure 4.32. The same as Figure 4.2, but for ENSO years during the above-normal part of the decadal cycle only.

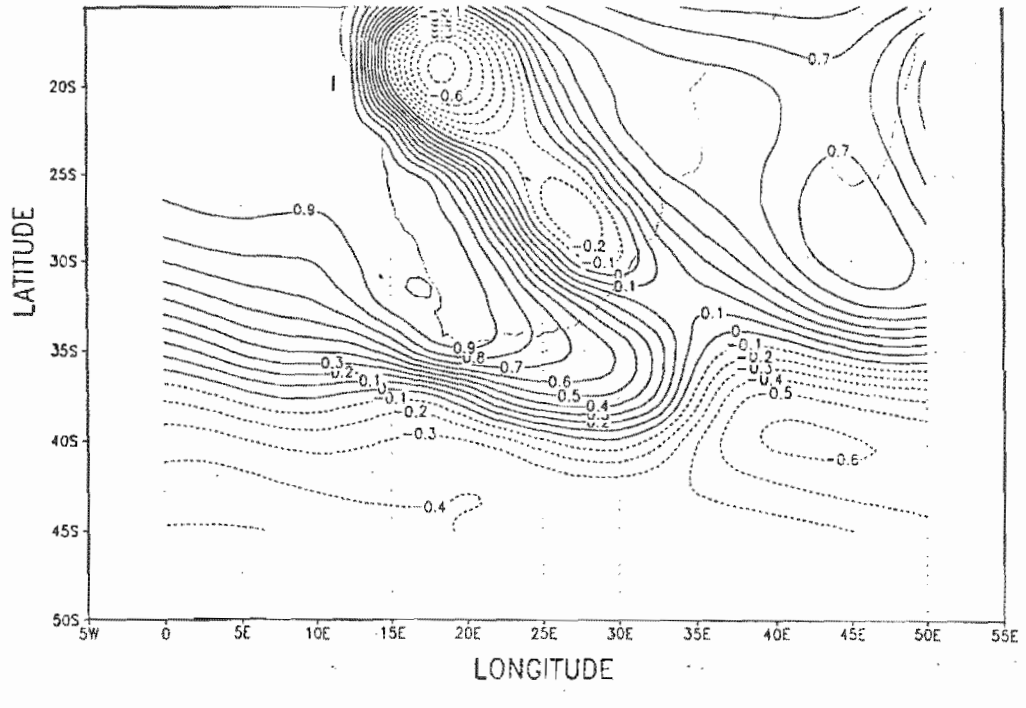

Figure 4.33. The same as Figure 4.3, but for ENSO years during the above-normal part of the decadal cycle only.

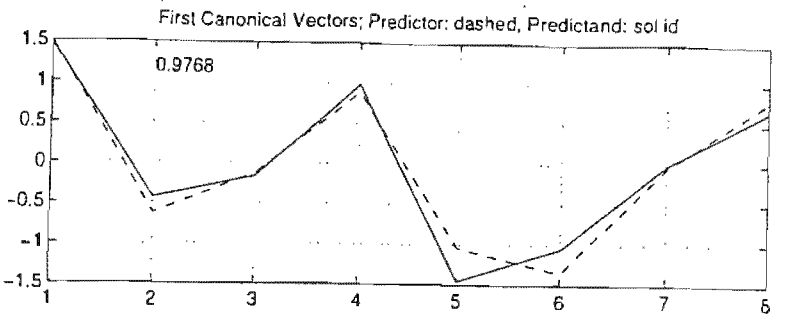

Figure 4.34. The same as Figure 4.7, but for ENSO years during the above-normal part of the decadal cycle only.

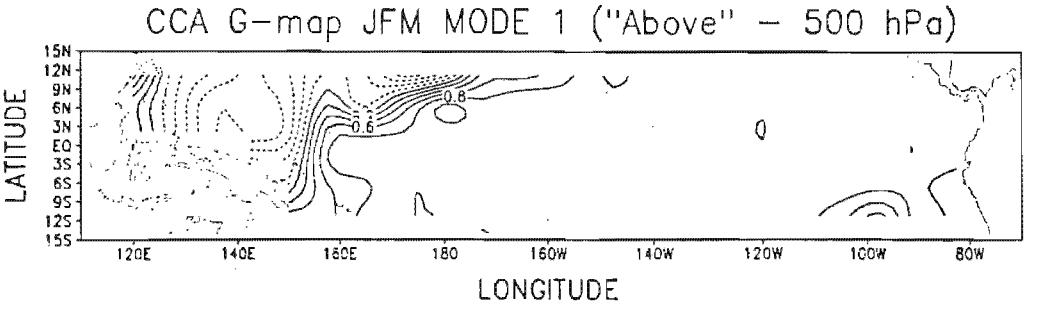

Figure 4.35. The same as Figure 4.8, but for ENSO years during the above-normal part of the decadal cycle only.

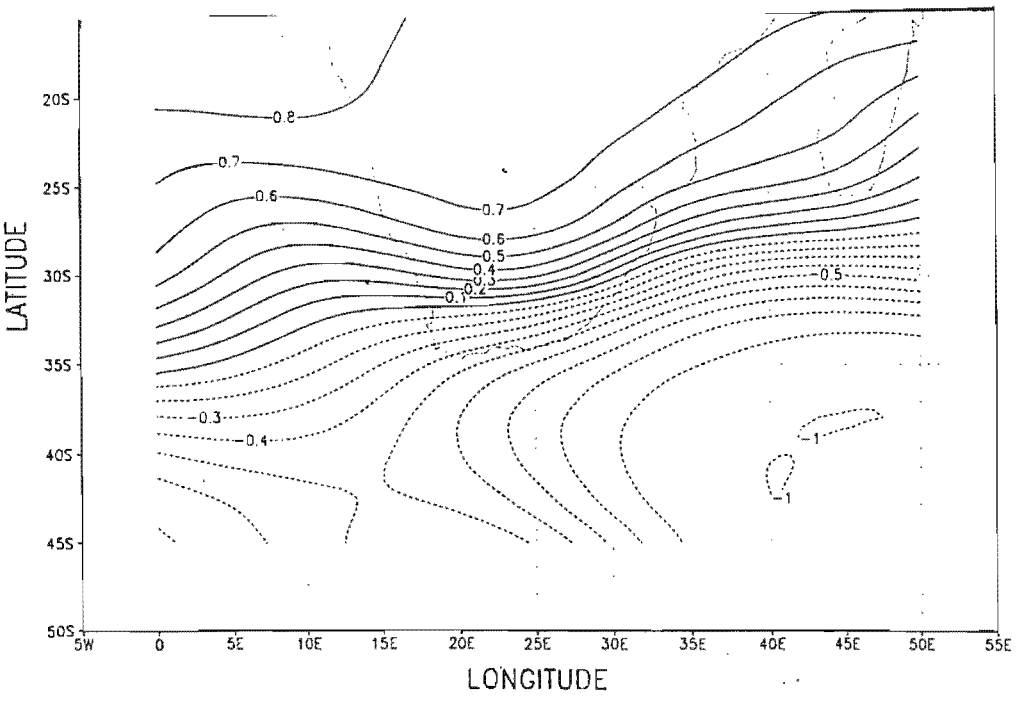

Figure 4.36. The same as Figure 4.9, but for ENSO years during the above-normal part of the decadal cycle only.

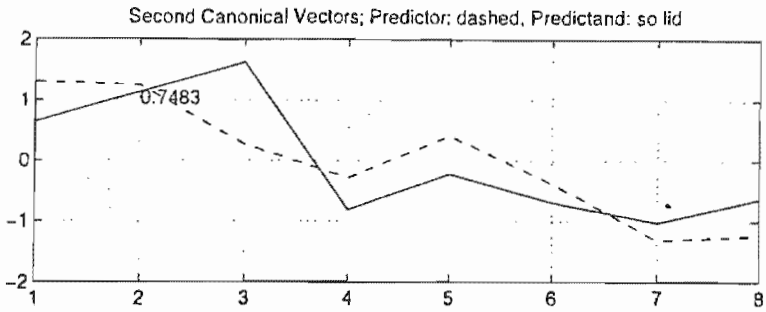

Figure 4.37. The same as Figure 4.10, but for ENSO years during the above-normal part of the decadal cycle only.

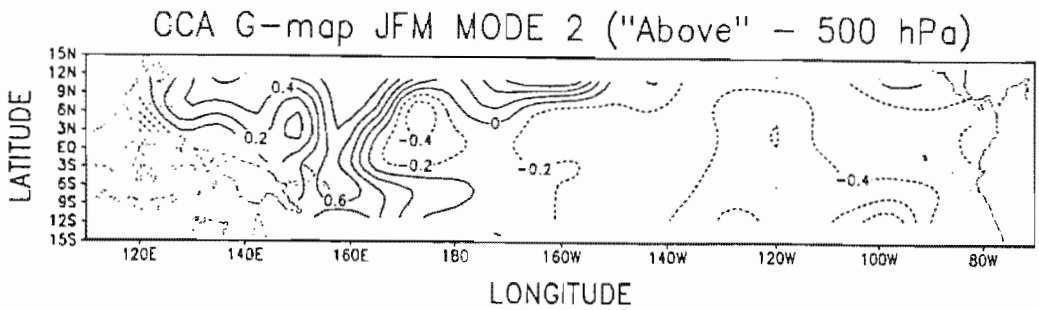

Figure 4.38. The same as Figure 4.11, but for ENSO years during the above-normal part of the decadal cycle only.

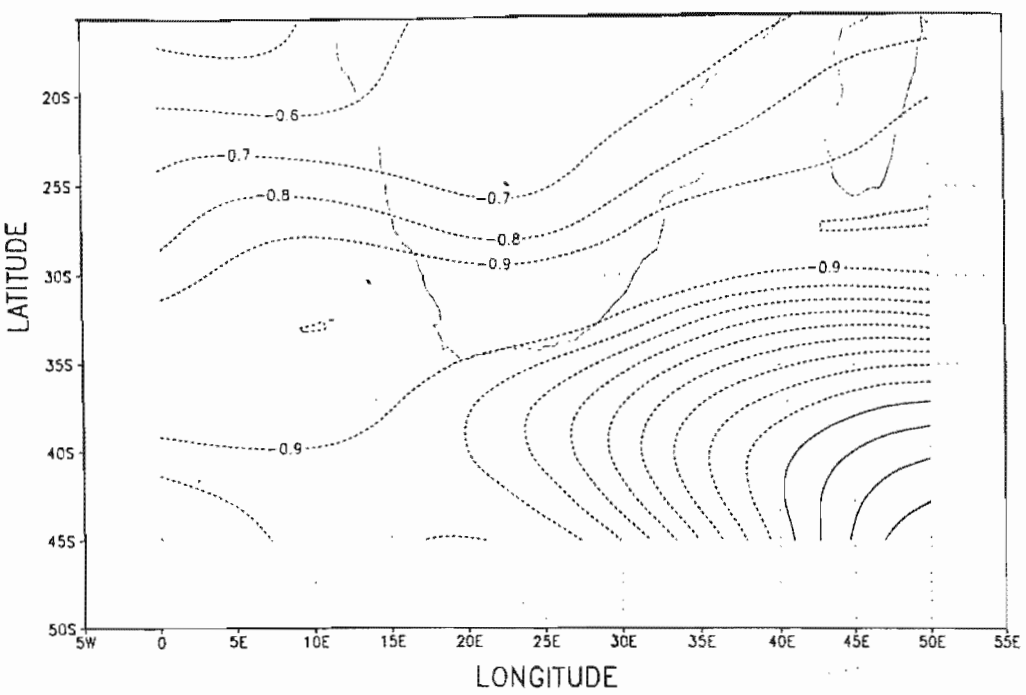

Figure 4.39. The same as Figure 4.12, but for ENSO years during the above-normal part of the decadal cycle only.

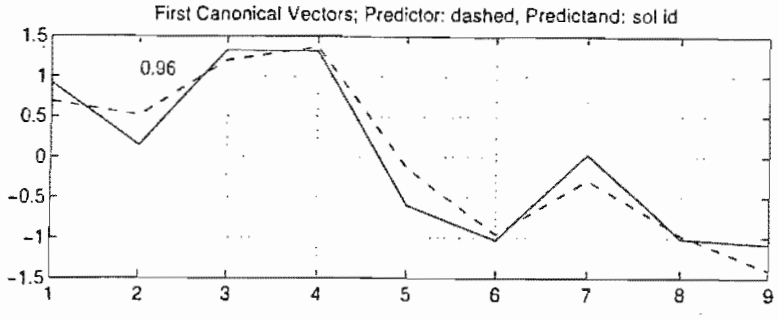

Figure 4.40. The same as Figure 4.1, but for ENSO years during the below-normal part of the decadal cycle only.

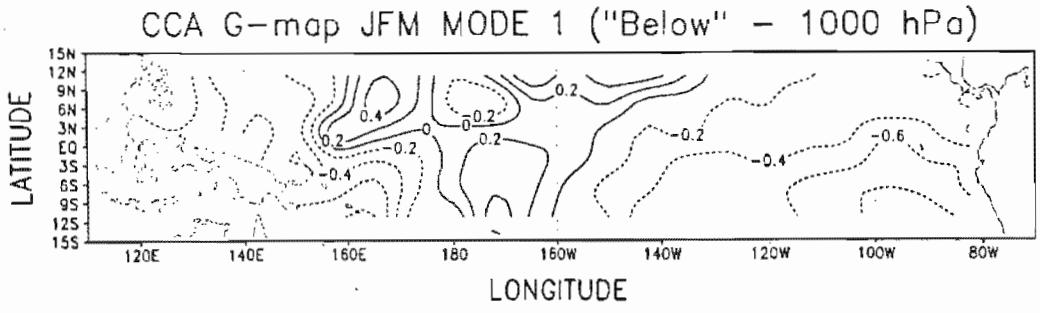

Figure 4.41. The same as Figure 4.2, but for ENSO years during the below-normal part of the decadal cycle only.

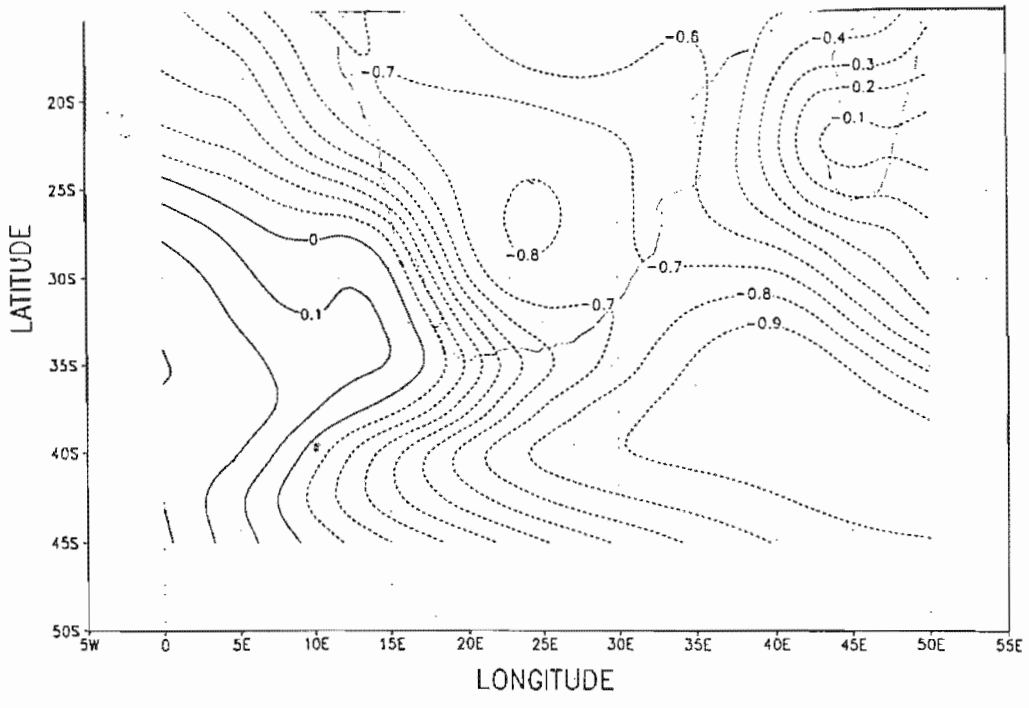

Figure 4.42. The same as Figure 4.3, but for ENSO years during the below-normal part of the decadal cycle only.

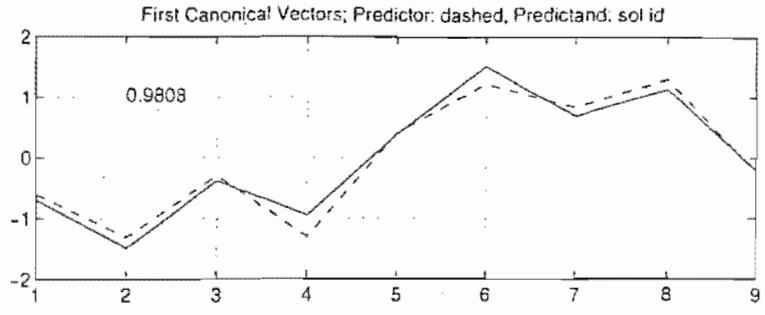

Figure 4.43. The same as Figure 4.7, but for ENSO years during the below-normal part of the decadal cycle only.

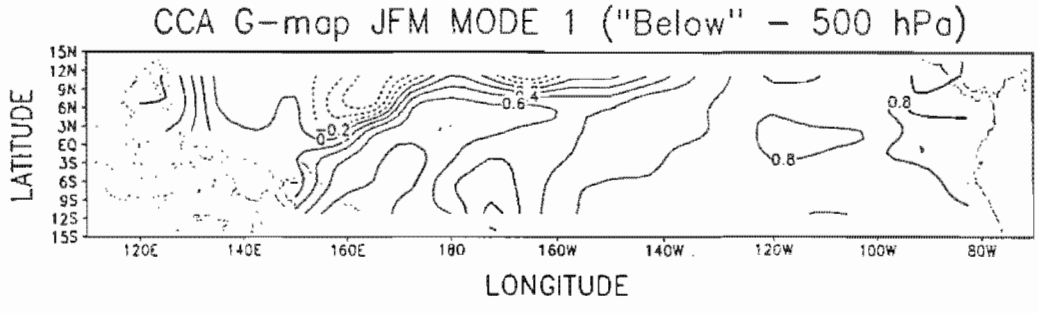

Figure 4.44. The same as Figure 4.8, but for ENSO years during the below-normal part of the decadal cycle only.

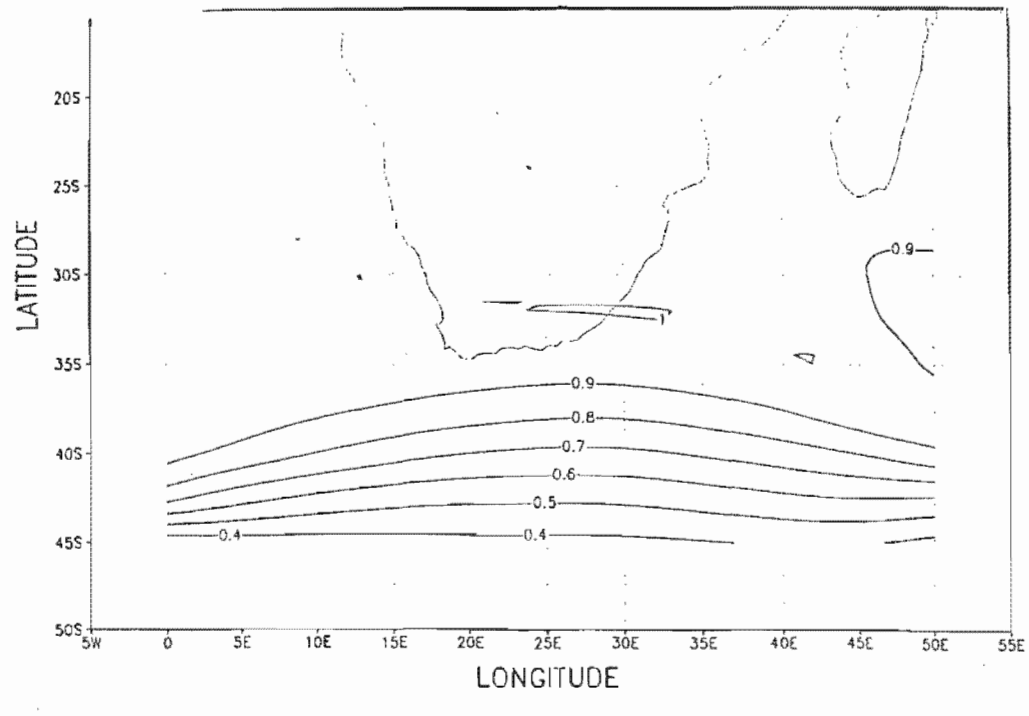

Figure 4.45. The same as Figure 4.9, but for ENSO years during the below-normal part of the decadal cycle only.

4.5. Verification of results with model runs

To verify that the relationships found between Pacific equatorial SST's, precipitation and 1000 hPa and 500 hPa geopotential height anomalies over the subcontinent found by CCA are not coincidental, these were compared to the Atmospheric Model Intercomparison Project (AMIP) (Gates, 1992) atmospheric model runs of the T31 GENESIS general circulation model (GCM) (version 2.0a), which was readily available for the period 1979 to 1988 (10 years). The AMIP model simulations use observed SST's as boundary conditions. Therefore, comparisons were made between averaged observed NINO3 SST's, 1000 hPa and 500 hPa geopotential height field simulations and rainfall simulations for the period JFM for 1979 to 1988. Unfortunately the behaviour of the model during above-normal periods of the near-decadal rainfall cycle could not be examined with the available simulations, but this should become possible as more AGCM model runs become available.

The GENESIS GCM (version 2.0a) consists of an atmospheric general circulation model (AGCM) coupled to multilayer models of vegetation, soil- and land-ice, snow, sea-ice, and a 50 m slab oceanic layer with prescribed heat transport. The AGCM has a T31 resolution with 18 atmospheric levels, while the surface models have a 2° x 2° grid resolution (Hudson, 1997). A more detailed description of the model can be found in Thompson and Pollard (1997).

4.5.1. Average AMIP simulations for late-summer 1979 to 1988

The average simulations for late-summer precipitation, 1000 hPa and 500 hPa geopotential heights for the period 1979 to 1988 for southern Africa are shown in Figures 4.46, 4.47 and 4.48 respectively. For rainfall (in $mm.day^{-1}$) one can see the expected minimum over the western parts of the subcontinent, increasing towards the north-east during this time of the year, although somewhat overestimated (Hudson, 1997). The average 1000 hPa geopotential

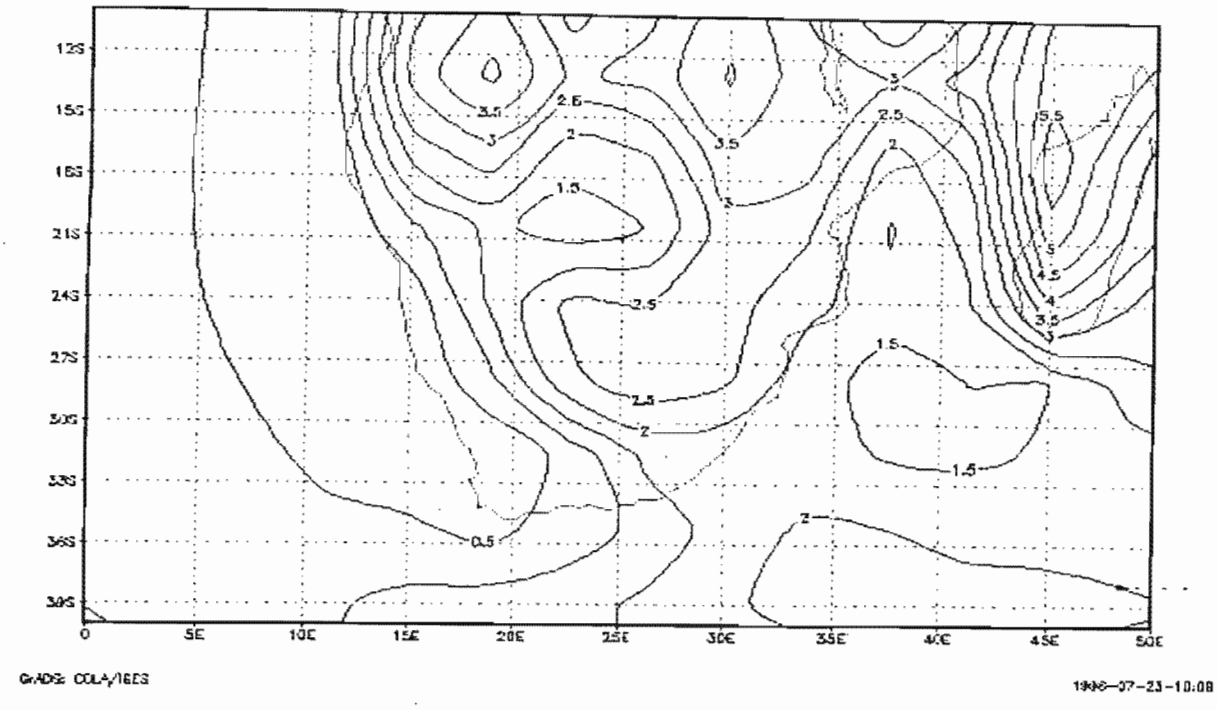

Figure 4.46. Average simulation for precipitation for JFM for the period 1979 to 1988 by the GENESIS GCM (version 2.0a) ($mm.day^{-1}$).

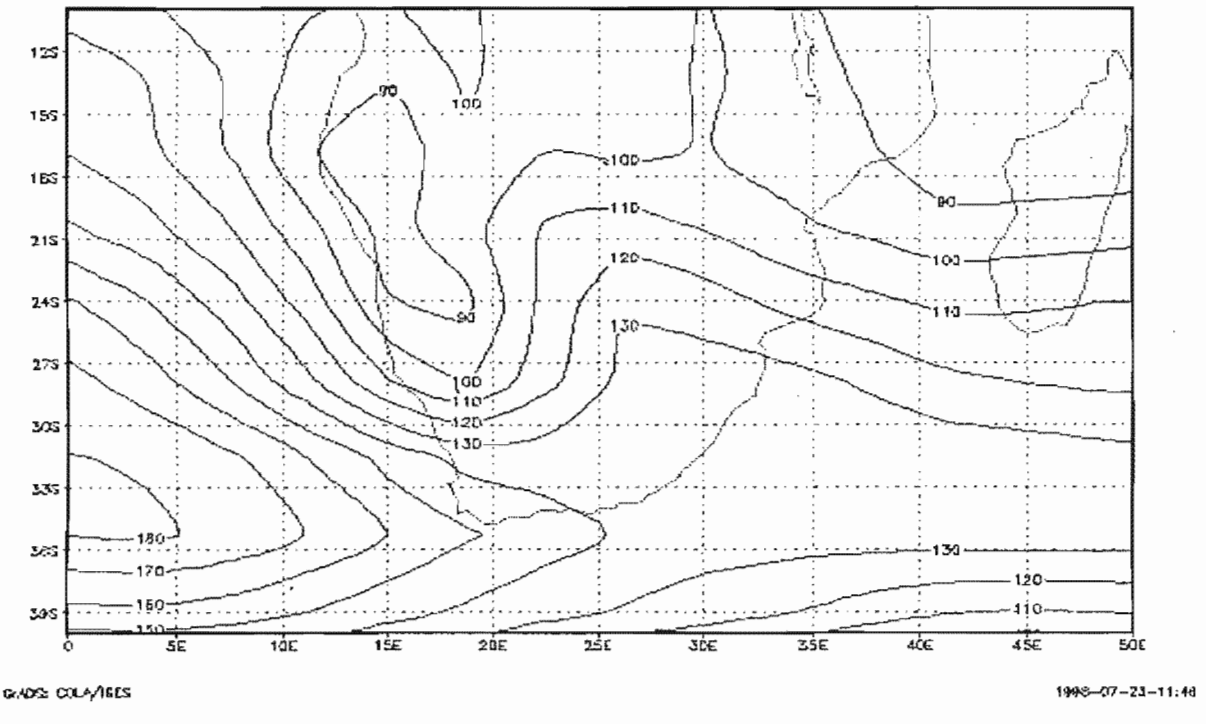

Figure 4.47. The same as Figure 4.46, but for 1000 hPa geopotential heights (gpm).

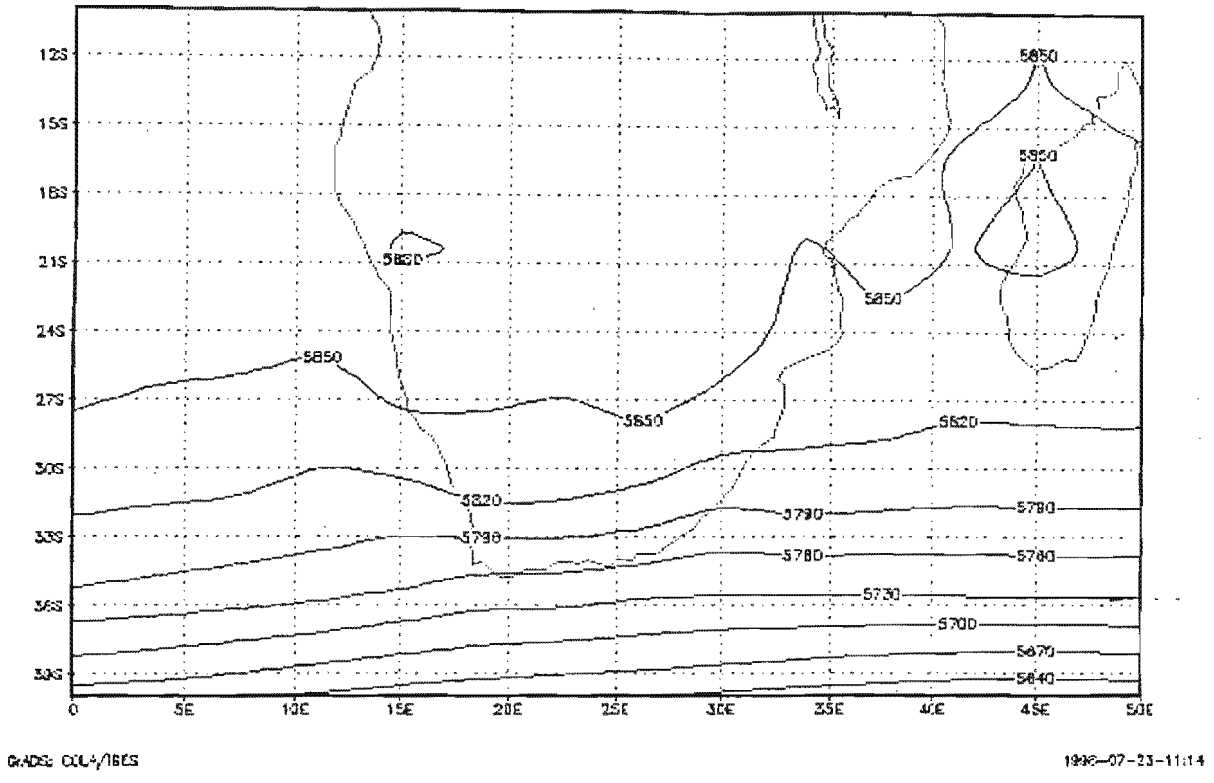

Figure 4.48. The same as Figure 4.46, but for 500 hPa heights (gpm).

heights (Figure 4.46) shows an underestimation of the subtropical high-pressure cell east of the subcontinent. Hudson (1997) also found that the spatial extent of the high pressure cells are less than observed. The reason for the eastern high-pressure cell to be underestimated more than the western high, may be due to the period of simulation, which falls mostly in the drier part of the near-decadal rainfall cycle described in Chapter 3.During these periods the western high is stronger than the eastern, causing a probably stronger influx of drier air from the south-west and reduced influx of moist air from the east. Regarding simulations of 500 hPa geopotential heights, Hudson (1997) found them to be good, with discrepancies between simulations and observed values due to the coarse resolution of the AGCM, such that it is unable to simulate the steep meridional pressure gradients.

4.5.2. Results

As mentioned, the average NINO3 SST anomalies are compared with the precipitation and 1000 hPa and 500 hPa geopotential height anomaly simulations for JFM for each season. The

average observed SST anomalies for the period are shown in Table 4.2. Here it must be noted that all available years in the AGCM runs were utilized according to their NINO3 anomalies, regardles whether they can be defined as ENSO years or not.

4.5.2.1. Observed SST's compared to precipitation anomaly simulations

Figures 4.49 to 4.58 show the average precipitation anomaly simulations for JFM for 1979 to 1988 respectively. Except for the 1980, 1986 and 1988 seasons, the relationship found, that above (below)-normal SST's are associated with below (above)-normal precipitation over the regions indicated in Figure 2.3(b) was confirmed in seven of the 10 cases by the simulations, i.e. 70%. The precipitation anomalies simulated for 1980, however, does not show the opposite relationship but a more neutral character with near zero rainfall anomalies simulated for the period over the major part of South Africa. Here it must also be kept in mind that the 1980 season falls in the above-normal period of the near-decadal rainfall cycle, and it is not an El Niño year. The 1986 season also has a simulation that does not deviate from the normal for almost the whole of South Africa. The 1988 season, however, shows an opposite association to the remainder of the precipitation simulations that indicates that it cannot be explained by the methods used in this study alone.

Table 4.2. Average NINO3 SST anomalies for JFM for 1979 to 1988.

Year	Average NINO3 SST anomaly for JFM (°C)
1979	0.18
1980	0.38
1981	-0.32
1982	0.27
1983	2.89
1984	-0.10
1985	-0.90
1986	-0.39
1987	1.29
1988	0.47

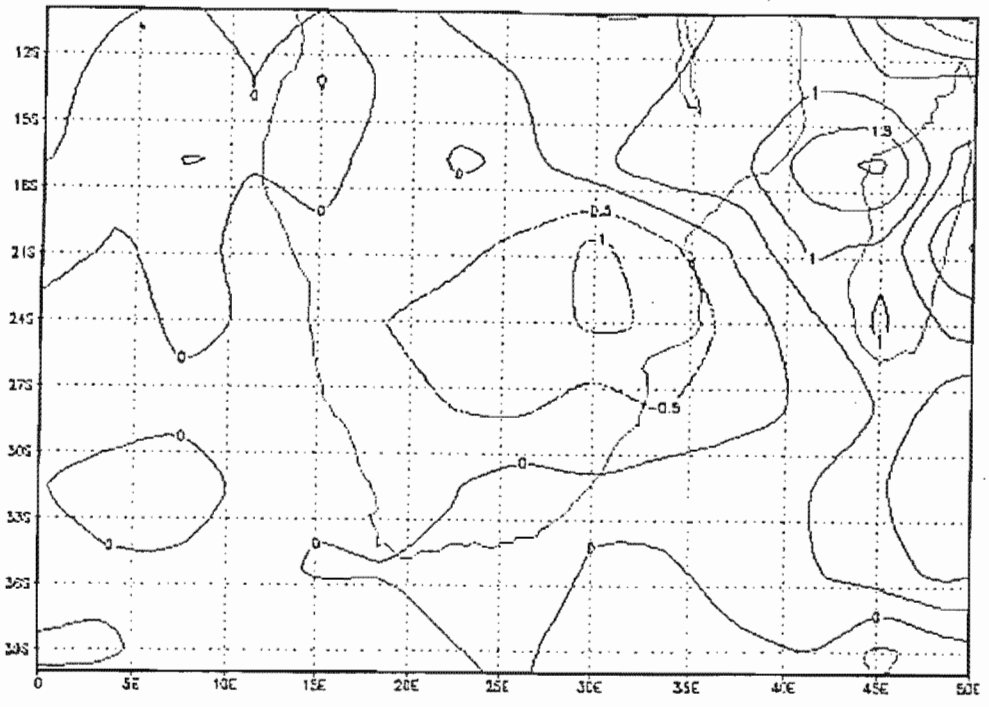

Figure 4.49. Average precipitation anomaly simulation for JFM for 1979 (mm.day^{-1}).

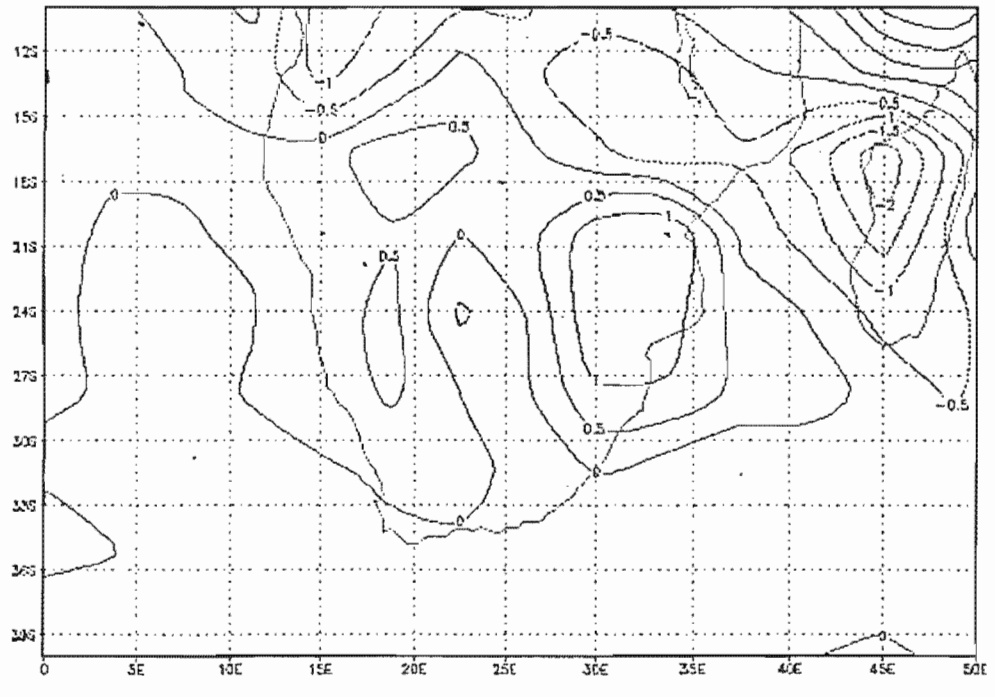

Figure 4.50. The same as Figure 4.49, but for 1980.

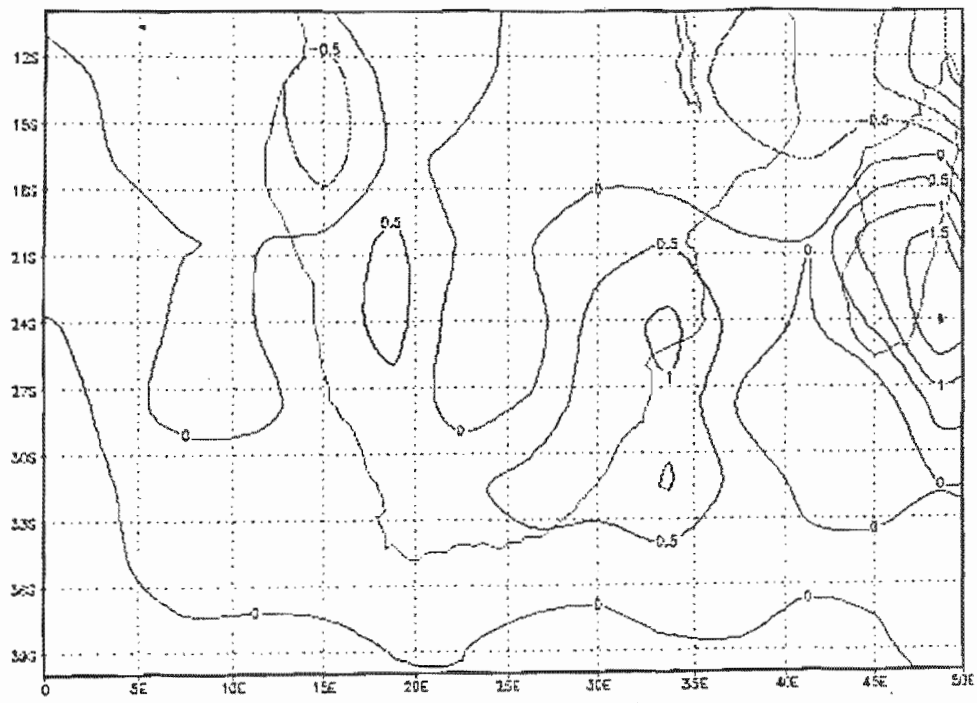

Figure 4.51. The same as Figure 4.49, but for 1981

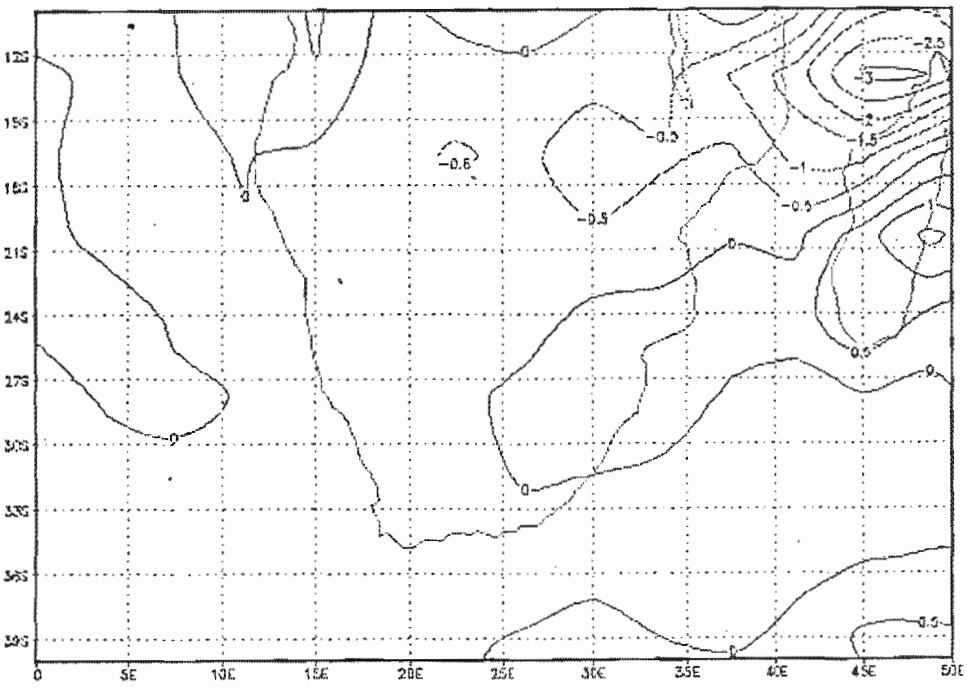

Figure 4.52. The same as Figure 4.49, but for 1982

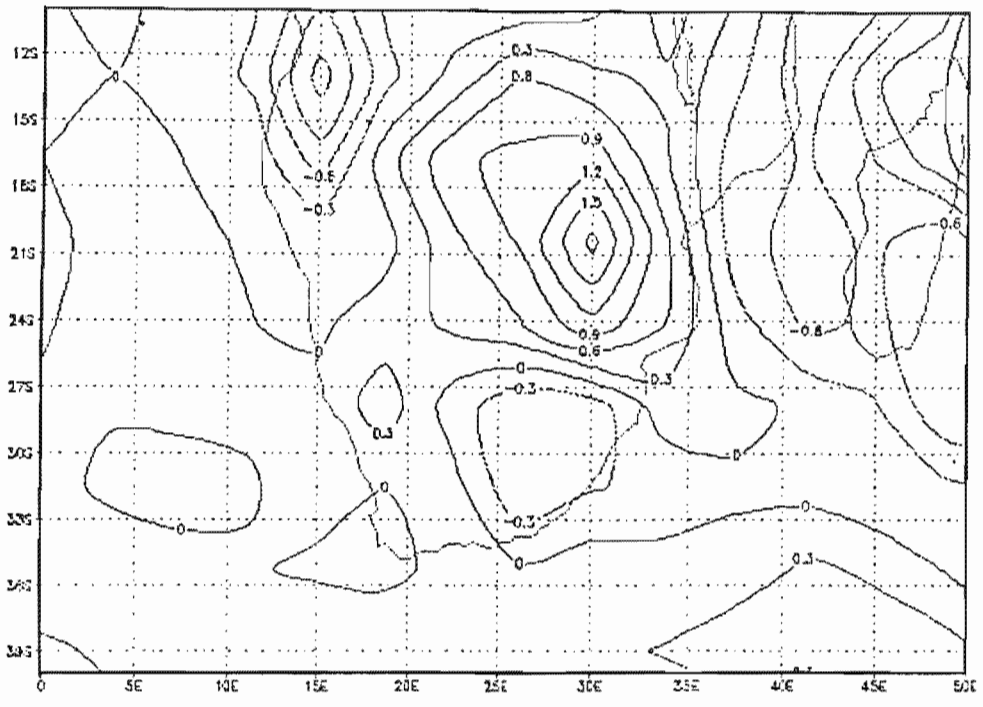

Figure 4.55. The same as Figure 4.49, but for 1985

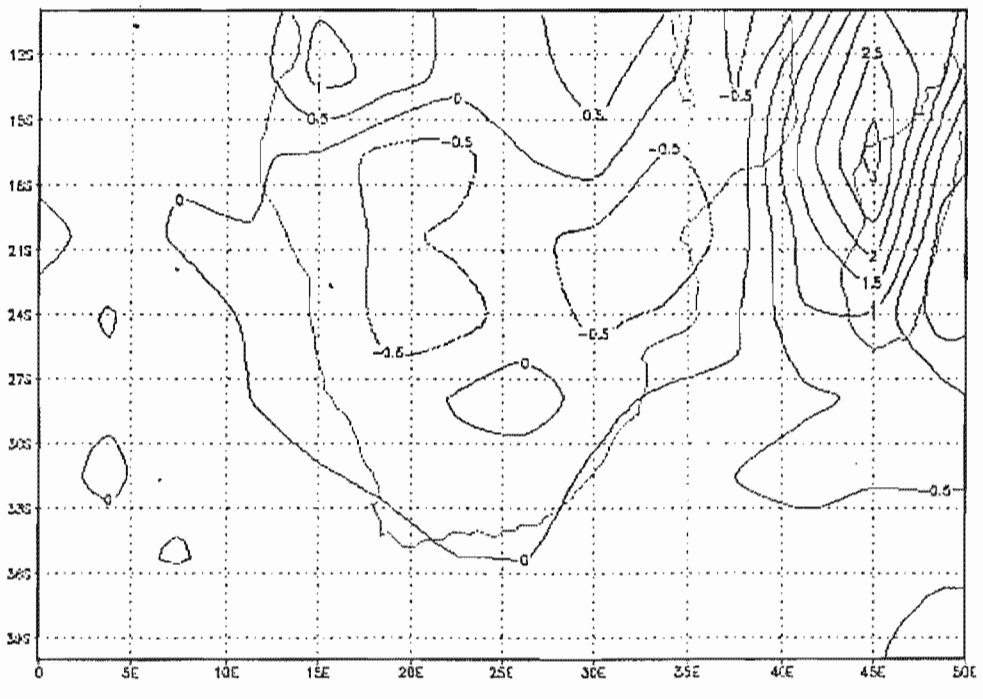

Figure 4.56. The same as Figure 4.49, but for 1986.

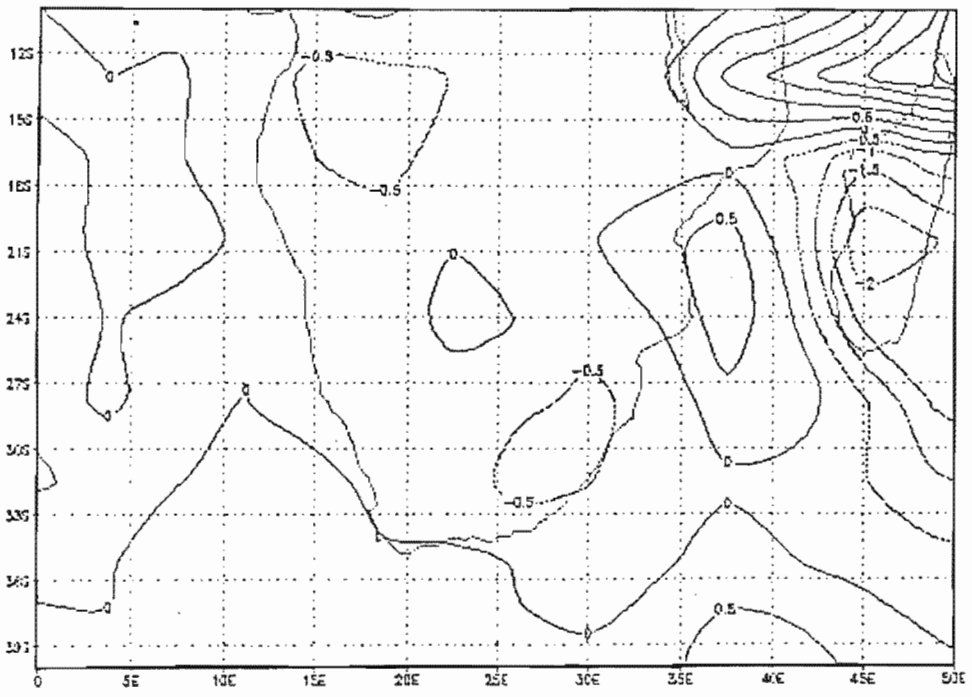

Figure 4.57. The same as Figure 4.49, but for 1987.

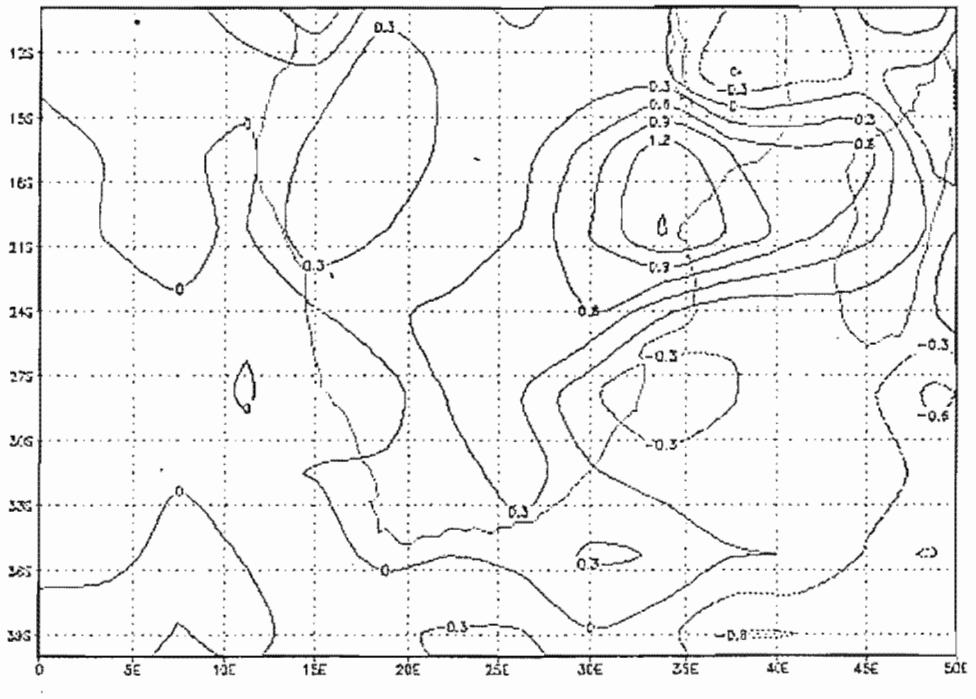

Figure 4.58. The same as Figure 4.49, but for 1988.

4.5.2.2. Observed SST's compared to 1000 hPa and 500 hPa geopotential height anomaly simulations

Figures 4.59 to 4.68 show the average 1000 hPa geopotential height anomalies for JFM for 1979 to 1988 respectively while Figures 4.69 to 4.78 show the same for the 500 hPa level. For the pressure simulations to show the same relationships as that found with CCA analysis, above (below)-normal 1000 hPa and 500 hPa heights over the subcontinent and adjacent areas should be associated with above (below)-normal NINO3 SST's. These relationships are indeed confirmed with the results of the model simulations, except for the 500 hPa height anomalies for 1979, 1980, 1984 (with an opposite association towards the east of the subcontinent), and 1988 (only the 500 hPa height anomalies). Thus a positive verification is obtained for 14 of the 20 simulations, i. e. 70%.

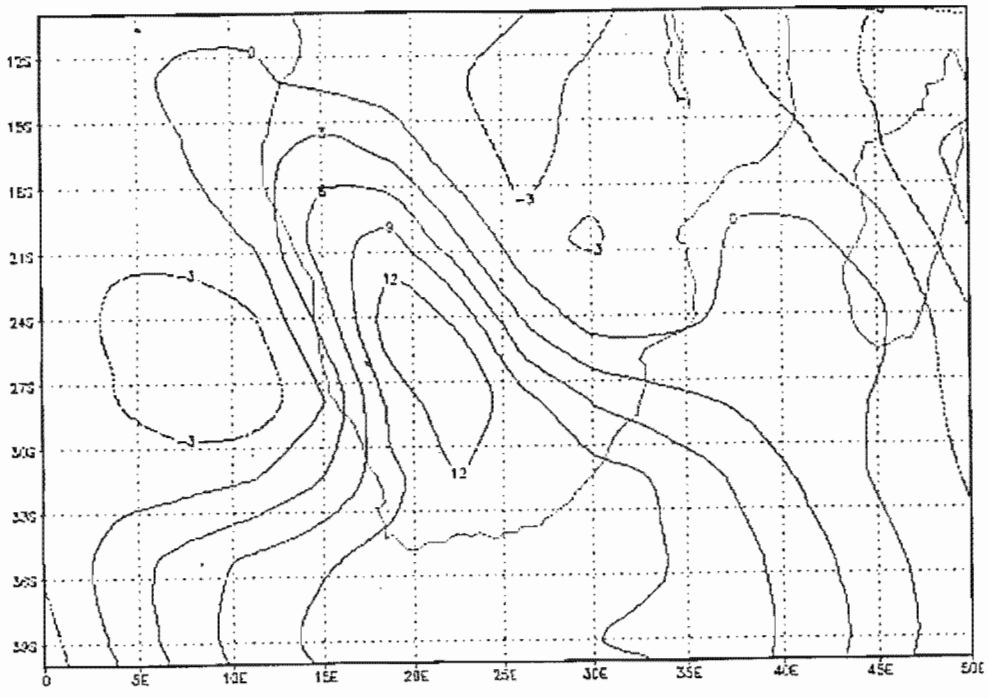

Figure 4.59. Average GCM simulation for 1000 hPa level for JFM for 1979 (gpm).

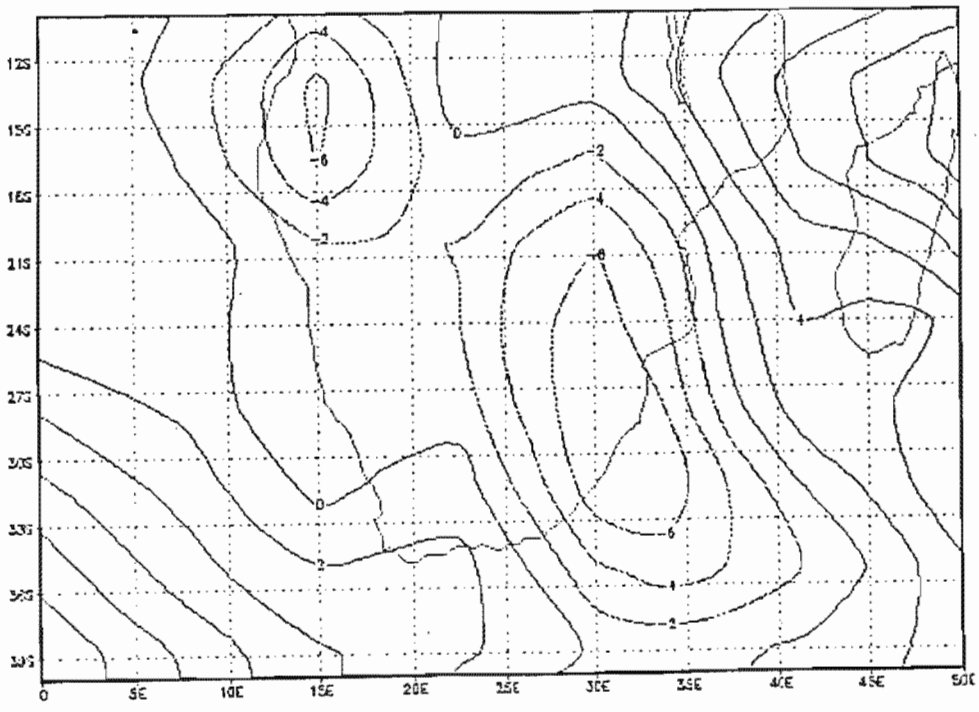

Figure 4.60. The same as Figure 4.59, but for 1980.

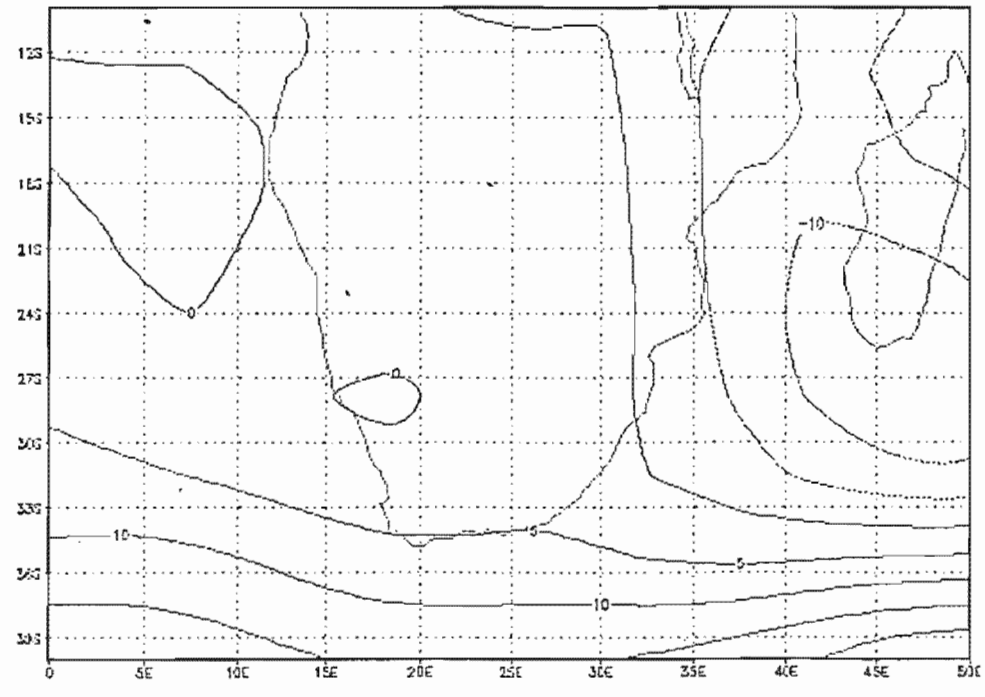

Figure 4.61. The same as Figure 4.59, but for 1981.

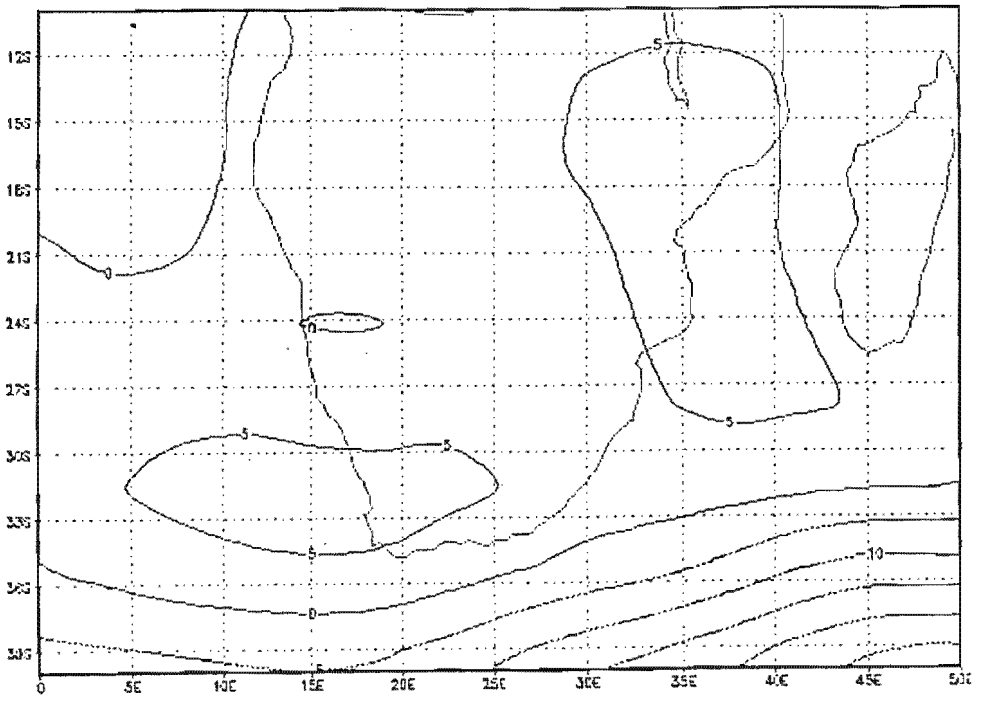

Figure 4.62. The same as Figure 4.59, but for 1982.

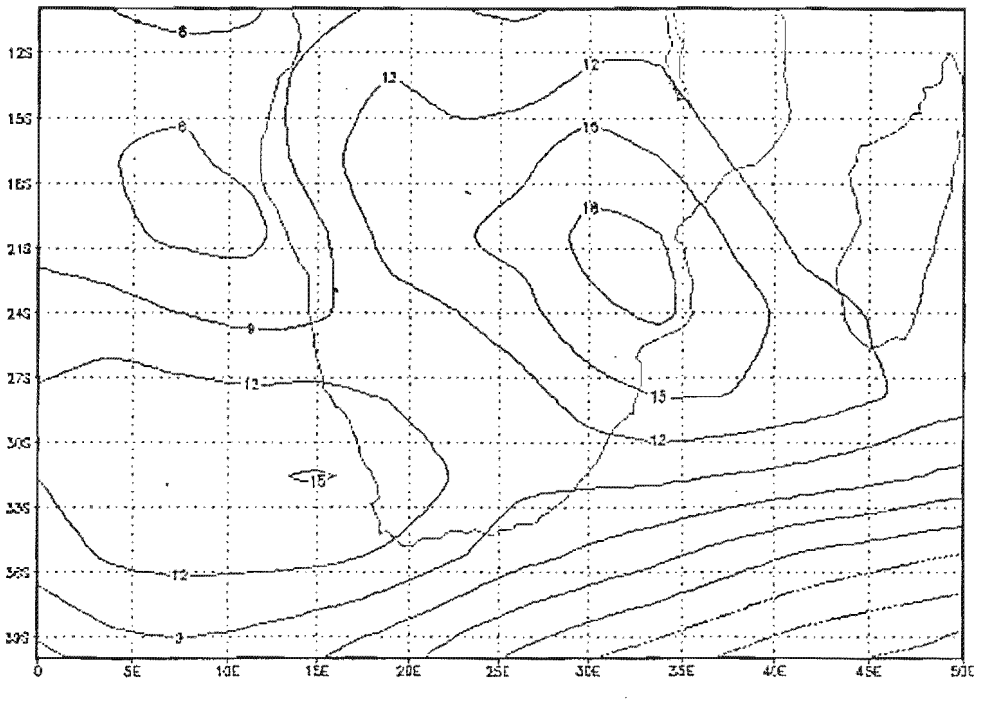

Figure 4.63. The same as Figure 4.59, but for 1983.

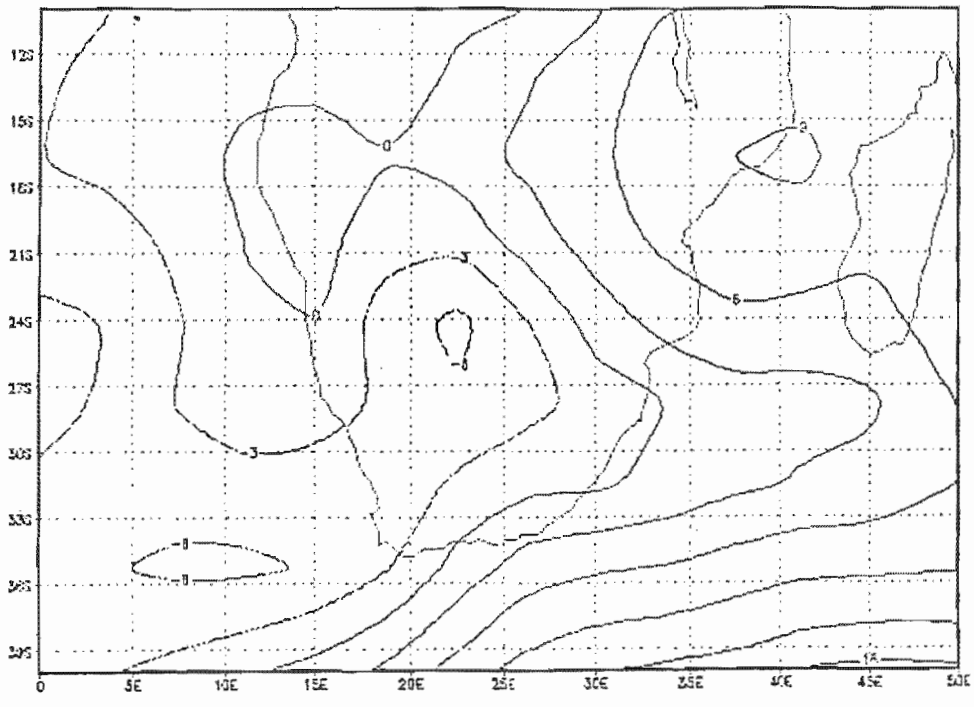

Figure 4.64. The same as Figure 4.59, but for 1984.

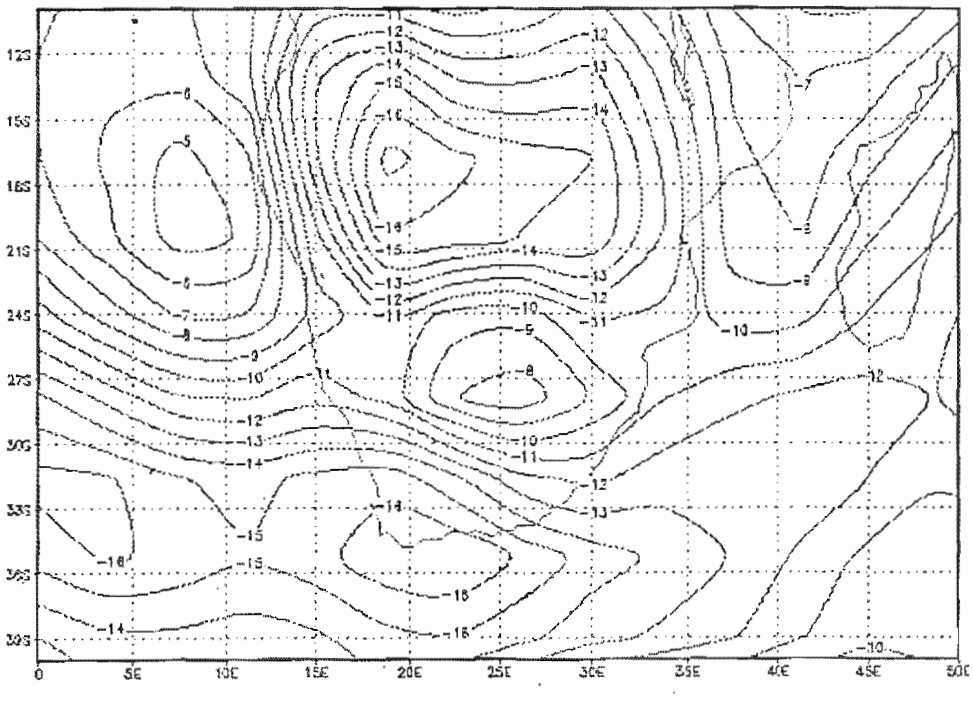

Figure 4.65. The same as Figure 4.59, but for 1985.

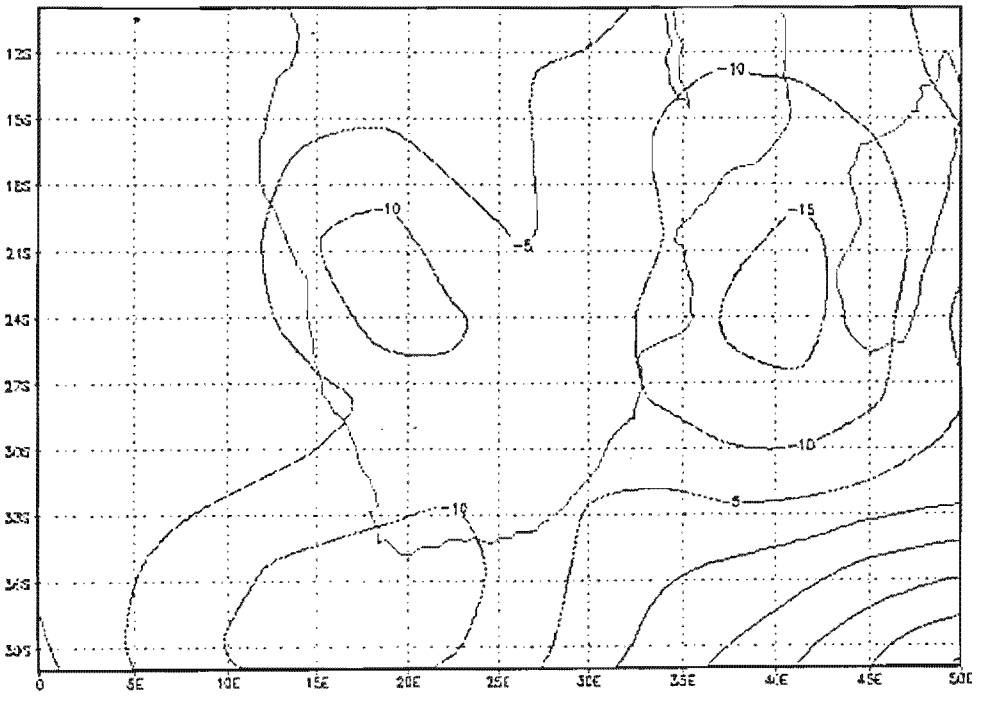

Figure 4.66. The same as Figure 4.59, but for 1986.

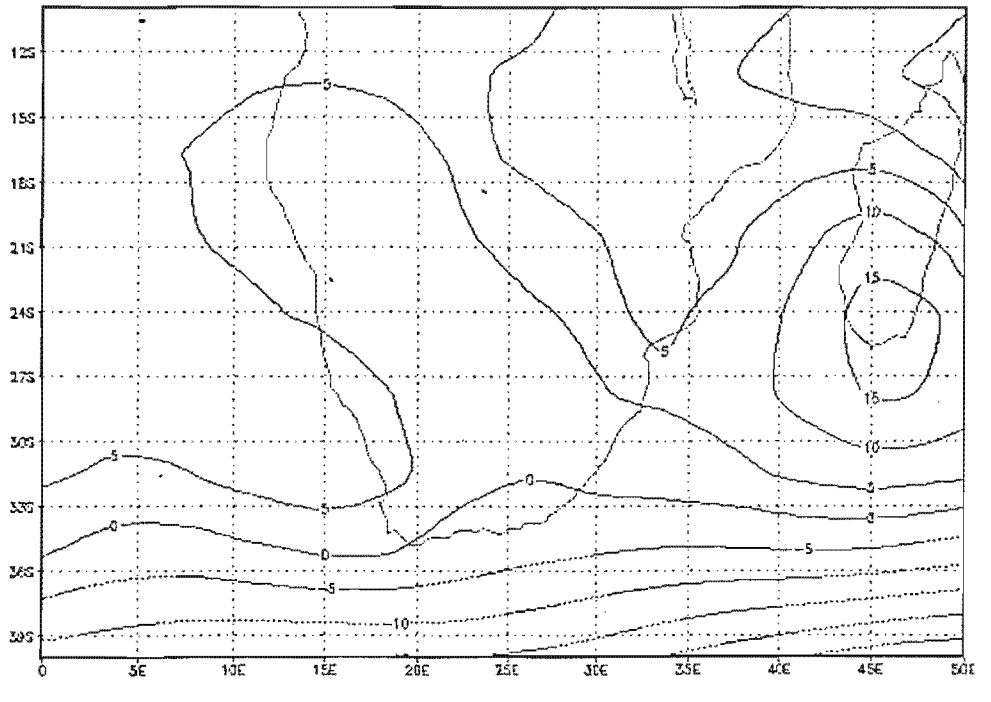

Figure 4.67. The same as Figure 4.59, but for 1987.

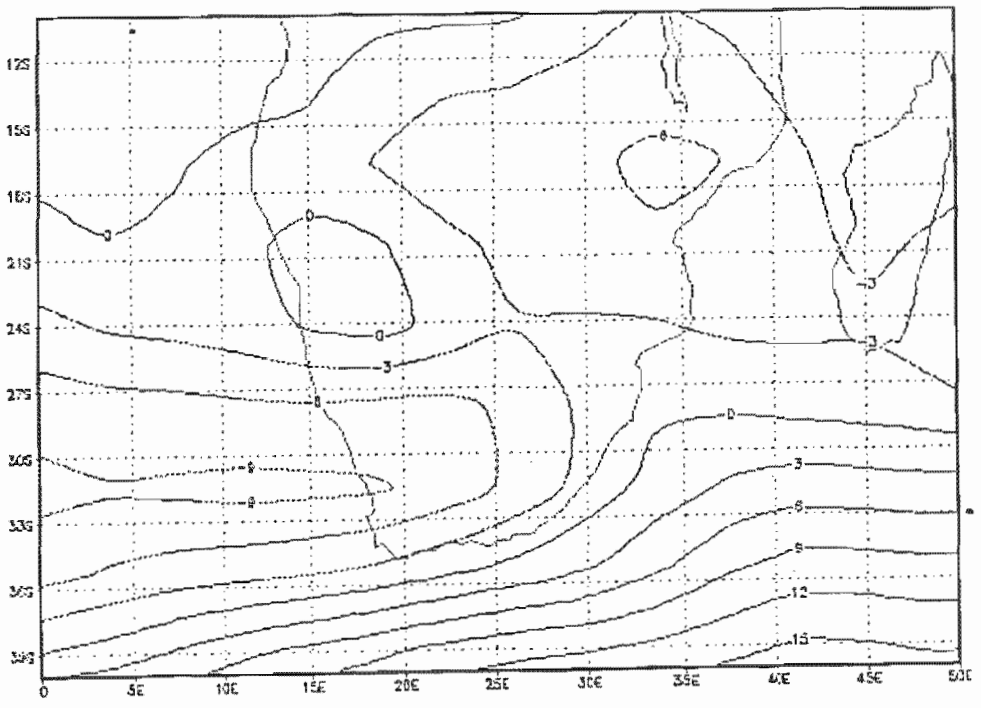

Figure 4.68. The same as Figure 4.59, but for 1988.

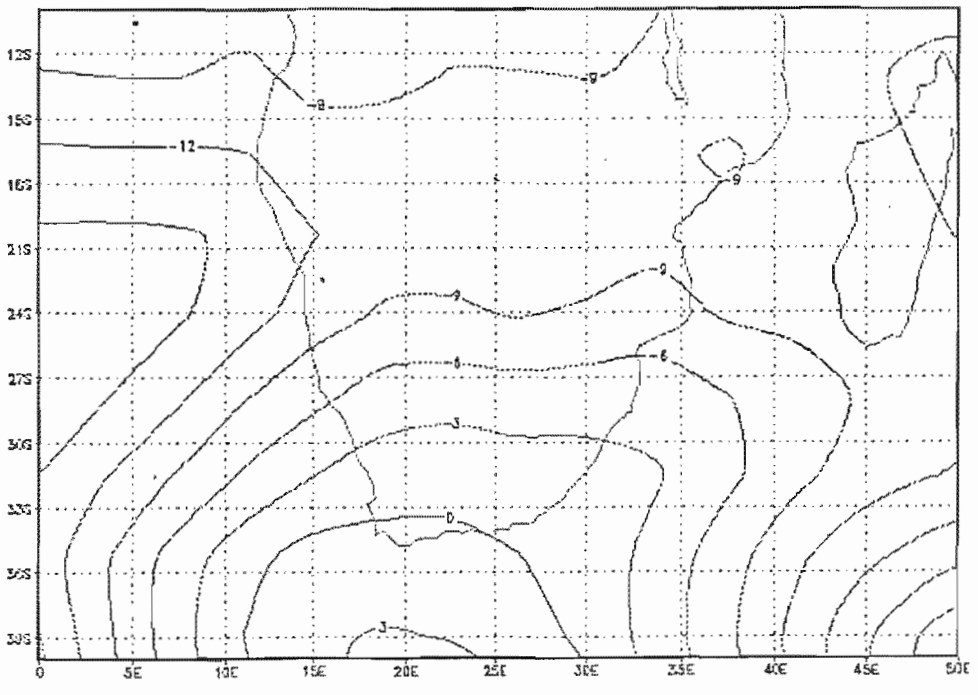

Figure 4.69. Average GCM simulation of the 1000 hPa level for JFM for 1979 (gpm).

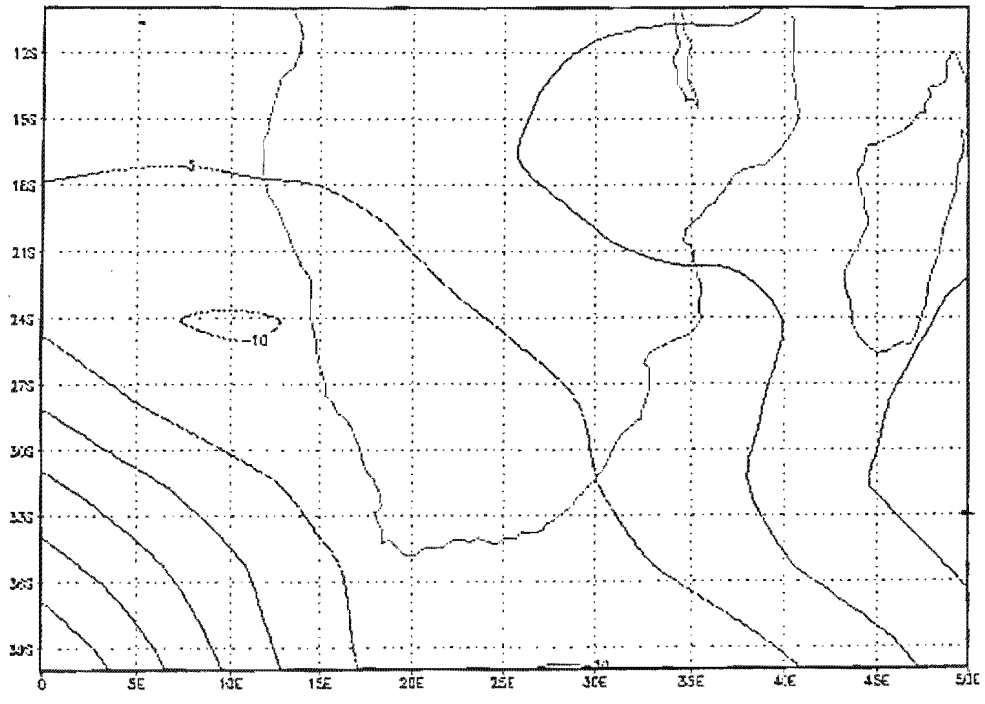

Figure 4.70. The same as Figure 4.69, but for 1980.

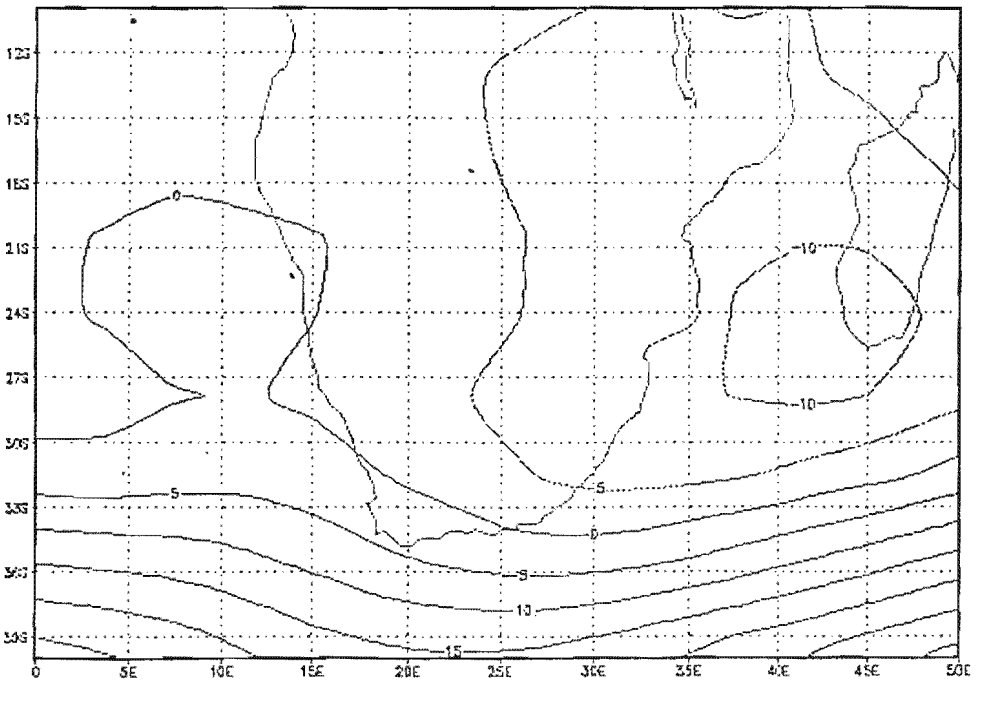

Figure 4.71. The same as Figure 4.69, but for 1981.

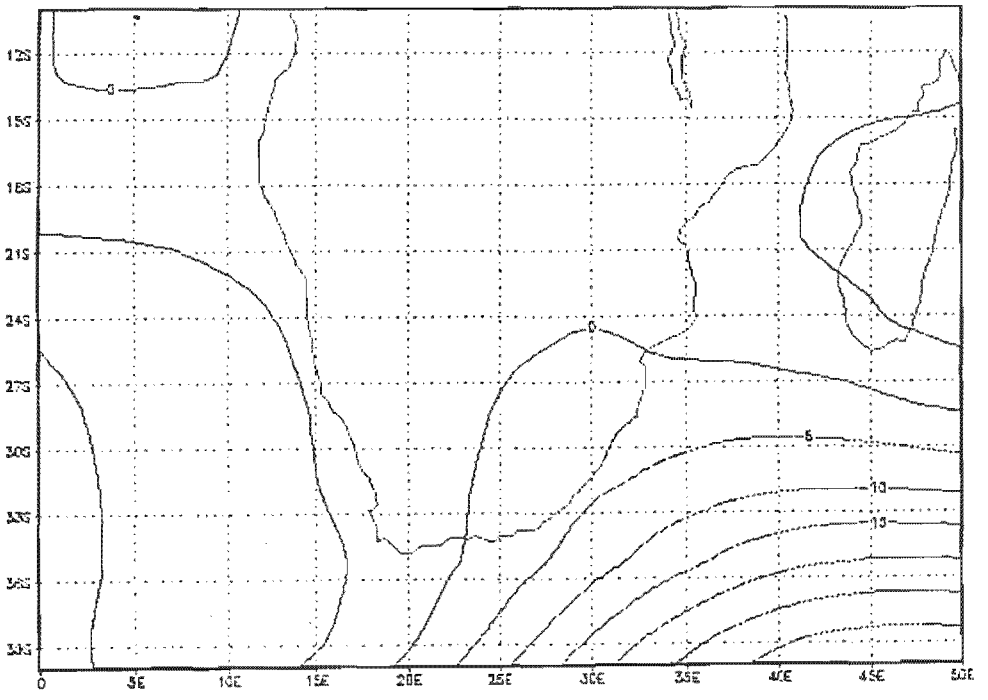

Figure 4.72. The same as Figure 4.69, but for 1982.

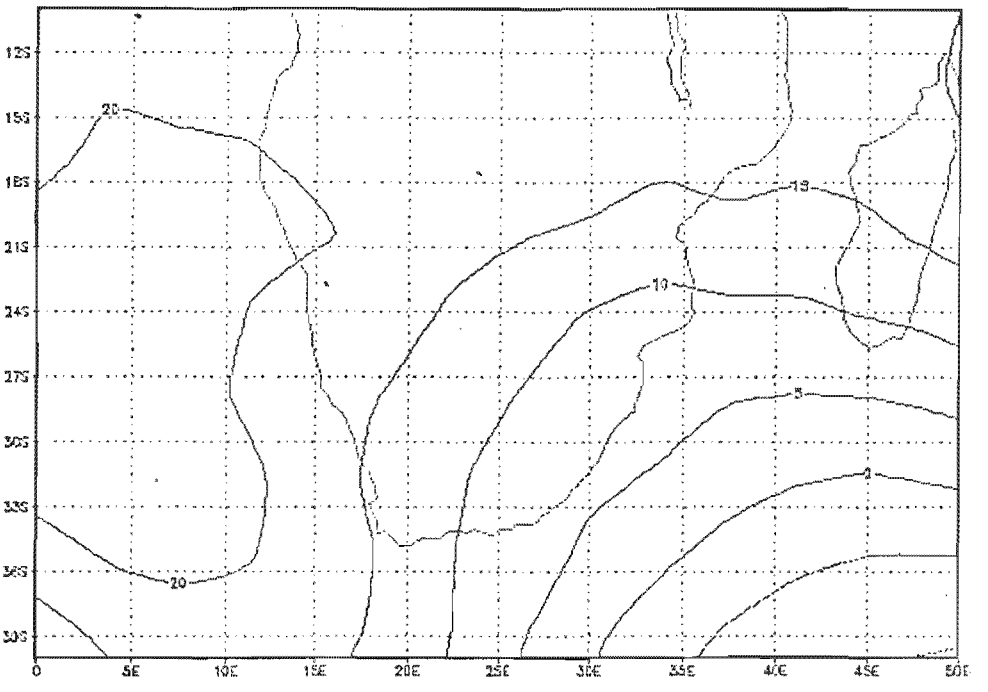

Figure 4.73. The same as Figure 4.69, but for 1983.

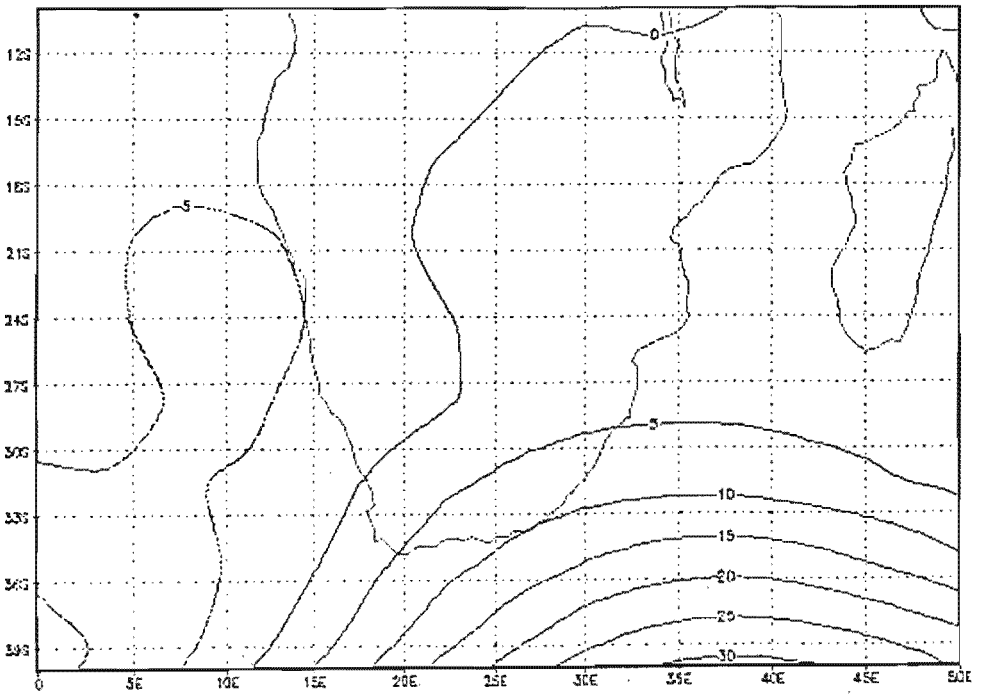

Figure 4.74. The same as Figure 4.69, but for 1984.

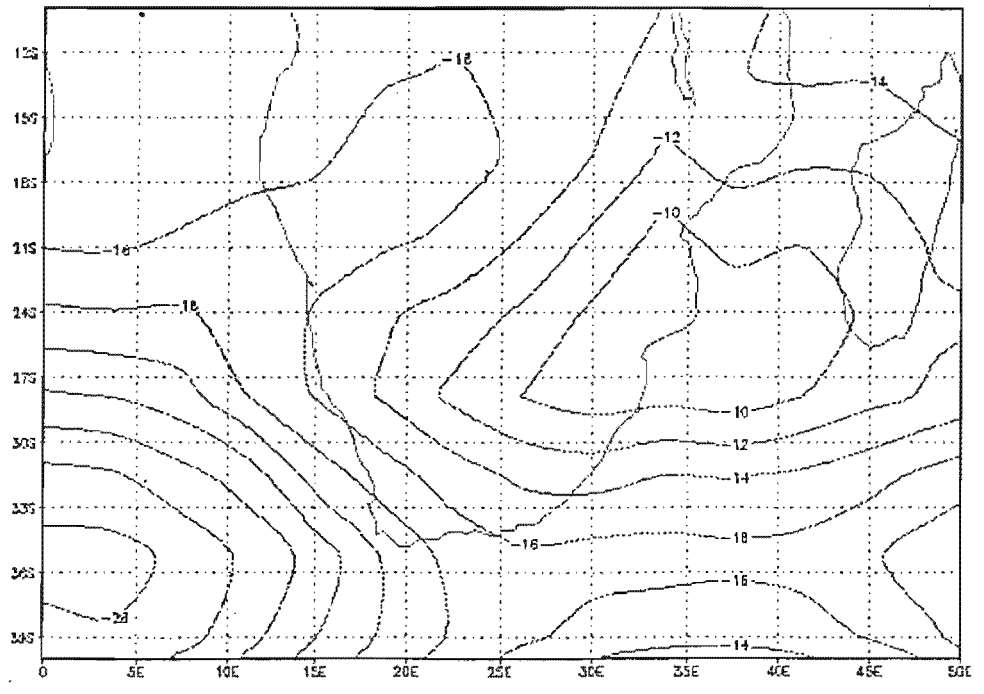

Figure 4.75. The same as Figure 4.69, but for 1985.

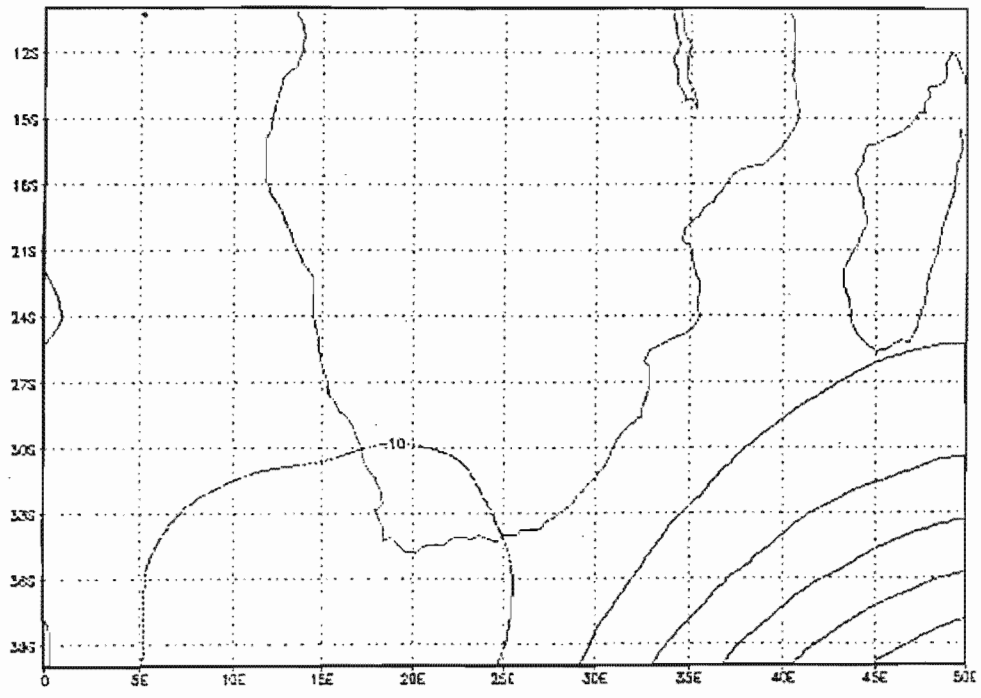

Figure 4.76. The same as Figure 4.69, but for 1986.

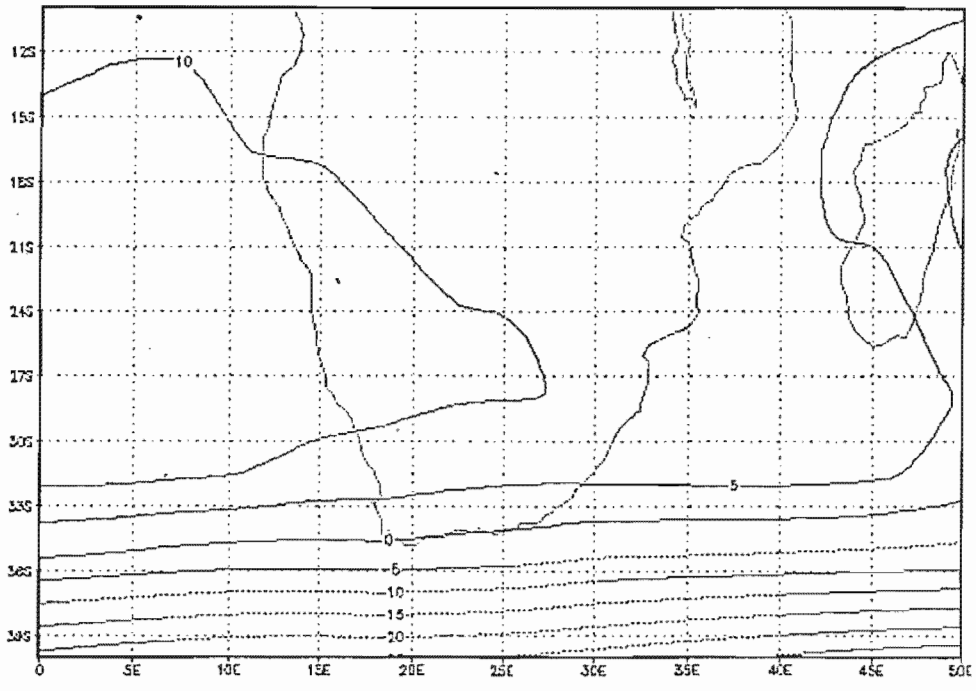

Figure 4.77. The same as Figure 4.69, but for 1987.

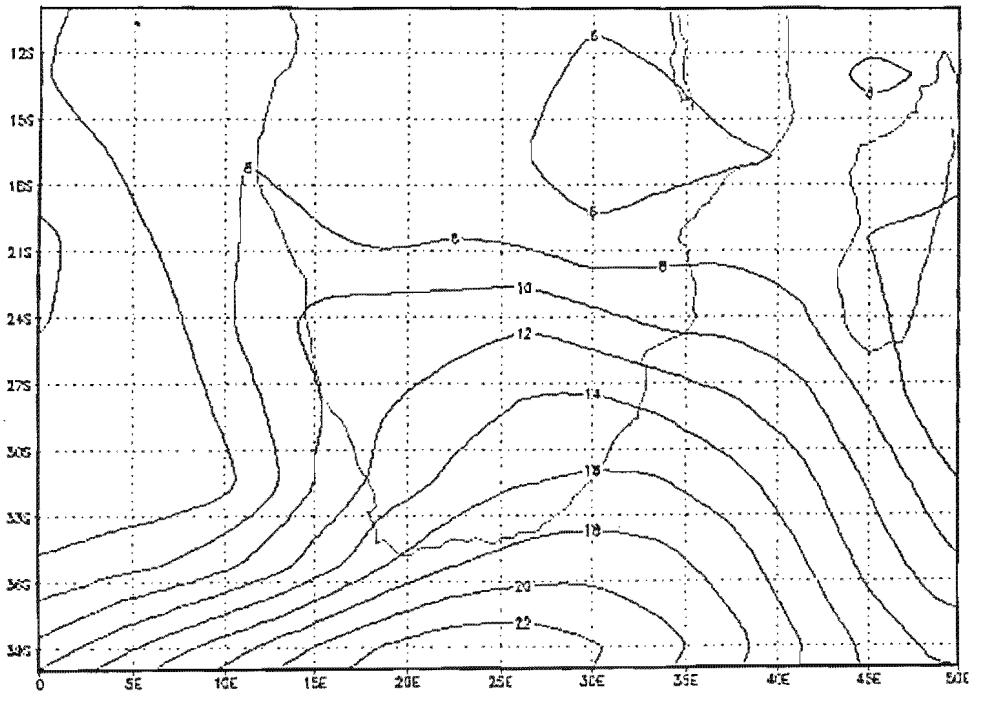

Figure 4.78. The same as Figure 4.69, but for 1988.

4.5.2.3. Precipitation anomaly simulations compared to 1000 hPa and 500 hPa geopotential height simulations

To verify the relationships obtained with CCA, above (below)-normal 1000 hPa and 500 hPa height anomalies should correspond to below (above)-normal precipitation anomalies over the area of the subcontinent shown in Figure 2.3(b). This is indeed the case for most of the seasons except again for the 500 hPa height anomalies for 1979, the 1984 geopotential height anomalies for both levels toward the south, east and northeast of the subcontinent, the 1985 precipitation anomalies in the southeast, 1986, and the 1988 500 hPa geopotential height anomalies. Thus the relationships hold again for 14 of the 20 cases, i.e. 70%.

4.5.3. Conclusions from comparison of CCA results with model runs

The AMIP model runs of the GENESIS (version 2.0a) model confirm in general the relationships between observed NINO3 SST anomalies, precipitation and 1000 hPa and 500 hPa geopotential height anomalies obtained from CCA. In all comparisons, a 70 % correspondence was found with the above relationships established with CCA. Fortunately most of the model simulations fall in the same part (below-normal) of the inter-decadal rainfall cycle, so that comparisons between seasons could easily be made without the additional complications that can be brought about by this cyclic behaviour of the rainfall. Although the AGCM outputs have been used to provide additional degrees of freedom, it can also provide a means of, e.g. why the atmospheric pressure increases during dry years, and decrease during wetter years. This, however, falls beyond the scope of this study.

CHAPTER 5

INTERPRETATION OF RESULTS

5.1. Introduction

With the results in Chapter 4 it can be inferred that, in general, periods or seasons associated with anomalously high equatorial Pacific SST's, are also associated with anomalously high 1000 hPa as well as 500 hPa geopotential heights over the subcontinent. As anomalously high (low) SST's are associated with high (low) rainfall (Chapter 2), this result merely confirms the findings of Hofmeyr and Gouws (1964), Tyson (1981, 1984, 1986), Matarira (1990), Matarira and Jury (1992), Shinoda and Kawamura (1996) and others. It is only with more detailed inspection of the results of Chapter 4, that other associations become apparent. To assess the effect of anomalous SST's on the atmospheric circulation over the subcontinent, average circulation maps for the six combinations of years, identified in Chapter 4, for both pressure levels under consideration (1000 hPa and 500 hPa), are obtained. Interpretation of the effects of circulation anomalies associated with anomalously high or low equatorial Pacific SST's on this average circulation during specific conditions (e. g. only El Niño years) is then attempted.

5.2. Interpretation of results

5.2.1. All years

The maps for the average geopotential heights for the 1000 hPa and 500 hPa levels for the period 1958 to 1997 for JFM, are shown in Figure 5.1.1 and 5.1.2 respectively. From Figure 5.1.1 one can see that the average circulation at the surface over the southern African subcontinent is roughly characterized by two high pressure cells situated on either side of the subcontinent, a low pressure over the Namibia/Botswana region, as well as a deeper but spatially smaller low pressure in the Mozambique Channel. From Figure 5.1.2 the average 500 hPa geopotential heights show a ridge from the west over the subcontinent at about 20 to

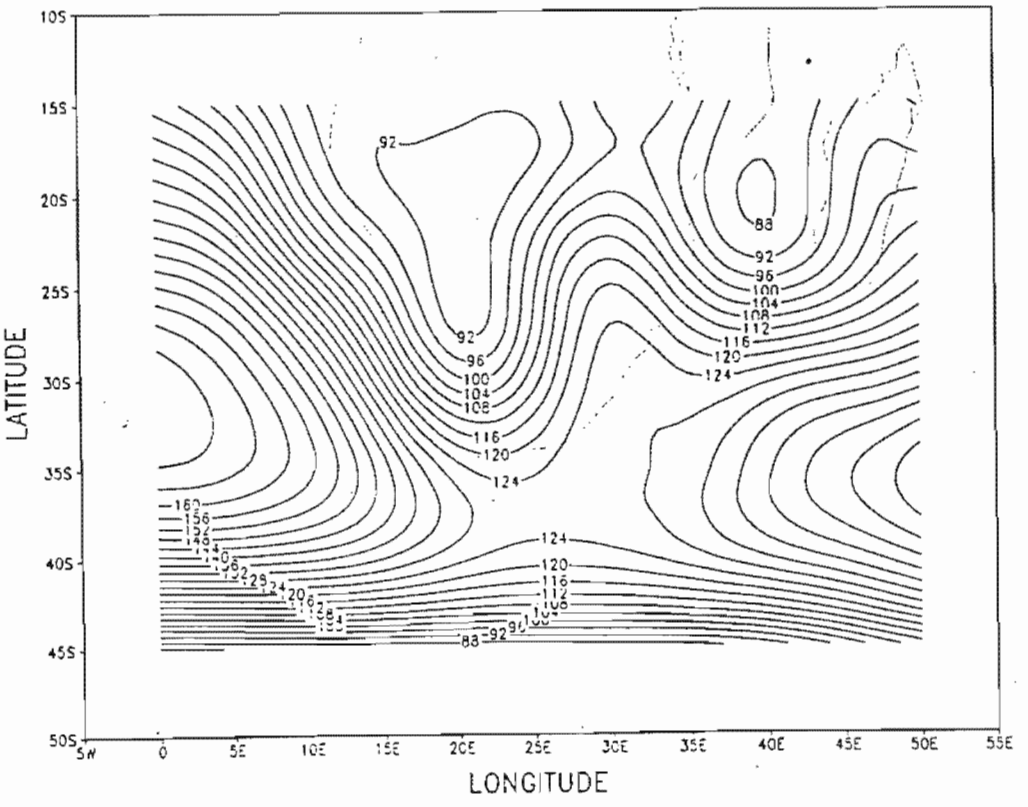

Figure 5.1.1. Average geopotential height of the 1000 hPa level for JFM for the period 1958 to 1997.

25°S with a gradual decrease in heights southwards.

Referring to section 4.4.1 to 4.4.2, one can see that anomalously high equatorial Pacific SST's are associated with a strengthening of the ridge on the western side of the subcontinent and a weakening of the ridge on the eastern side. This is significant in the sense that the ridge on the eastern side is usually responsible for the influx of moist air from the east, while the western ridge is associated with a southern to south-western influx of dry air. If this ridge should strengthen, as is inferred, more dry air will be transported into the area over the subcontinent while the weakening of the eastern ridge causes less moist air to be transported from the east. The net result of this is less rain over the subcontinent during the JFM period. For the case of anomalously low equatorial Pacific SST's, the opposite situation is inferred

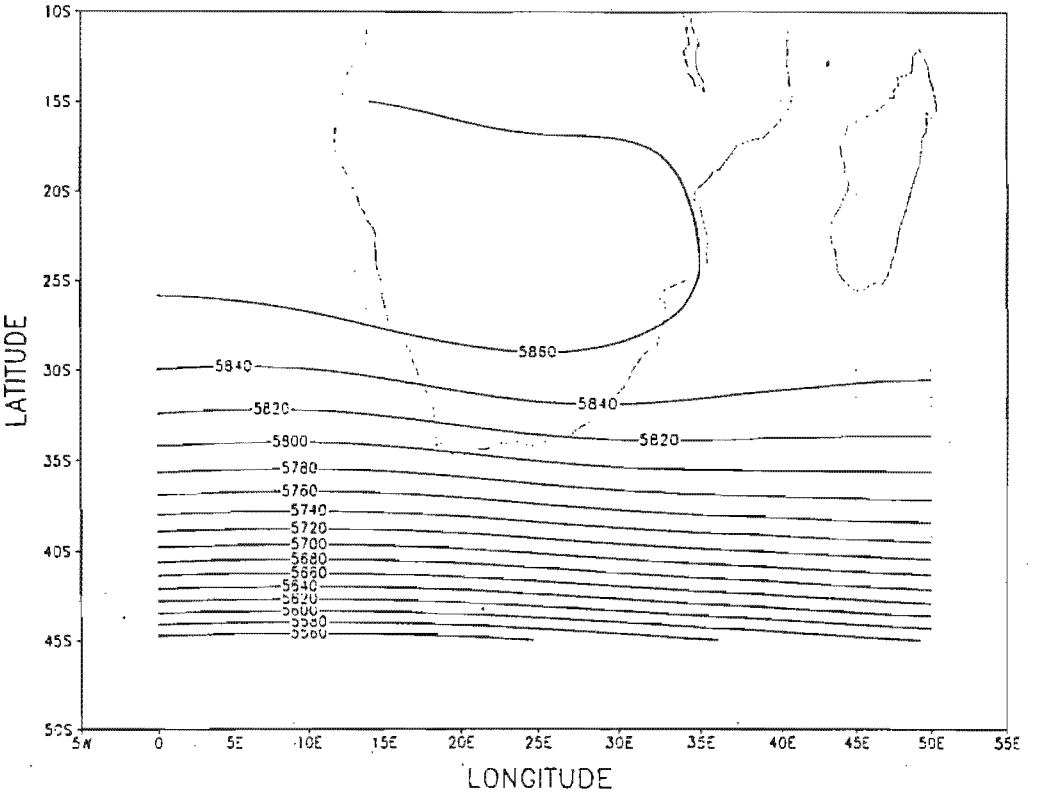

Figure 5.1.2. The same as Figure 5.1.1, but for the 500 hPa level.

with a stronger influx of moisture from the east and less dry air from the south to south-west, with the result that more rain can be expected over the interior. For the 500 hPa level an increase (decrease) of geopotential heights is suggested over the subcontinent and surrounding oceans during periods of anomalously high (low) SST's. This means that the ridge on this level over the subcontinent will strengthen (weaken), inhibiting (encouraging) the development of strong troughs over the interior that are associated with rain-bearing synoptic systems.

5.2.2. Only ENSO years

Figures 5.2.1 and 5.2.2 show the average 1000 hPa and 500 hPa geopotential heights for ENSO years, i. e. El Niño and La Niña years. These maps look roughly similar to Figures

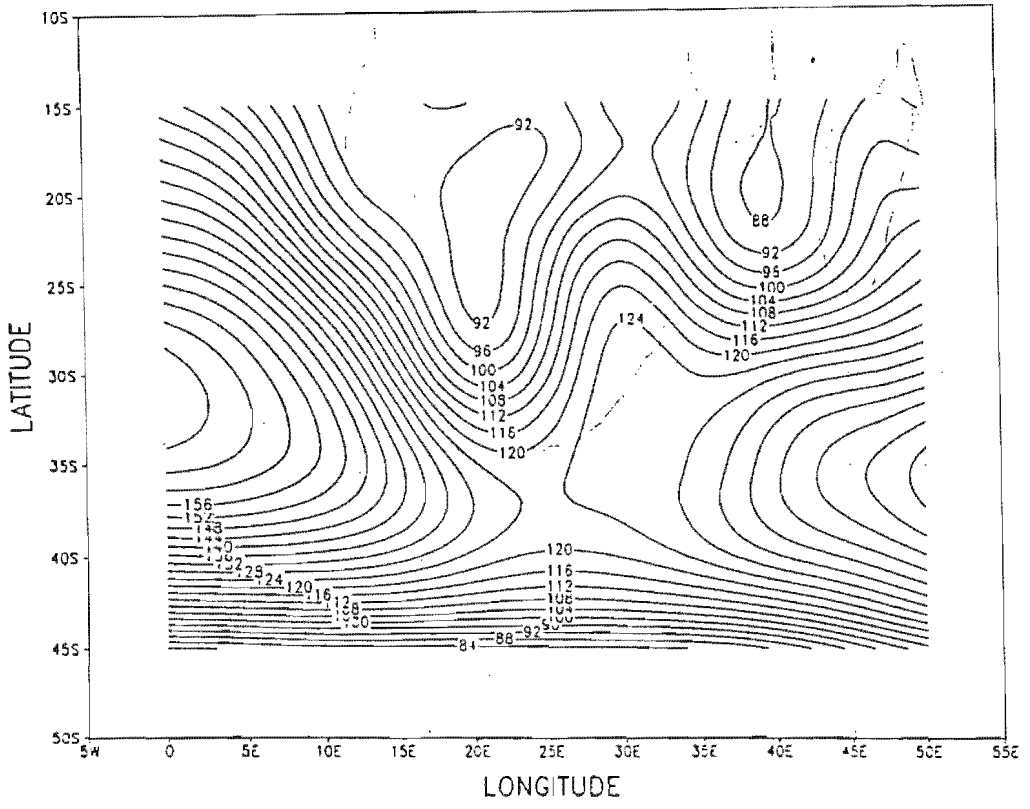

Figure 5.2.1. The same as Figure 5.1.1, but for ENSO years only

5.1.1 and 5.1.2 because ENSO years are years where the equatorial Pacific SST's can be either very high or very low. The highs and lows are at about the same positions and strengths at both 1000 hPa and 500 hPa. Referring to sections 4.4.3 and 4.4.4 one can infer that anomalously high (low) SST's trigger the same anomalous conditions in the 1000hPa and 500 hPa heights as was the case where all years were taken into consideration.

5.2.3. Only El Niño years

The average synoptic situations during El Niño years only are shown in Figure 5.3.1 and 5.3.2 for the 1000 hPa and 500 hPa levels respectively. This is thus the average situation associated with very high equatorial Pacific SST's. If we compare the circulation at the surface to the average situation for all years we see that the ridges on either side of the subcontinent are slightly stronger, especially on the eastern side. The low pressures over

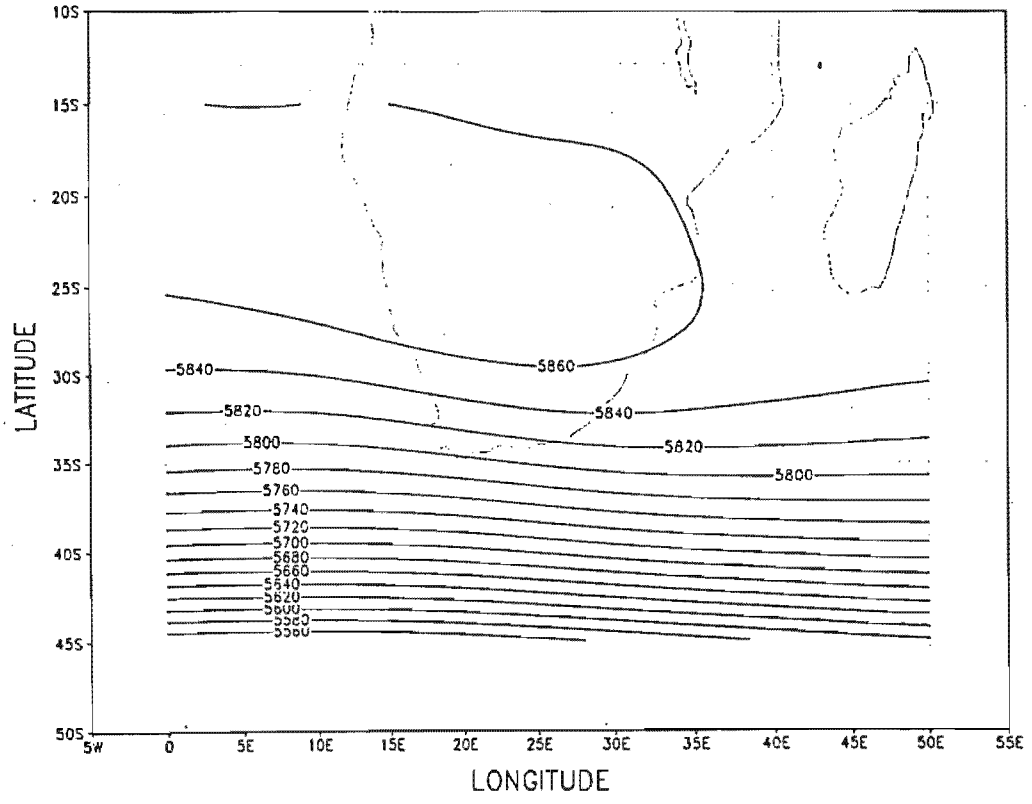

Figure 5.2.2. The same as Figure 5.1.2, but for ENSO years only.

Botswana/Namibia and in the Mozambique Channel are both weaker and smaller in aerial extent. While the slight strengthening of the eastern ridge can cause a stronger influx of moist air, the weakening of the Namibia/Botswana trough causes reduced convective development, the main source of precipitation over the interior, as well as reduced influx of moisture laden air from the tropics. The 500 hPa level for El Niño years only, shows higher geopotential heights for that level as well as a closed high pressure cell over the western side of the subcontinent compared to a ridge in the average situation where all years are taken into account. This shows again that usually during El Niño seasons, the formation of troughs over the subcontinent is inhibited so that reduced rainfall can be expected.

Referring to sections 4.4.5 and 4.4.6 one can see that anomalously high (low) SST's during El Niño years are generally associated with higher (lower) geopotential heights over the

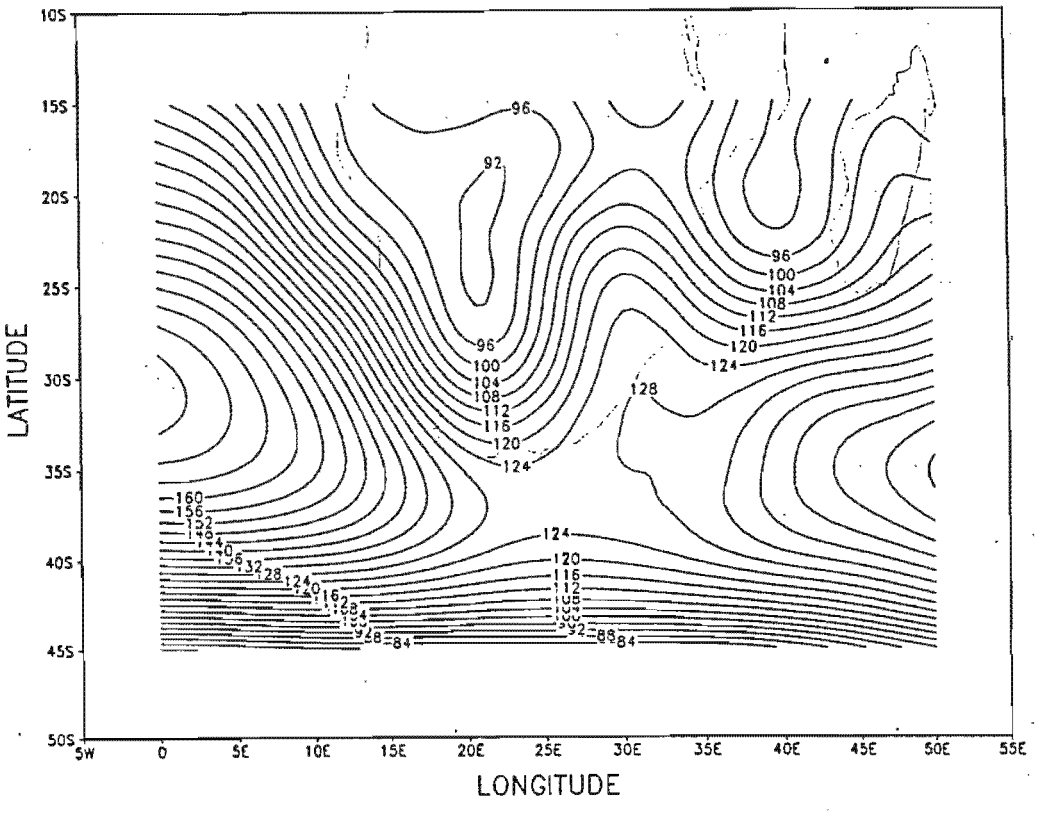

Figure 5.3.1. The same as Figure 5.1.1, but for El Niño seasons only.

whole subcontinent at the 1000 hPa level, decreasing (increasing) southwestwards. These higher (lower) geopotential heights are especially prominent just west of the subcontinent and over an area in the south of the Mozambique Channel. This suggests a strengthening (weakening) of the ridge west of the subcontinent which can be associated with a stronger (weaker) influx of dry air from the south-west over the subcontinent. Also a possible northward (southward) displacement and slight weakening (strengthening) of the ridge to the east of the country is suggested so that influx of moist air from the east will be displaced north (south). These all suggest drier (moister) air over the subcontinent with the result that less (more) rain can be expected when SST's are anomalously high (low) for an El Niño event. For the 500 hPa level anomalously high (low) SST's between about 150°W and the South American coast causes an increase (decrease) in geopotential heights over the whole

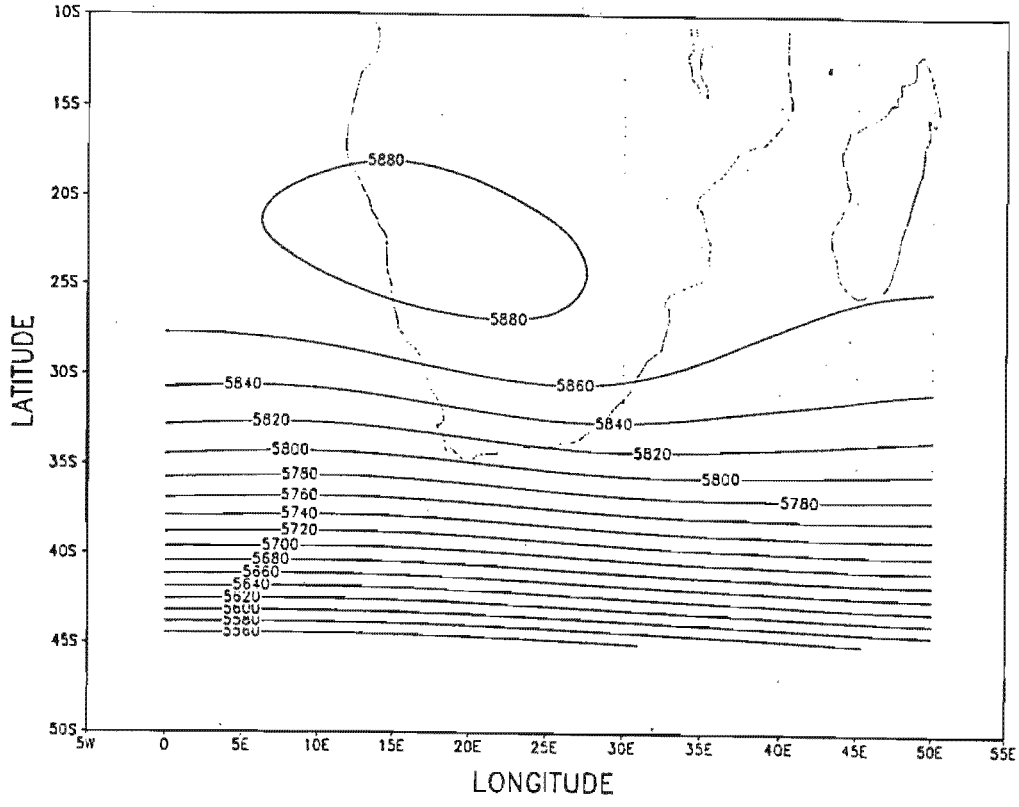

Figure 5.3.2. The same as Figure 5.1.2, but for El Niño seasons only.

subcontinent so that weakening (strengthening) of troughs can be expected, with the result of a weaker (stronger) influx of moist air from the tropics, with the associated probability of less (more) rain over the interior. For the SST's from about 140°W to 180°W the opposite applies.

5.2.4. Only La Niña years

Figures 5.4.1 and 5.4.2 show the average 1000 hPa and 500 hPa heights during La Niña years only. The differences between these maps and that for the average circulation in general (Figures 5.1.1 and 5.1.2), show a slight weakening of the ridges on either side of the

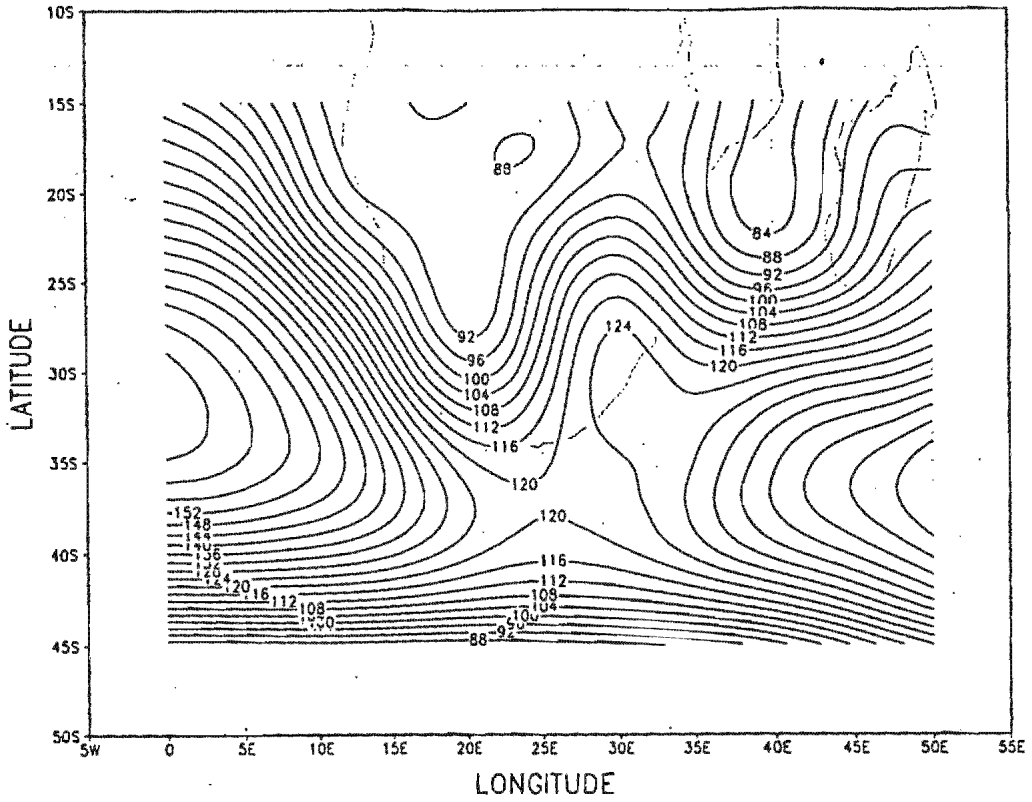

Figure 5.4.1. The same as Figure 5.1.1, but for La Niña seasons only.

subcontinent, but a significant deepening of the low pressure over Botswana/Namibia and accompanying strengthening of the associated trough extending southwards at the surface. This improves the chances for convective development over the interior as well as influx of tropical moist air from the tropics. At the 500 hPa level a reduction in heights over the whole area under consideration compared to the average situation in general is evident. This also enhances the chances for troughs to develop over the interior with improved influx of moist air from the tropics.

The analyses in sections 4.4.7 and 4.4.8 associate higher (lower) SST's with higher (lower) 1000 hPa geopotential heights adjacent to the Northern Cape and Namibian coast; also lower (higher) over the interior, especially Namibia, and to the south. This suggests a probable northward (southward) displacement of the ridge to the west of the subcontinent as well as a

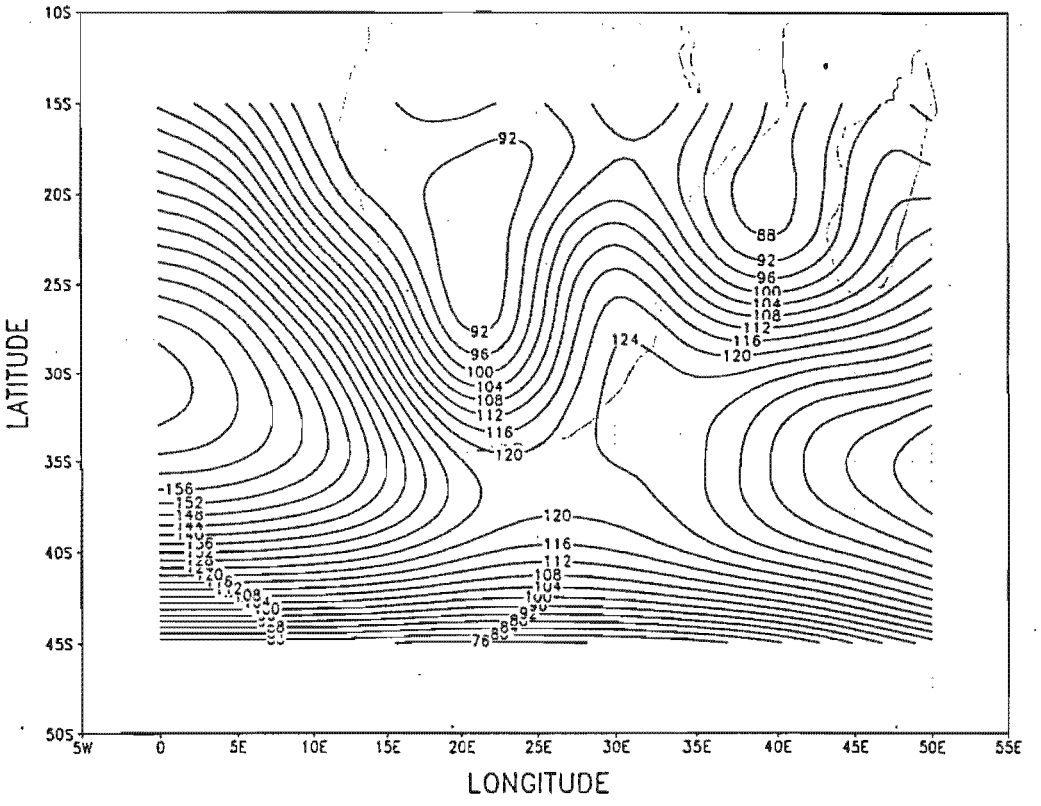

Figure 5.6.1. The same as Figure 5.1.1, but for ENSO seasons during the below-normal part of the decadal rainfall cycle only.

Zimbabwe, might even receive slightly more (less) rainfall.

5.2.6. Only ENSO years occurring during the below-normal part of the decadal rainfall cycle

Figures 5.6.1 and 5.6.2 show the average geopotential heights during ENSO years occurring during the below-normal part of the decadal rainfall cycle for the 1000 hPa level and 500 hPa level respectively. Comparing these maps with the average situation where all years are taken into account, one can see that the maps are similar in the distribution of high and low pressure, but the high pressures are somewhat weaker while the low pressure area in the Mozambique Channel is a bit deeper at the 1000 hPa level. This suggests that influx of moist

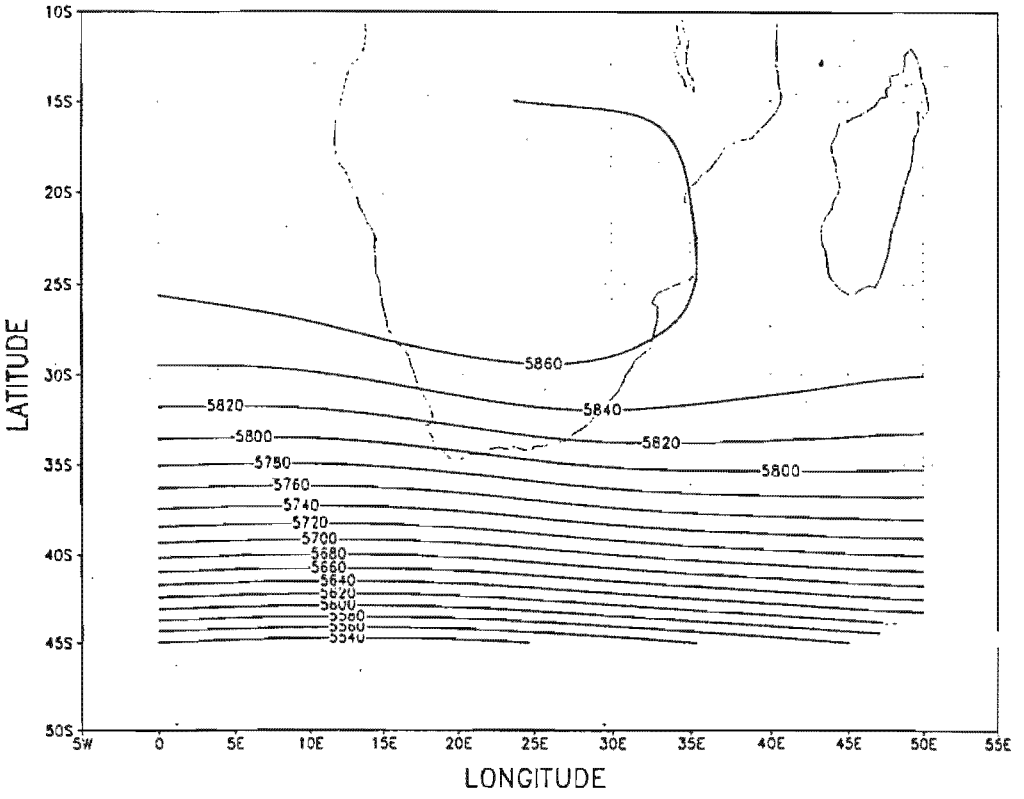

Figure 5.6.2. The same as Figure 5.1.2, but for ENSO seasons during the below-normal part of the decadal rainfall cycle only.

air from the east will be weaker, and might even be diverted towards the north because of the deeper low pressure in the Channel. The above suggest lower average rainfall in the interior.

From sections 4.4.11 and 4.4.12 one can see that there is an association between anomalously high (low) SST's in the NINO4 region and anomalously low (high) SST's in the NINO1 to NINO3 regions, and anomalously high (low) 1000 hPa heights west of the subcontinent and very low (high) 1000 hPa heights over the central parts of the interior and the east south eastern ocean area, suggesting a strengthening (weakening) of the western high and a weakening (strengthening) of the eastern high, causing stronger (weaker) influx of dry air from the south-west and weaker (stronger) influx of moist air from the east. Contrary to the above a stronger (weaker) influx of moist air from the tropics can be expected with the deeper

(weaker) trough over the interior. Anomalously high (low) SST's over the whole equatorial Pacific area is also associated with very high (low) 1000 hPa heights west of the subcontinent, as well as in the Mozambique Channel, suggesting a strengthening (weakening) of the western high pressure and a weakening (deepening) of the low pressure area in the Channel. This causes a probable weaker (stronger) influx of dry air from the south-west. Also, because of lower (higher) heights south of the subcontinent, more (less) frontal activity is suggested. Considering the 500 hPa pressure field, higher (lower) SST's is associated with higher (lower) 500 hPa geopotential heights over the whole area, but less (more) so south of the subcontinent, suggesting less (more) frontal activity and a weaker (stronger) influx of moist tropical air from the north. Less (more) rain can then be expected.

CHAPTER 6

SUMMARY

An overview of previous studies on relationships between anomalous SST's, seasonal rainfall, and atmospheric circulation anomalies is given in Chapter 1. In this study it was attempted to broaden our knowledge on the above by:

a) The use of more comprehensive data-sets than in previous studies.

b) The use of more combinations of data to find more detailed relationships or associations between anomalous SST's, seasonal rainfall, and atmospheric circulation.

In all aspects of the study, this approach produced the desired results. Although relationships between equatorial Pacific SST's and summer rainfall have already been established it was possible, in Chapter 2, to find a much better idea of the temporal and spatial extent of the summer-rainfall region that can be associated with equatorial Pacific SST's. This proved useful to the extent that only studies on late summer-rainfall were conducted in further parts of the study, because of the more coherent spatial structure of the rainfall region associated with equatorial Pacific SST's. Consider Figure 2.3 in this regard.

In Chapter 3 impacts of different ENSO events on the late summer-rainfall of South Africa during different periods since 1950 to 1996, based on the well researched quasi 18-20 year cycle, which is evident over the summer-rainfall region, were investigated. Above- and below-normal periods of this cycle with turning points between these periods were established. El Niño and La Niña seasons were grouped into the periods in which they occurred, i. e. in above- or below-normal periods. Average rainfall totals were then compared. In summarizing the results it was found that during an epoch of above-normal rainfall a moderating influence was evident on the impact of El Niño events so that, on average, even above normal rainfall is experienced during such events, e.g. the 1998 late summer rainfall season. Rainfall during La Niña events was further enhanced during above-normal epochs e. g. the 1976 late summer rainfall season. It was found that the opposite is also true in that during an epoch of below-normal rainfall, El Niño seasons are more severe e. g. the 1983 rainfall season. There is also significantly less rainfall during La Niña seasons

during below-normal rainfall epochs. See Table 3.3 for a summary of the results. These results gave more scope to the study, in that differences in the associations between circulation anomalies during different epochs and equatorial Pacific SST's were investigated, to find more detailed relationships that possibly exist between equatorial Pacific SST's, atmospheric circulation anomalies and rainfall over the subcontinent.

Subsequently, in Chapter 4, different combinations of data sets for the 1000 hPa and 500 hPa heights over the subcontinent and surrounding oceans, from 1958 to 1997, were used to find associations between circulation anomalies at those levels and equatorial Pacific SST's. In general a confirmation of previous studies was found that above-normal equatorial Pacific SST's are associated with above-normal heights at both the 1000 hPa and 500 hPa levels over the subcontinent, although different results were found for regions over the surrounding oceans. But other associations also became evident. The most important of these are that higher (lower) equatorial Pacific SST's are especially associated with higher (lower) 1000 hPa geopotential heights on the western side of the subcontinent. Also, when only ENSO, i. e. El Niño and La Niña years, were used in analysis, the associations found for all years were emphasized, because more extreme high and low equatorial Pacific SST's were taken into account. El Niño (La Niña) is associated with higher (lower) geopotential heights at both the 1000 hPa and 500 hPa levels over the subcontinent, while the opposite association is evident over the southern oceanic areas, similar to the findings of Miron and Tyson (1984). When intercomparisons between different El Niño seasons were made it was found that the stronger the El Niño, the stronger the negative factors for rainfall become at the surface as well as the 500 hPa level, where geopotential heights are higher in conjunction with stronger El Niño seasons. Again, when intercomparisons between La Niña seasons were made, it was found that the stronger the La Niña, the stronger the positive factors for rainfall become at the surface, where stronger troughs over the interior and a weakening and southward displacement of the western high pressure cell are suggested in conjunction with stronger La Niña seasons. Other associations were more fully discussed in Chapter 5, with the aid of long-term average maps.

It was demonstrated in Chapter 5 that it is possible to physically explain rainfall anomalies during specific types of rainfall seasons by considering the anomalies at the 1000 hPa and 500 hPa levels over the subcontinent and surrounding oceans during those seasons, while these seasons were also associated with anomalously high or low equatorial Pacific SST's.

This was done by investigating the effects of these associations on the Atlantic and Indian Ocean high pressure cells as well as the troughs that usually occur over the interior of the subcontinent at the surface, as shown by the average circulation maps at the surface. Also assessed was the strengthening and weakening of circulation features at the 500 hPa level. The differences between the circulation patterns for the above- and below-normal parts of the inter-decadal rainfall cycles could also be somewhat assessed: it seems that above-normal rainfall during the above-normal part of the inter-decadal rainfall cycle is caused by a stronger inflow of moisture from the east of the subcontinent because of a stronger Indian Ocean high, while a stronger low pressure area in the Mozambique channel causes moisture flow to be diverted northwards during the below-normal part of the inter-decadal rainfall cycle, with subsequently less rainfall over the more southern parts of the subcontinent.

To verify that the relationships found between Pacific equatorial SST's, precipitation and 1000 hPa and 500 hPa geopotential height anomalies over the subcontinent found in Chapter 4 are not coincidental but can be explained by known and proven physical processes, these relationships were compared to the AMIP atmospheric model runs of the T31 GENESIS general circulation model. These model runs were available for the period 1979 to 1988. The associations found by these runs compared well with the associations found by CCA in about 70% of cases assessed, and it can therefore be concluded that these associations found between equatorial Pacific SST's, 1000 hPa and 500 hPa height anomalies, and rainfall over southern Africa, are supported by the GCM simulations.

Comparing this study to previous ones in the same field, it is proven that, the more variables and data used, the more intricate the relationship between Pacific equatorial SST's and rainfall over the subcontinent of southern Africa becomes.

By using, e.g. more levels of geopotential height data by applying CCA to more atmospheric pressure levels, the associations between Pacific equatorial SST's and rainfall over South Africa might be proven to be even more complex as already shown. It is hoped, however, that the results obtained herein will enhance the possibility of further studies into the relationships between Pacific equatorial SST's and rainfall over South Africa, making these associations more clear to both the climatologist and long-term rainfall forecaster.

REFERENCES

ALEXANDER, W. J. R. (1984): *The current drought - a challenge to a hydrologist.* Preprints, South African National Hydrological Symposium, WRC, Technical Report No. TR119, p180-194.

BARNETT, T. P. and R. PREISENDORFER (1987): *Origins and levels of monthly and seasonal forecast skill for United States surface air temperatures determined by canonical correlation analysis.* Monthly Weather Review, **115**, 1825-1850.

BHALATRA, Y. P. R. (1985): *The drought of 1981-85 in Botswana.* Department of Meteorological Services, Ministry of Works and Commerce, Gaborone, Botswana, 78 pp.

D'ABRETON, P. C. and J. A. LINDESAY (1993): *Water vapour transport over southern Africa during wet and dry early and late summer months.* International Journal of Climatology, **13**, 151-170.

D'ABRETON, P. C. and P. D. TYSON (1995): *Divergent and non-divergent water vapour transport over southern Africa during wet and dry conditions.* Meteorology and Atmospheric Physics, **55**, 47-59.

D'ABRETON, P. C. and P. D. TYSON (1996): *Three-dimensional kinematic trajectory modelling of water vapour transport over southern Africa.* Water SA, **22**, 297-305.

DENT, M. C., R. E. SCHULZE, H. M. M. WILLS and S. D. LYNCH (1987): *Spatial and temporal analysis of the recent drought in the summer rainfall region of Southern Africa.* Water SA, **13**, 37-42.

DYER, T. G. J. (1976): *Meridional interactions between rainfall and surface pressure.* Nature, **264**, 48-49.

DYER, T. G. J. (1979): *Rainfall along the east coast of southern Africa, the Southern*

Oscillation, and the latitude of the subtropical high pressure belt. Quarterly Journal of the Royal Meteorological Society, **105**, 445-451.

DYER, T. G. J. and P. D. TYSON (1978): *Inter-hemisphere associations in the year-to-year variations of major components of the general circulation of the atmosphere: 1910-1963.* South African Journal of Science, **74**, 325-328.

ERSKINE, J. M. (1983): *Impact of drought in Natal/KwaZulu.* South African Journal of Science, **79**, 439-440.

GATES, L. W. (1992): *AMIP: The Atmospheric Model Intercomparison Project.* Bulletin of the American Meteorological Society, **73**, 1962-1970.

GILLOOLY, J. F. and T. G. J. DYER (1979): *Spatial variations in rainfall during abnormally wet and dry years.* South African Journal of Science, **75**, 261-262.

HALPERT, M. S. and C. F. ROPELEWSKI (1992): *Surface temperature patterns associated with the Southern Oscillation.* Journal of Climate, **5**, 577-593.

HARANGOZO, S. A. and M. S. J. HARRISON (1983): *On the use of synoptic data in indicating the presence of cloud bands over southern Africa.* South African Journal of Science, **79**, 413-414.

HARRISON, M. S. J. (1983): *The Southern Oscillation, zonal equatorial circulation cells and South African rainfall.* Preprints, 1st ICSHM, American Meteorological Society, 302-305.

HARRISON, M. S. J. (1986): *A synoptic climatology of South African rainfall variations.* Unpublished PhD Thesis, University of the Witwatersrand, 341 pp.

HASTENRATH, S., L. GREISCHAR and J. VAN HEERDEN (1995): *Prediction of the summer rainfall over South Africa.* Journal of Climate, **8**, 1511-1518.

HATTLE, A. D. and P. WEBSTER (1984): *Drought management tools and strategies.* Proceedings of the S. A. Nat. Hydrol. Symp., WRC, Technical Report No. TR119, 299-308.

HOFMEYR, W. L. and V. GOUWS (1964): *A statistical and synoptic analysis of wet and dry conditions in northwestern Transvaal.* Notos, **13**, 37-48.

HUDSON, D. A. (1997): *Southern African climate change simulated by the GENESIS GCM.* South African Journal of Science, **93**, 389-403.

JANOWIAK, J. E. (1988): *An investigation of interannual rainfall variability in Africa.* Journal of Climate, **1**, 240-255.

JURY, M. R. (1992): *A climatic dipole governing the interannual variability of convection over the SW Indian Ocean and SE Africa region.* Trends in Geophysical Research, **1**, 165-172.

JURY, M. R. (1996): *Regional teleconnection patterns associated with summer rainfall over South Africa, Namibia and Zimbabwe.* International Journal of Climatology, **16**, 135-153.

JURY, M. R. and B. M. R. PATHACK (1991): *A study of climate and weather variability over the tropical southwest Indian Ocean.* Meteorology and Atmospheric Physics, **47**, 37-48.

JURY, M. R., B. PATHACK and B. J. SOHN (1992): *Spatial structure and interannual variability of summer convection over southern Africa and the SW Indian Ocean.* South African Journal of Science, **88**, 275-280.

JURY, M. R. and B. M. R. PATHACK (1993): *Composite climatic patterns associated with extreme modes of summer rainfall over southern Africa: 1975-1984.* Theoretical and Applied Climatology, **47**, 137-145.

JURY, M. R., C. A. MCQUEEN and K. M. LEVEY (1994): *SOI and QBO signals in the African region.* Theoretical and Applied Climatology, **50**, 103-115.

JURY, M. R., B. A. PARKER, N. RAHOLIJAO and A. NASSOR (1995): *Variability of summer rainfall over Madagascar: climatic determinants at interannual scales.* International Journal of Climatology, **15**, 1323-1332.

KRIPALANI, R. H. and A. KULKARNI (1997a): *Climatic impact of El Niño/La Niña on the Indian monsoon: A new perspective.* Weather, **52**, 39-46.

KRIPALANI, R. H. and A. KULKARNI (1997b): *Rainfall variability over South-East Asia-Connections with Indian Monsoon and ENSO extremes: New perspectives.* International Journal of Climatology, **17**, 1155-1168.

KRUGER, A. C. (1996): *Oscillatory variations of Seasonal Rainfall in South Africa.* South African Weather Bureau Internal Report No. CLI/5, South African Weather Bureau, 42 pp.

LANDMAN, W. A. and S. J. MASON (1999): *Operational long-lead prediction of South African rainfall using canonical correlation analysis.* International Journal of Climatology, **19**, 1073-1090.

LAU, N. C. and M. J. NATH (1994): *A modelling study of the relative roles of tropical and extratropical SST anomalies in the variability of the global atmosphere-ocean system.* Journal of Climate, **7**, 1184-1207.

LINDESAY, J. A. (1984): *Spatial and temporal variability of rainfall over South Africa, 1963 to 1981.* South African Geographical Journal, **66**, 168-175.

LINDESAY, J. A. (1988): *South African Rainfall, the Southern Oscillation and a Southern Hemisphere Semi-Annual Cycle.* Journal of Climatology, **8**, 17-30.

LINDESAY, J. A. and M. R. JURY (1991): *Atmospheric circulation controls and characteristics of a flood event in central South Africa.* International Journal of Climatology, **11**, 609-627.

LYONS, S. W. (1991): *Origins of convective variability over equatorial southern Africa during austral summer.* Journal of Climate, **4**, 23-39.

MAIN, J. P. L. and B. C. HEWITSON (1995): *Regionalization of daily precipitation in Botswana 1972-1989.* South African Geographical Journal, **77**, 51-55.

MASON, S. J. and M. R. JURY (1997): *Climate variability and change over southern Africa: a reflection on underlying processes.* Progress in Physical Geography, **21**, 23-50.

MASON, S. J. and J. A. LINDESAY (1993): *A Note on the Modulation of Southern Oscillation-Southern African Rainfall Associations With the Quasi-Biennial Oscillation.* Journal of Geophysical Research, **98**, 8847-8850.

MASON, S. J. and G. M. MIMMACK (1992): *The use of bootstrap correlation coefficients for the correlation coefficient in climatology.* Theoretical and Applied Climatology, **45**, 229-233.

MATARIRA, C. H. (1990): *Drought over Zimbabwe in a regional and global context.* International Journal of Climatology, **10**, 609-625.

MATARIRA, C. H. and M. R. JURY (1992): *Contrasting meteorological structure of intra-seasonal wet and dry spells in Zimbabwe.* International Journal of Climatology, **12**, 165-176.

MIRON, O. and J. A. LINDESAY (1983): *A note on changes in airflow patterns between wet and dry spells over South Africa, 1963 to 1979.* South African Geographical Journal, **65**, 141-147.

MIRON, O. and P. D. TYSON (1984): *Wet and dry conditions and pressure anomaly fields over South Africa and the adjacent oceans, 1963-1979.* Monthly Weather Review, **112**, 2127-2132.

MO, K. C. and G. H. WHITE (1985): *Teleconnections in the Southern Hemisphere.* Monthly Weather Review, **113**, 22-37.

MORON, V., S. BIGOT and P. ROUCOU (1995): *Rainfall variability in subequatorial America and Africa and relationships with the main sea-surface temperature modes.* International Journal of Climatology, **15**, 1297-1322.

NICHOLSON, S. E. (1986a): *Rainfall variability in southern and equatorial Africa, its*

relation to Atlantic sea-surface temperatures and the Southern Oscillation. Preprints, 2nd International Conference on Southern Hemisphere Meteorology, American Meteorological Society, 472-475.

NICHOLSON, S. E. (1986b): *The nature of rainfall variability in Africa south of the equator.* Journal of Climatology, **6**, 515-530.

NICHOLSON, S. E. (1986c): *The spatial coherence of African rainfall anomalies interhemispheric teleconnections.* Journal of Climate and Applied Meteorology, **25**, 1365-1381.

NICHOLSON, S. E. and D. ENTEKHABI (1986): *The quasi-periodic behaviour of rainfall variability in Africa and its relationship to the Southern Oscillation.* Archiv für Meteorologie, Geophysik und Bioklimatologie, **34**, 311-348.

NICHOLSON, S. E. and D. ENTEKHABI (1987): *Rainfall variability in equatorial and southern Africa: Relationships with sea-surface temperatures along the south-western coast of Africa.* Journal of Climate and Applied Meteorology, **26**, 561-578.

NICHOLSON, S. E. and J. KIM (1996): *The relationship of the El Niño-Southern Oscillation to African rainfall.* International Journal of Climatology, **17**, 117-135.

PAN, J. P. and A. H. OORT (1990): *Correlation analysis between sea surface temperature anomalies in the eastern equatorial Pacific and the world ocean.* Climate Dynamics, **4**, 191-205.

PANOFSKY, H. A. and W. BRIER (1958): *Some applications of statistics to Meteorology.* Pennsylvania State University, Pennsylvania, 224 pp.

PRESTON-WHYTE, R. A. and P. D. TYSON (1988): *The Atmosphere and Weather of Southern Africa.* Oxford University Press, Cape Town, 374 pp.

REYNOLDS, R. W. (1988): *A real-time global sea-surface temperature analysis.* Journal of Climate, **1**, 75-86.

REYNOLDS, R. W. and T. M. SMITH (1994): *Improved global sea surface temperature analyses using optimum interpolation.* Journal of Climate, **7**, 929-948.

ROCHA, A. and I. SIMMONDS (1997): *Interannual variability of south-eastern African summer rainfall. Part II: modelling the impact of sea-surface temperatures on rainfall and circulation.* International Journal of Climatology, **17**, 267-290.

ROPELEWSKI, C. F. and M. S. HALPERT (1987): *Precipitation patterns associated with El Niño/Southern Oscillation.* Monthly Weather Review, **115**, 1606-1626.

ROPELEWSKI, C. F. and M. S. HALPERT (1989): *Precipitation patterns associated with the high index phase of the Southern Oscillation.* Journal of Climate, **2**, 268-284.

SCHULZE, B. R. (1965): *Climate of South Africa. Part 8. General survey.* South African Weather Bureau, 330 pp.

SCHULZE, G. C. (1984): *'n Oorsigtelike bespreking van drukveranderings en sinoptiese drukpatrone in die Suidelike Halfrond in die tydperk Oktober 1982 tot Februarie 1983.* South African Journal of Science, **80**, 94-97.

SCHULZE, G. C. (1989): *Seisoenvariasies van reënval oor die somerreënstreke van Suid-Afrika.* Unpublished MSc dissertation, University of Pretoria, 205 pp.

SHINODA, M. and R. KAWAMURA (1996): *Relationships between rainfall over semi-arid southern Africa and geopotential heights, and sea-surface temperatures.* Journal of the Meteorological Society of Japan, **74**, 21-36.

STOECKENIUS, T. (1981): *Interannual variations of tropical precipitation patterns.* Monthly Weather Review, **109**, 1233-1247.

TALJAARD, J. J. (1986a): *Contrasting atmospheric circulation during dry and wet summers in South Africa.* SAWB Newsletter No. 445, 1-5.

TALJAARD, J. J. (1986b): *Change of rainfall distribution and circulation patterns over southern Africa in summer.* Journal of Climatology, **6**, 579-592.

TALJAARD, J. J. (1994): *Atmospheric circulation systems, synoptic climatology and weather phenomena of South Africa. Part 1. Controls of the Weather and Climate of South Africa.* Technical Note No. 27, South African Weather Bureau, 45 pp.

TALJAARD, J. J. (1995): *Atmospheric circulation systems, synoptic climatology and weather phenomena of South Africa. Part 2. Atmospheric circulation systems in the South African region.* Technical Note No. 28, South African Weather Bureau, 65 pp.

THOMPSON, L. S. and D. POLLARD (1997): *Greenland and Antarctic mass balances for present and doubled CO_2 from the GENESIS version-2 Global Climate Model.* Journal of Climate, **10**, 871-900.

TORRANCE, J. D. (1979): *Upper windflow patterns in relation to rainfall in south-east central Africa.* Weather, **34**, 106-115.

TYSON, P. D. (1980): *Temporal and spatial variation of rainfall anomalies in Africa south of latitude 22 during the period of meteorological record.* Climate Change, **2**, 363-371.

TYSON, P. D. (1981): *Atmospheric circulation variations and the occurrence of extended wet and dry spells over southern Africa.* Journal of Climatology, **1**, 115-130.

TYSON, P. D. (1984): *The atmospheric modulation of extended wet and dry spells over South Africa, 1958-78.* Journal of Climatology, **4**, 621-635.

TYSON, P. D. (1986): *Climatic change and variability over southern Africa.* Oxford University Press, Cape Town, 220 pp.

TYSON, P. D., T. G. J. DYER and M. N. MAMETSE (1975): *Secular changes in South African rainfall: 1880-1972.* Quarterly Journal of the Royal Meteorological Society, **101**, 817-833.

TYSON, P. D. and T. G. J. DYER (1978): *The predicted above-normal rainfall of the seventies and the likelihood of droughts in the eighties in South Africa.* South African Journal of Science, **76**, 340-341.

VAN DEN HEEVER, S. C. (1994): *Modelling tropical-temperate troughs over southern Africa.* Unpublished MSc dissertation, University of the Witwatersrand, 216 pp.

VAN HEERDEN, J., D. E. TERBLANCHE and G. C. SCHULZE (1988): *The Southern Oscillation and South African Summer Rainfall.* Journal of Climatology, **8**, 577-597.

VAN LOON, H. and R. A. MADDEN (1981): *The Southern Oscillation Part I: Global associations with pressure and temperature in northern winter.* Monthly Weather Review, **109**, 1150-1162.

VINES, R. G. (1982): *Rainfall patterns in southern South America and possible relationships with similar patterns in South Africa.* South African Journal of Science, **78**, 457-459.

WALKER, G. T. and E. W. BLISS (1930): *World Weather IV - some applications to seasonal forecasting.* Memoirs of the Royal Meteorological Society, **3(24)**, 81-95.